

X-ray Photoelectron Spectroscopy

Roger Smart, Stewart McIntyre, Mike
Bancroft, Igor Bello & Friends

Department of Physics and Materials Science

City University of Hong Kong

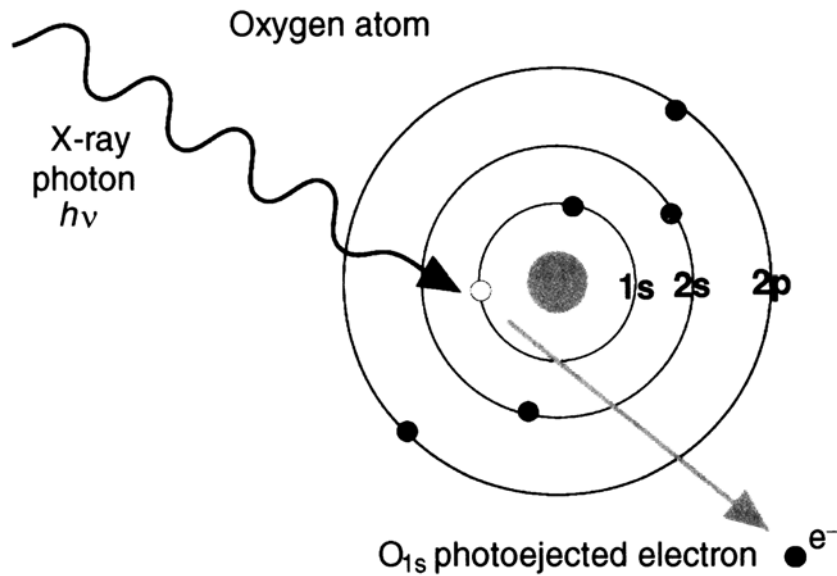
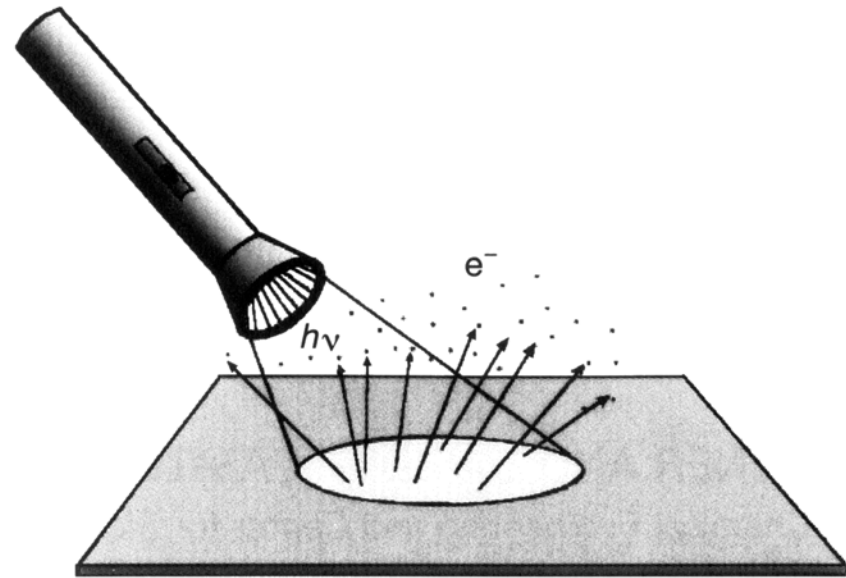
Surface Science Western, UWO

Introduction

Photoelectric effect

Photoelectric effect

Einstein, Nobel Prize 1921

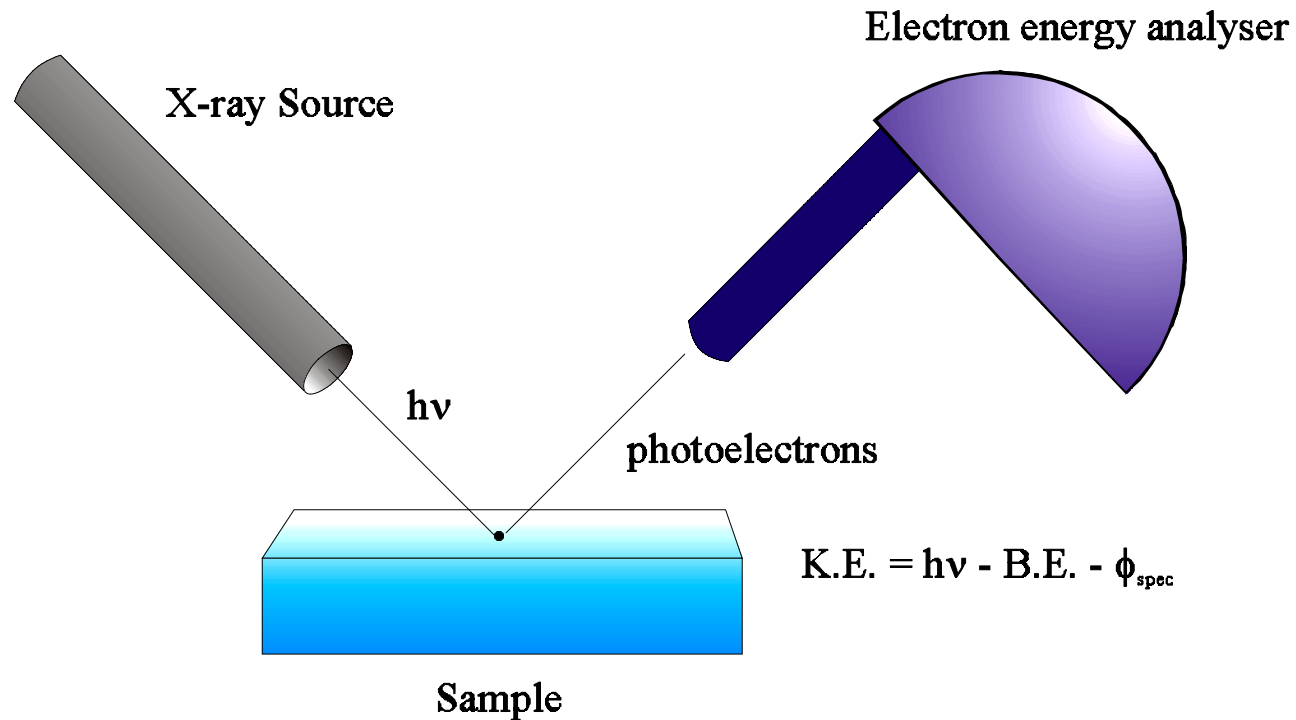


Photoemission as an analytical tool

Kai Siegbahn, Nobel Prize 1981

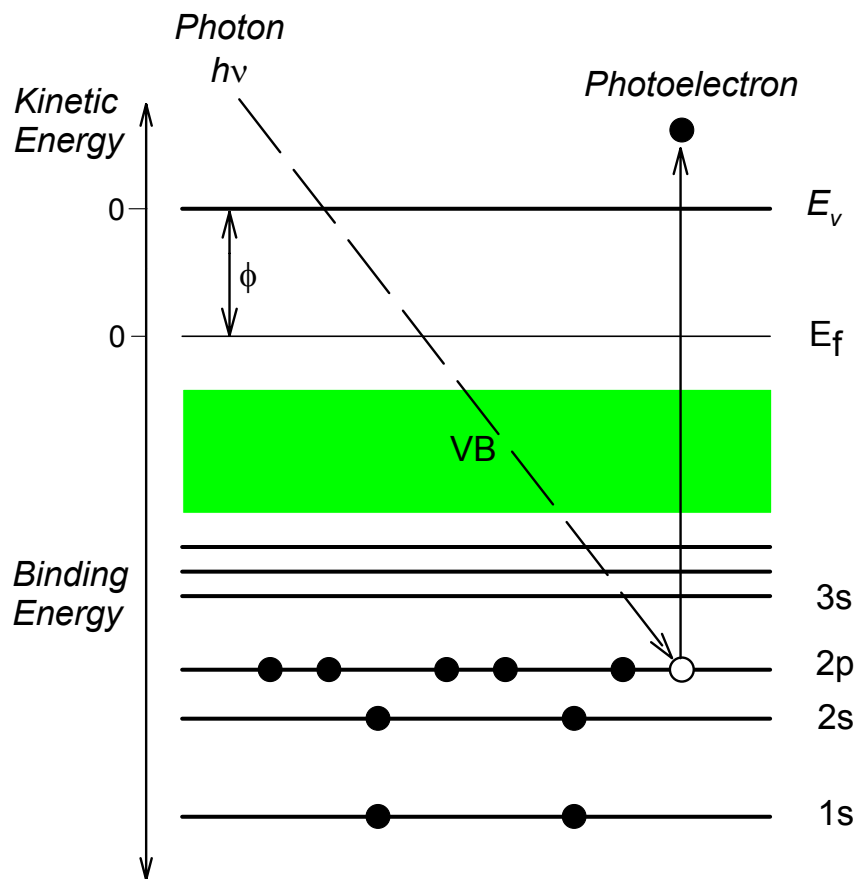
XPS, also known as ESCA, is the most widely used surface analysis technique because of its relative simplicity in use and data interpretation.

- XPS** X-ray Photoelectron Spectroscopy
- ESCA** Electron Spectroscopy for Chemical Analysis
- UPS** Ultraviolet Photoelectron Spectroscopy
- PES** Photoemission Spectroscopy



Analytical Methods

--- X-ray Photoelectron Spectroscopy (XPS)

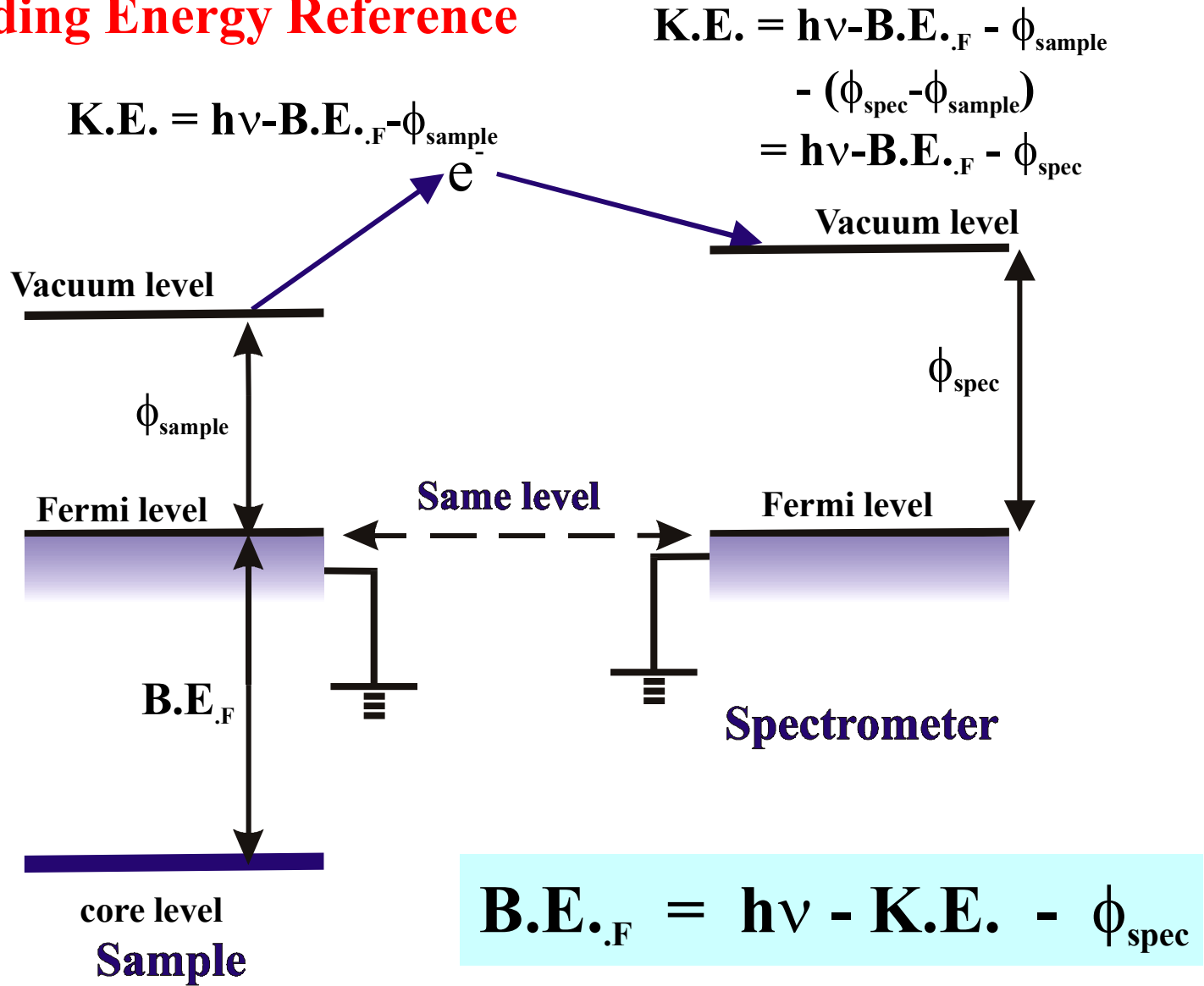


$$KE = h\nu - (E_B + \phi)$$

XPS spectrum:
Intensities of photoelectrons
versus E_B or KE

- Elemental identification and chemical state of element
- Relative composition of the constituents in the surface region
- Valence band structure

Binding Energy Reference

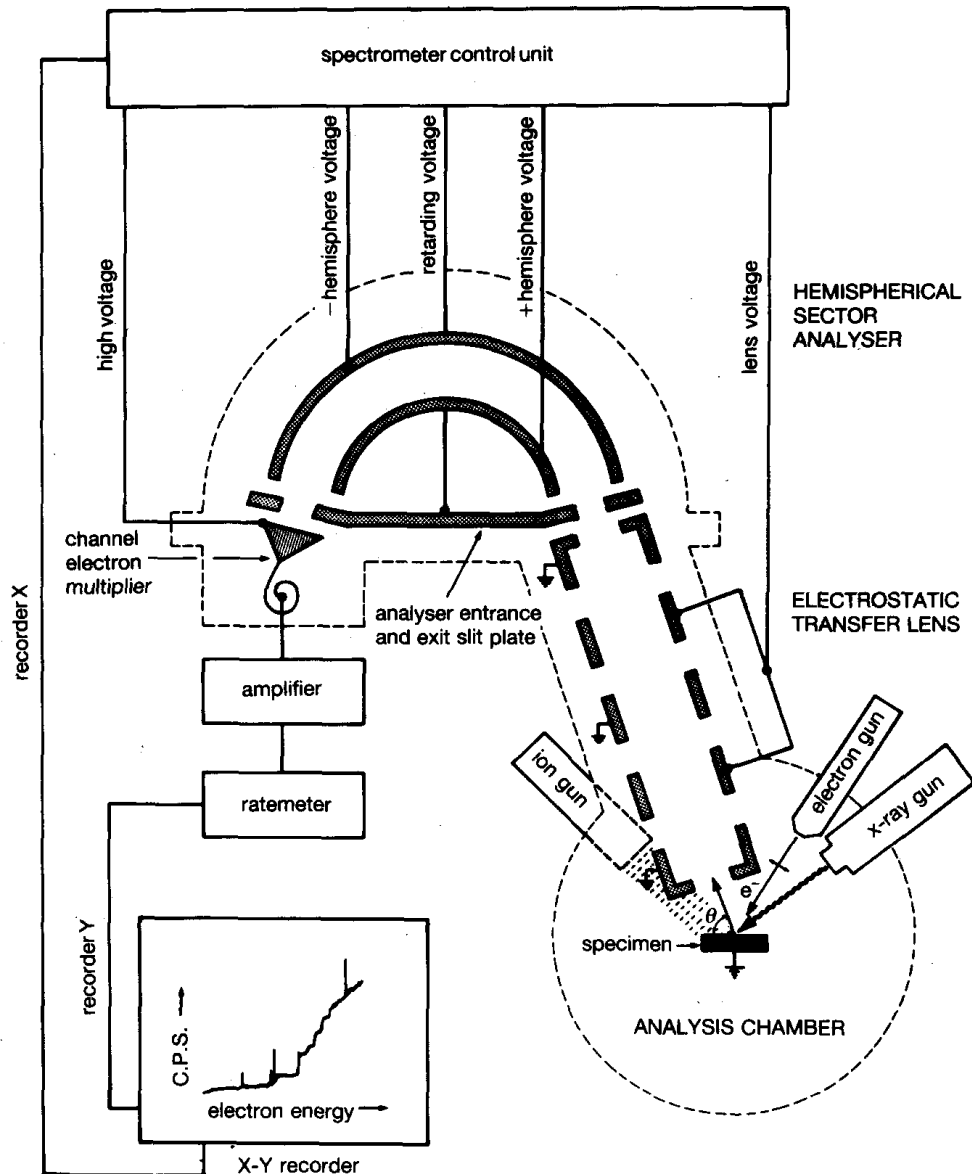


Instrumentation

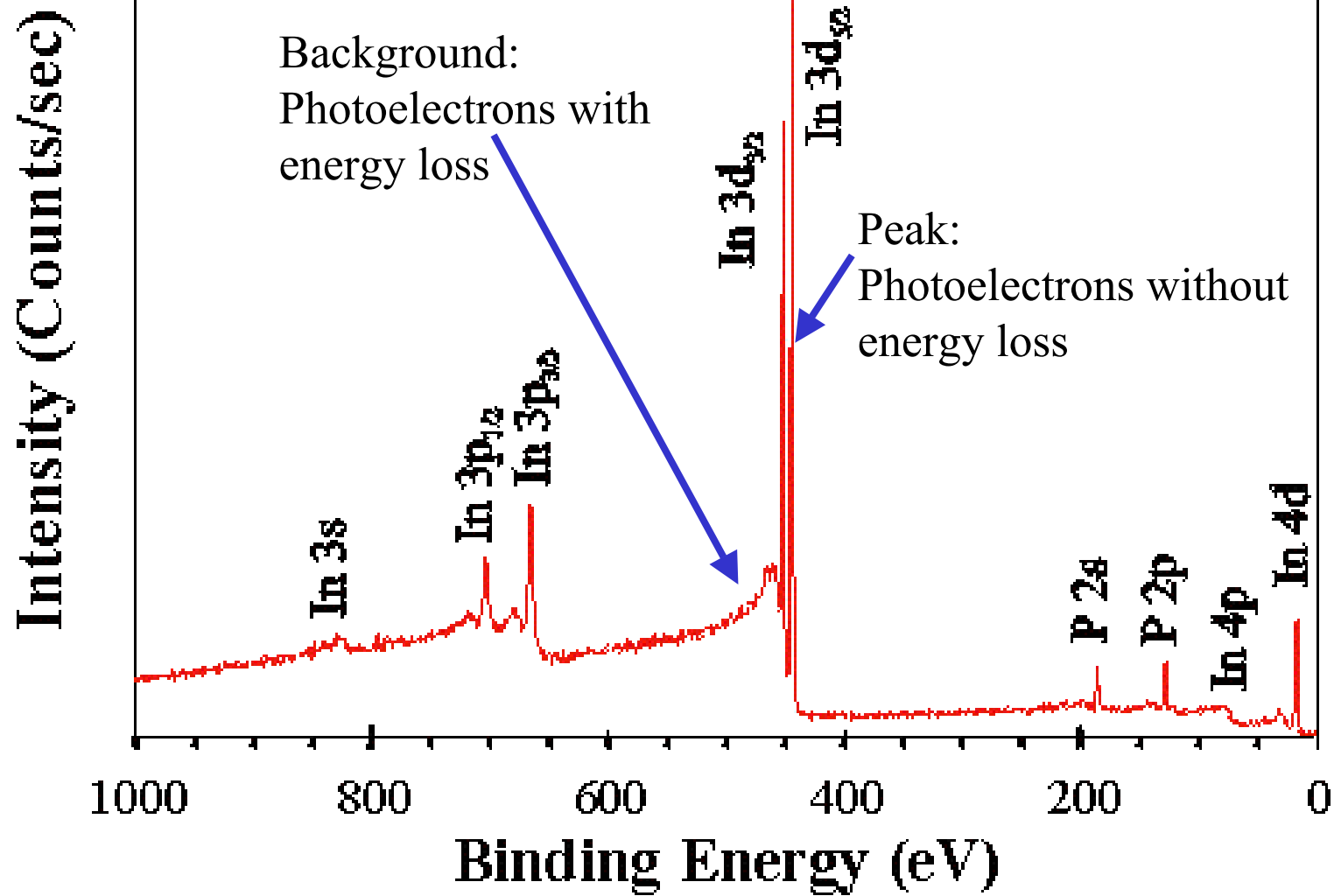
- Electron energy analyzer
- X-ray source
- Ar ion gun
- Neutralizer
- Vacuum system
- Electronic controls
- Computer system

Ultrahigh vacuum system
< 10^{-9} Torr (< 10^{-7} Pa)

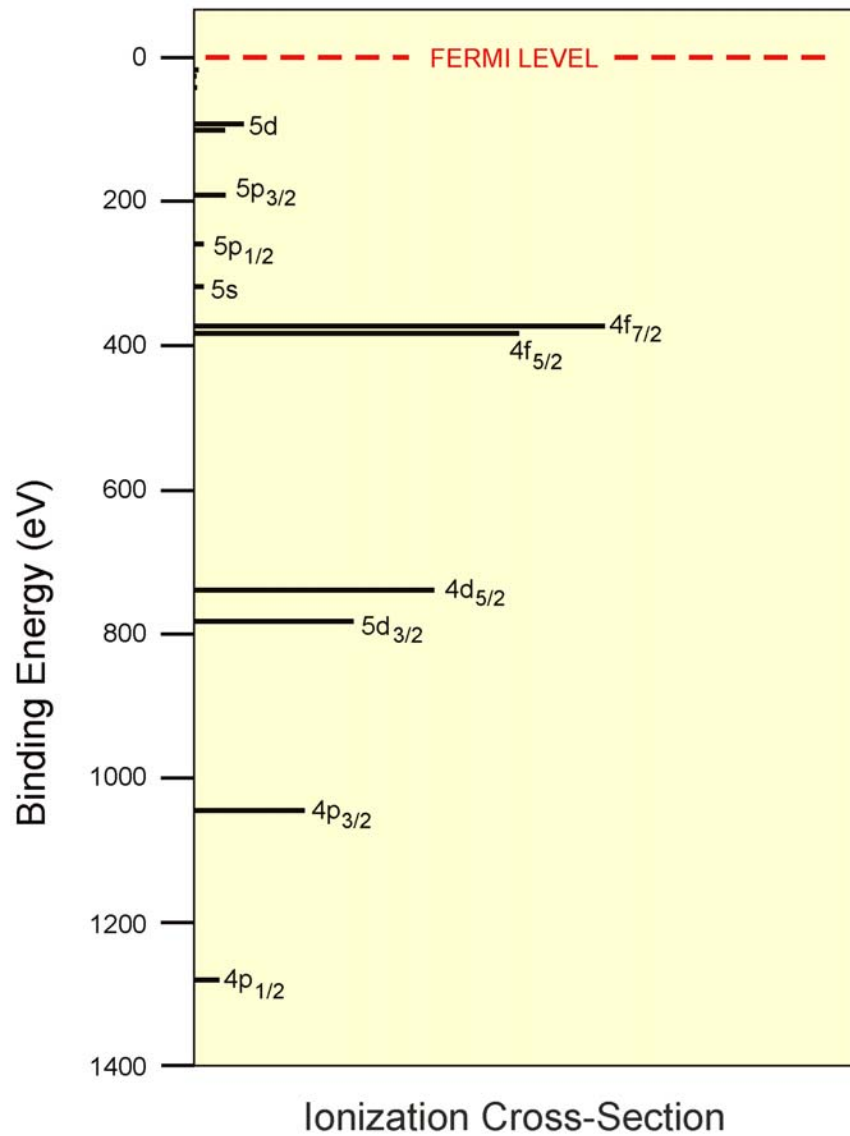
- Detection of electrons
- Avoid surface reactions/
contaminations



XPS spectrum of a UHV cleaved InP (110) surface.



Relative binding energies and ionization cross-section for U

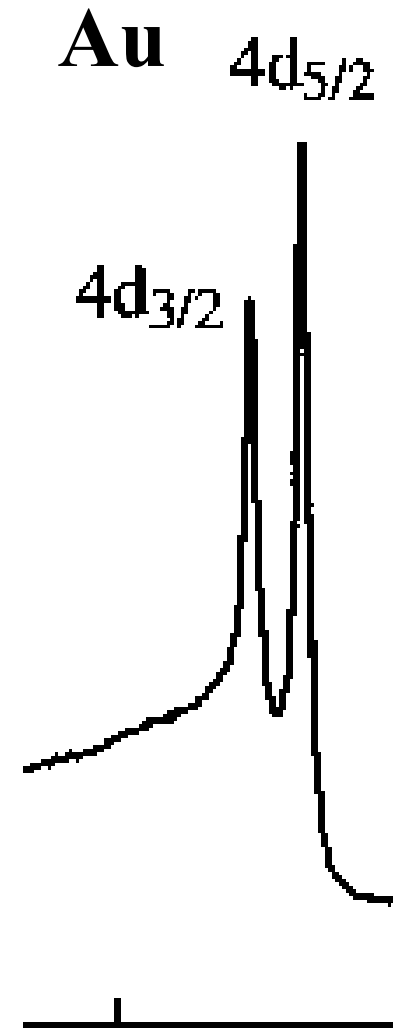


For p, d and f peaks, two peaks are observed.

The separation between the two peaks are named **spin orbital splitting**. The values of spin orbital splitting of a core level of an element in different compounds are nearly the same.

The **peak area ratios** of a core level of an element in different compounds are also nearly the same.

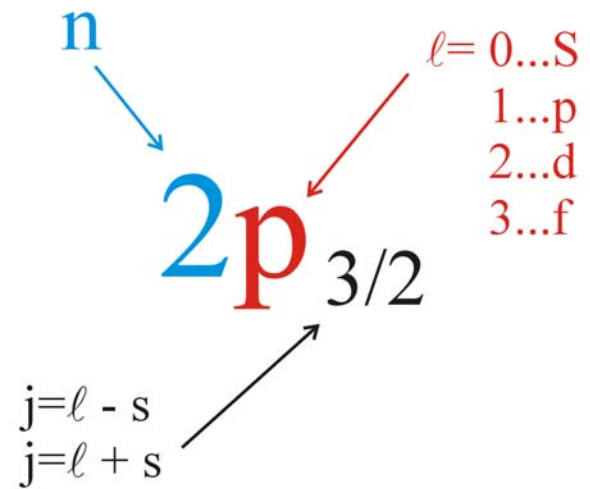
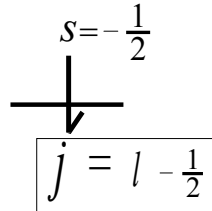
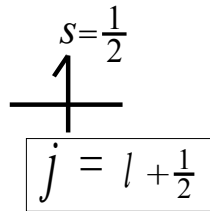
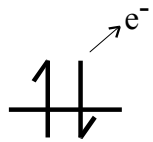
Spin orbital splitting and peak area ratios assist in element identifications.



Spin-orbital splitting

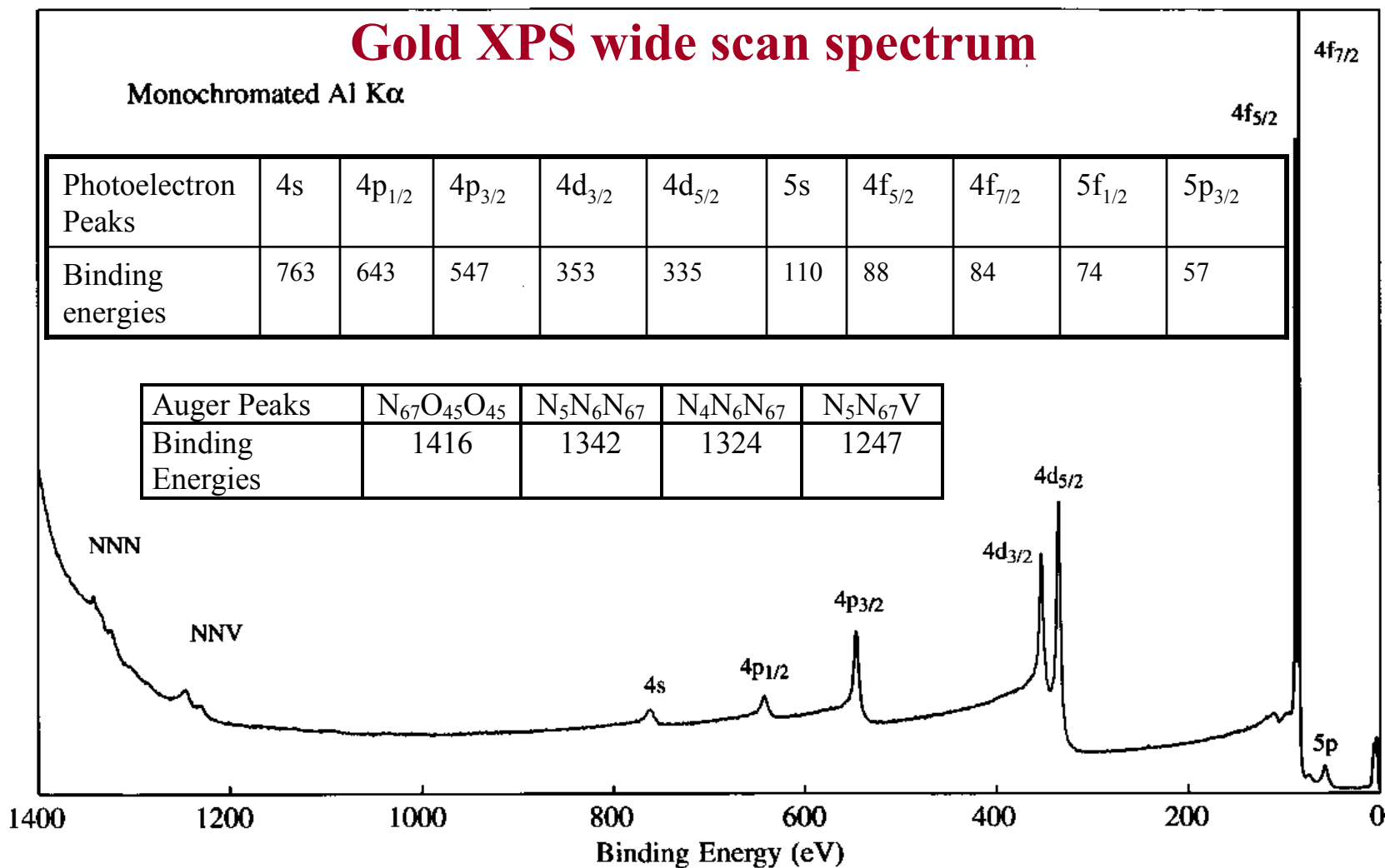
Peak Notations

L-S Coupling ($j = l \pm s$)

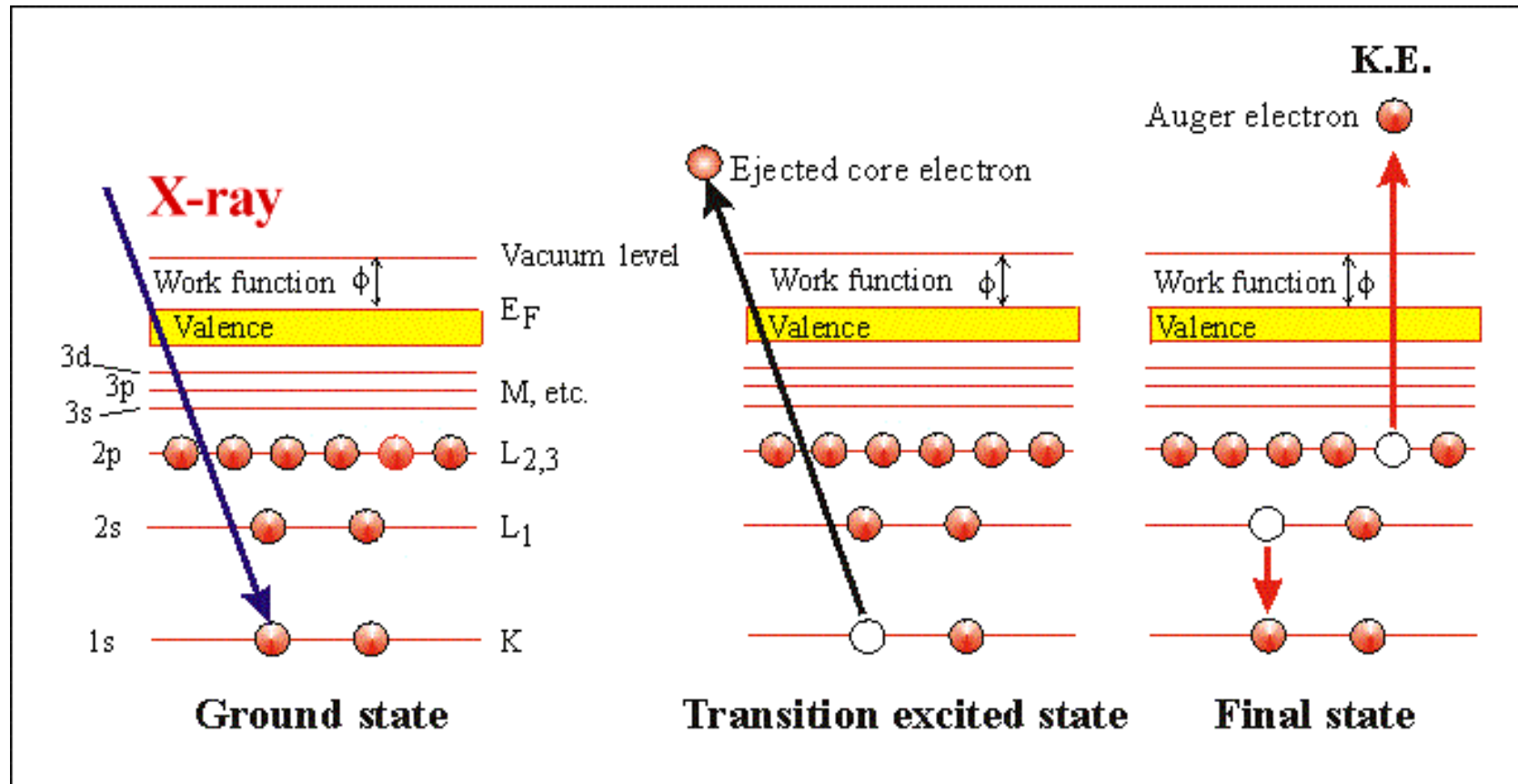


$l = 1$ $p_{1/2}$ $p_{3/2}$ $s = -1/2$ $s = +1/2$ Area ratio 1 : 2	$l = 2$ $d_{3/2}$ $d_{5/2}$ $s = -1/2$ $s = +1/2$ Area ratio 2 : 3	$l = 3$ $f_{5/2}$ $f_{7/2}$ $s = -1/2$ $s = +1/2$ Area ratio 3 : 4
--	--	--

Qualitative analysis



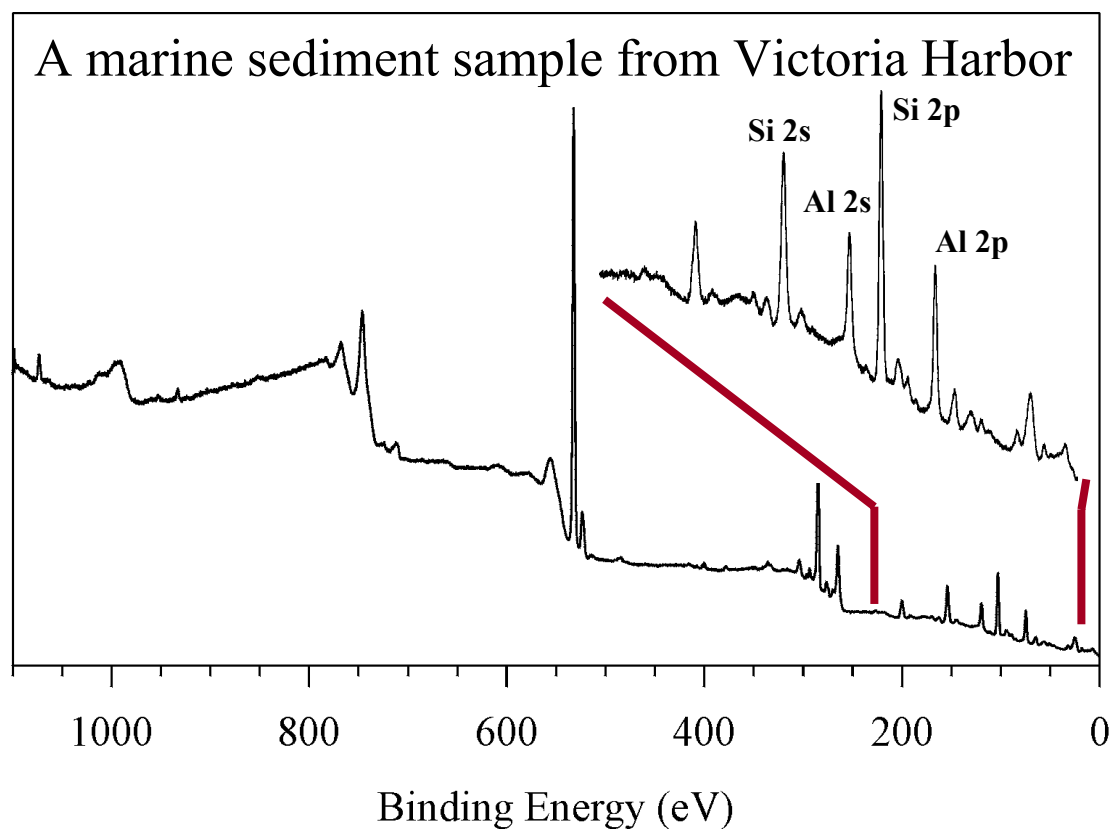
X-ray Induced Auger Electrons



K.E. is independent of the x-ray photon energy. However, in the B.E. scale, Auger peak positions depend on the x-ray source.

General methods in assisting peak identification

- (1) Check peak positions and relative peak intensities of 2 or more peaks (photoemission lines and Auger lines) of an element
- (2) Check spin orbital splitting and area ratios for p, d, f peaks



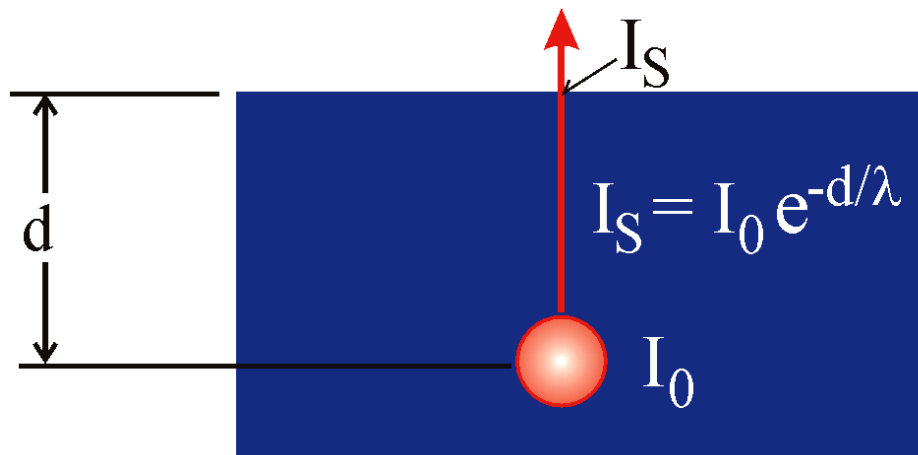
The following elements were found:
O, C, Cl, Si, F, N, S,
Al, Na, Fe, K, Cu,
Mn, Ca, Cr, Ni, Sn,
Zn, Ti, Pb, V

XPS Sampling Depth

λ_i = inelastic mean free path of an electron in a solid

For an electron of intensity I_0 emitted at a depth d below the surface, the intensity is attenuated according to the Beer-Lambert law. So, the intensity I_s of the same electron as it reaches the surface is

$$I_s = I_0 e^{-d/\lambda}$$



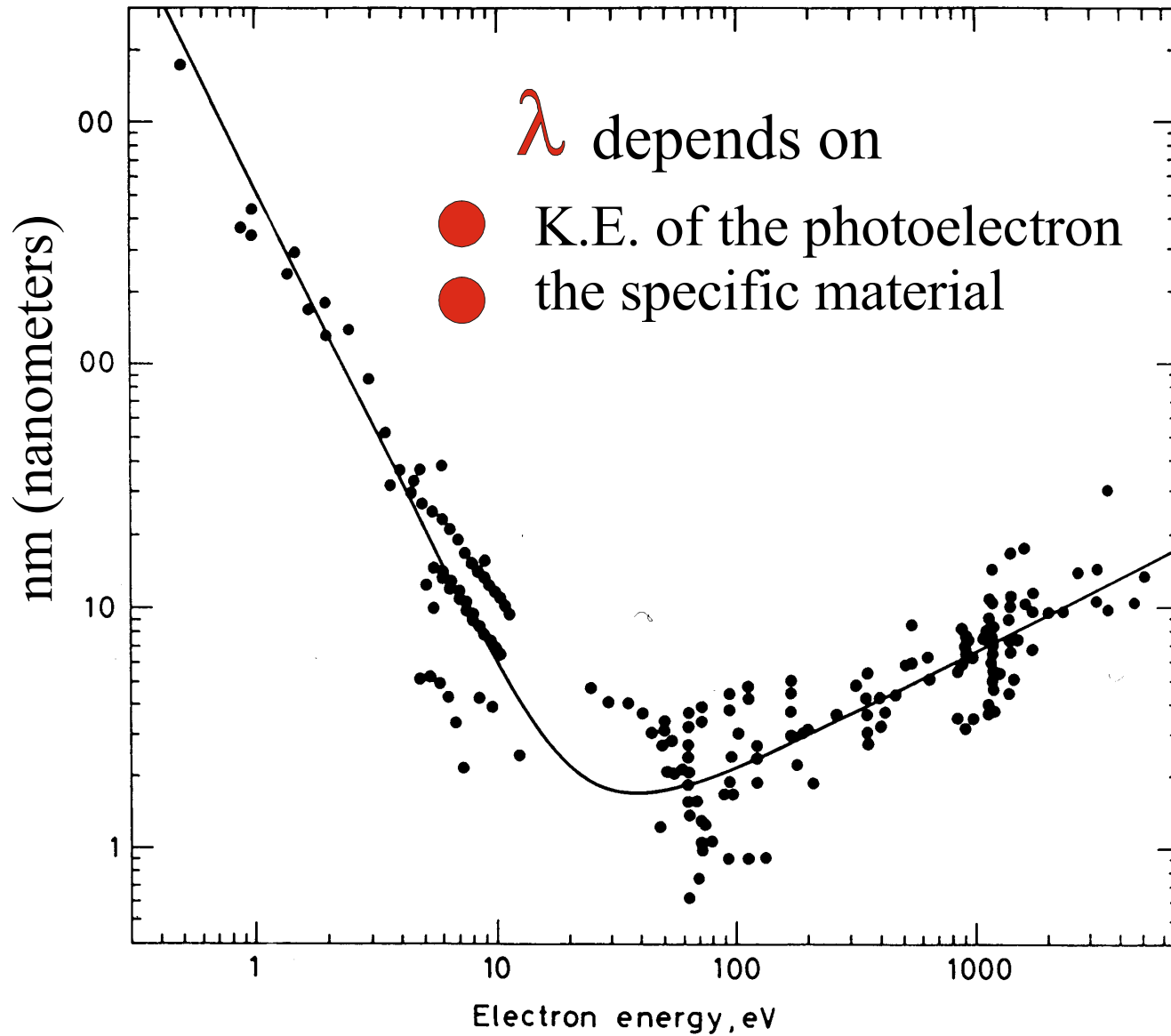
With a path length of one λ 63% of all electrons are scattered

Sampling Depth

- Sampling Depth is defined as the depth from which 95% of all photoelectrons are scattered by the time they reach the surface (3λ)
- Most λ 's are in the range of 1 – 3.5 nm for AlK α radiation
- So the sampling depth (3λ) for XPS under these conditions is 3-10 nm

1 monolayer = 0.3 nm

“Universal Curve” for IMFP



Quantitative XPS: I

Some XPS quantitative measurements are as accurate as $\pm 10\%$

$$I_i = N_i \sigma_i \lambda_i K$$

where: I_i = intensity of photoelectron peak “p” for element “i”

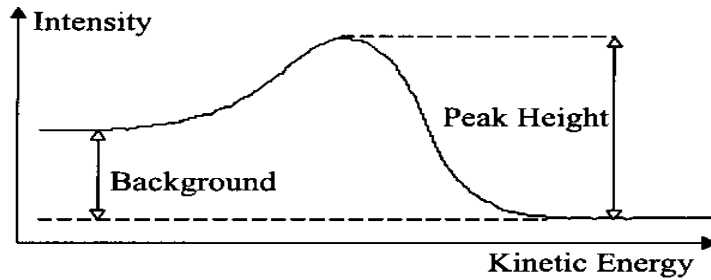
N_i = average atomic concentration of element “i” in the surface under analysis

σ_i = photoelectron cross-section (Scofield factor) for element “i” as expressed by peak “p”

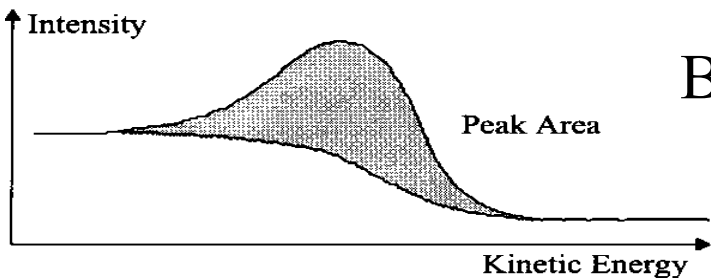
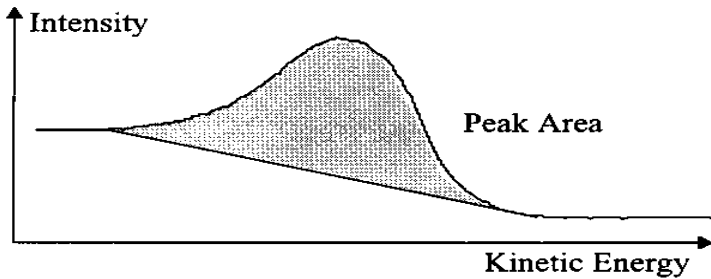
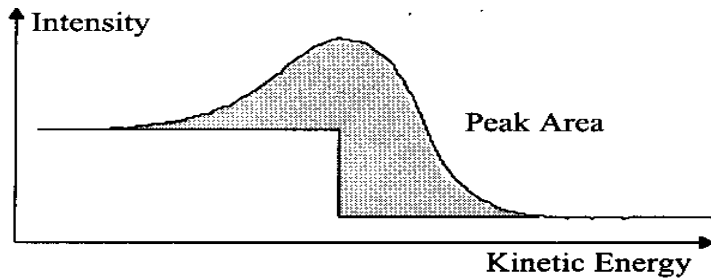
λ_i = inelastic mean free path of a photoelectron from element “i” as expressed by peak “p”

K = all other factors related to quantitative detection of a signal (assumed to remain constant during exp't)

How to measure I_{measured}



Worst



Best

Accuracy better than 15%
using ASF's

Use of standards measured
on same instrument or full
expression above accuracy
better than 5%

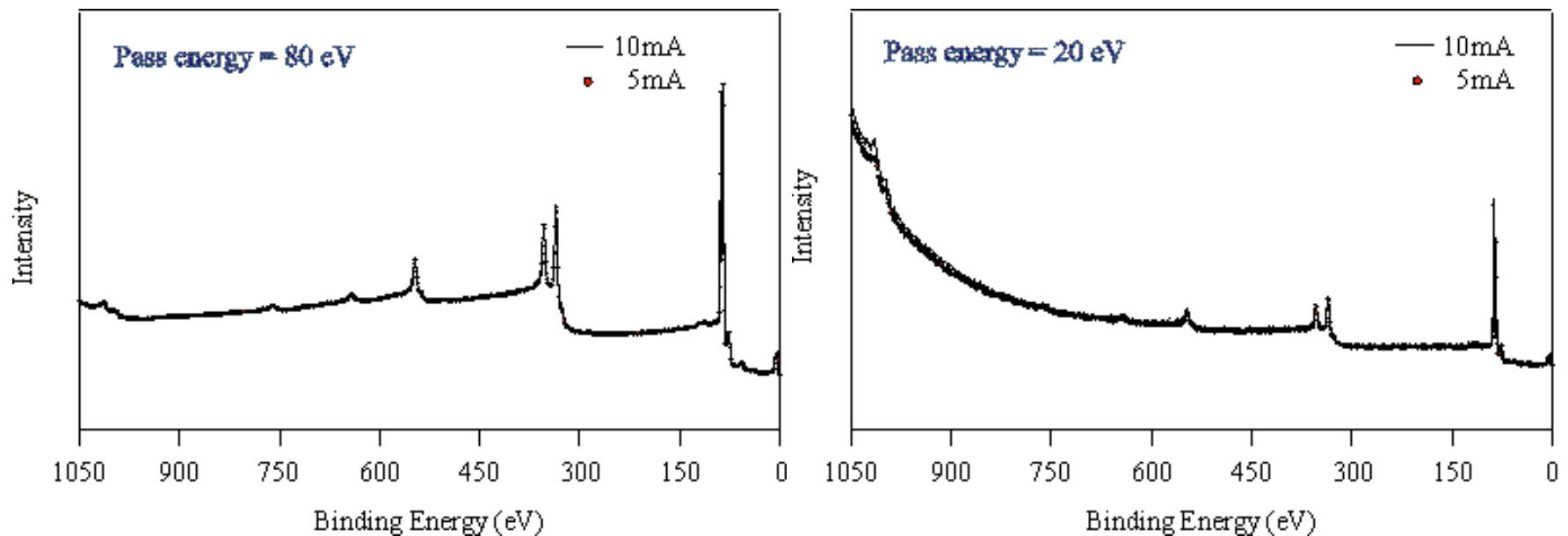
In both cases, reproducibility
(precision) better than 2%

Must include or correct for (i) x-ray satellites (ii) chemically shifted species (iii) shake-up peaks (iv) plasmon or other losses

Transmission Function

Transmission function is the detection efficiency of the electron energy analyzer, which is a function of electron energies. Transmission function also depends on the parameters of the electron energy analyzer, such as pass energy.

Pure Au after Ar⁺ sputtering



Quantitative Analysis: II

Scofield Cross-section Factors (σ_i) have been calculated for each element from scattering theory, specifically for AlK α and MgK α radiation

Inelastic Mean Free Paths (λ_i) varies with the kinetic energy of the photoelectron. It can be estimated from a “universal curve” or calculated (better).

For a multi-element surface layer consisting of elements i, j, k.

$$\frac{N_i}{N_i+N_j+N_k} = \frac{I_i}{\frac{I_i}{\sigma_i \lambda_i} + \frac{I_j}{\sigma_j \lambda_j} + \frac{I_k}{\sigma_k \lambda_k}}$$

Examples of Quantitation I

Table 1. Oxide surfaces: oxygen/metal atomic ratios determined from corresponding line intensities

Oxide and form	Oxygen/metal atomic ratios*						
	O 2s/M 2p	O 2s/M 3p	O 2s/M 3d	O 1s/M 2s	O 1s/M 2p	O 1s/M 3p	O 1s/M 3p
MgO, pelletized powder	0.95 ± 0.1	—	—	1.1 ± 0.1	1.0 ± 0.1	—	—
Al ₂ O ₃ , thin film	1.55 ± 0.1	—	—	1.5 ± 0.1	1.4 ± 0.1	—	—
SiO ₂ , several forms	1.55 ± 0.1	—	—	1.6 ± 0.1	1.6 ± 0.1	—	—
Fe ₂ O ₃ , thin film	—	1.6 ± 0.2	—	—	6.0 ± 2.0	2.2 ± 0.2	—
Cu ₂ O, thin film	0.5 ± 0.1	0.50 ± 0.1	—	—	0.5 ± 0.05	—	—
ZnO, thin film	—	—	—	—	1.8 ± 0.2	1.05 ± 0.1	—
MoO ₃ , thin film	—	—	2.95 ± 0.1	—	—	—	2.4 ± 0.1
CdO, pelletized powder	—	—	—	—	—	—	1.0 ± 0.1

* All ratios are the average of six measurements.

Examples of Quantitation II

Comparison of XPS and electron probe results for several feldspar minerals

Element	% Atomic Composition*													
	PIAG-02		PIAG-03		ALB-2		ALB-3		ANO-1		LAB-1		OLIG-1	
	XPS	EPMA	XPS	EPMA	XPS	EPMA	XPS	EPMA	XPS	EPMA	XPS	EPMA	XPS	EPMA
Silicon (Si 2p)	27.3	29.3	25.5	24.9	22.4	22.4	25.2	22.4	25.7	22.2	18.8	19.4	22.4	22.4
Aluminum (Al 2p)	11.9	12.4	15.0	15.6	8.4	8.3	9.3	8.4	7.2	8.6	11.0	11.4	8.4	8.6
Sodium (Na 2s)	5.7	6.6	2.3	3.2	4.3	7.2	8.4	6.6	4.5	6.6	4.4	3.6	7.9	6.3
Potassium (K 2p)	0.1	0.2	<0.1	0.2	<0.1	0.05	<0.1	0.12	<0.1	0.2	<0.1	0.2	<0.1	0.12
Calcium (Ca 2p)	2.2	3.7	4.9	9.0	0.6	0.6	0.9	0.8	2.1	0.9	3.1	3.9	0.8	1.0
Oxygen (O 1s)	52.8	47.8	52.3	47.1	64.3	61.5	56.2	61.8	59.4	61.6	62.8	61.6	60.5	61.7
Sum of % differences	9.0		11.5		4.7		11.5		9.1		3.9		3.0	

* Average of three determinations in the same location.

Errors in Quantitation

I_i = sometimes difficult to separate “intrinsic” photoelectrons for the “extrinsic” scattered photoelectrons which comprise the background ($\pm 5 - 100\%$)

σ_i = calculated value (unknown magnitude)

λ_i = estimated error $\pm 50\%$

Session 2

Chemical shifts in XPS

Initial and final states

Koopman's theorem

Equivalent core approximation

Calculations for binding energies and chemical shifts

Line widths and resolution

Chemical Effects in XPS

Chemical shift: change in binding energy of a core electron of an element due to a change in the chemical bonding of that element.

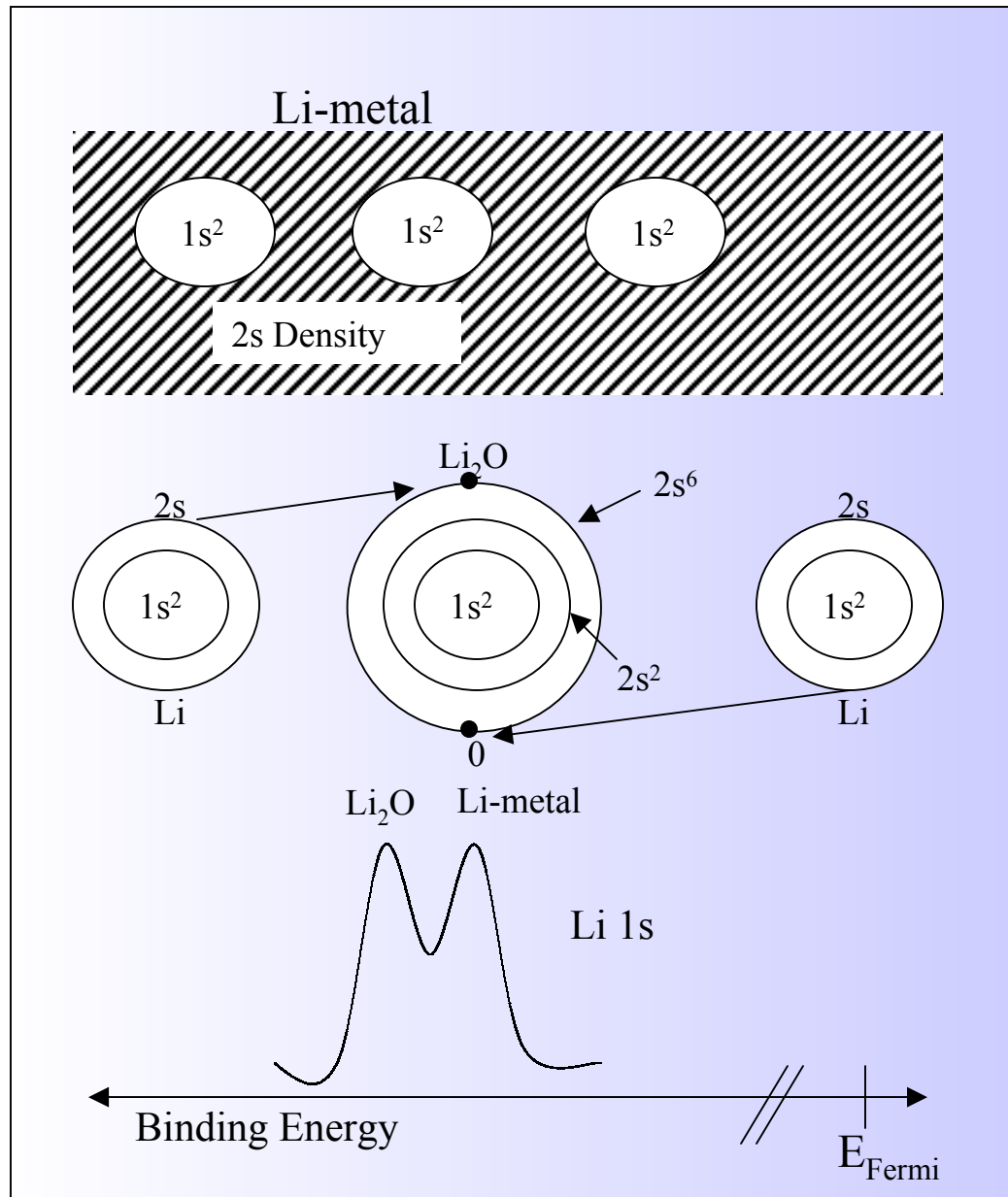
Qualitative view: Core binding energies are determined by:

- electrostatic interaction between it and the nucleus, and reduced by:
- the electrostatic shielding of the nuclear charge from all other electrons in the atom (including valence electrons)
- removal or addition of electronic charge as a result of changes in bonding will alter the shielding

Withdrawal of valence electron charge \longrightarrow increase in BE
(oxidation)

Addition of valence electron charge \longrightarrow decrease in BE

Chemical Shifts: Oxide Compared to Metal



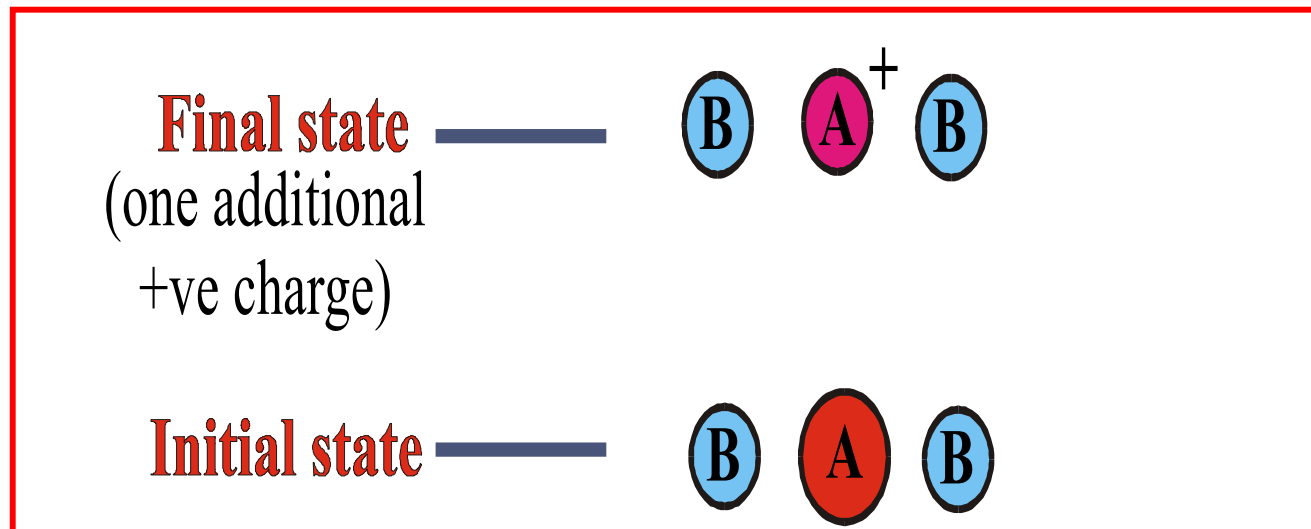
Binding Energy is lower due to increased screening of the nucleus by 2s conduction by 2s electrons

Binding Energy is higher because Li 2s electron density is lost to oxygen

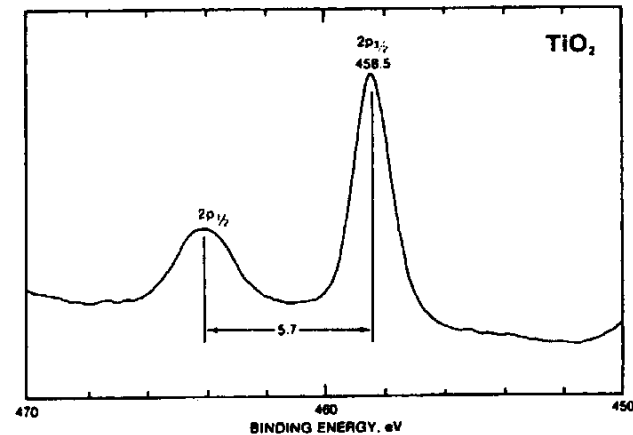
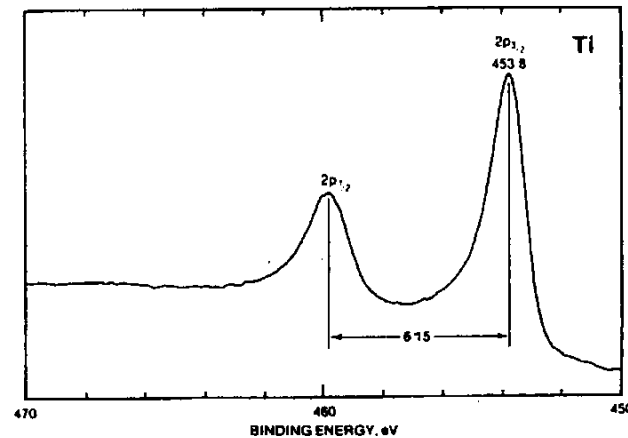
PE spectrum

Photoemission Process can be thought of as 3 steps:

- (a) Photon absorption and ionisation (initial state effects)
- (b) Response of atom and creation of photoelectron (final state effects)
- (c) Transport of electron to surface (extrinsic effects)



Usually chemical shifts are thought of as initial state effect (i.e. relaxation processes are similar magnitude in all cases)



Ti $2p_{1/2}$ and $2p_{3/2}$ chemical shift for Ti and Ti^{4+} . Charge withdrawn $\text{Ti} \rightarrow \text{Ti}^{4+}$ so 2p orbital relaxes to higher BE

Note: Spin-orbit splitting is approximately constant - confirming SOS is largely an initial state effect

Chemical shift information very powerful tool for functional group, chemical environment, oxidation state

Koopman's Theorem

The BE of an electron is simply the difference between the initial state (atom with n electrons) and final state (atom with n-1 electrons (ion) and free photoelectron)

$$BE = E_{\text{final}}(n-1) - E_{\text{initial}}(n)$$

If no relaxation* followed photoemission, $BE = -$ orbital energy, which can be calculated from Hartree Fock. *this “relaxation” refers to electronic rearrangement following photoemission – not to be confused with relaxation of surface atoms.

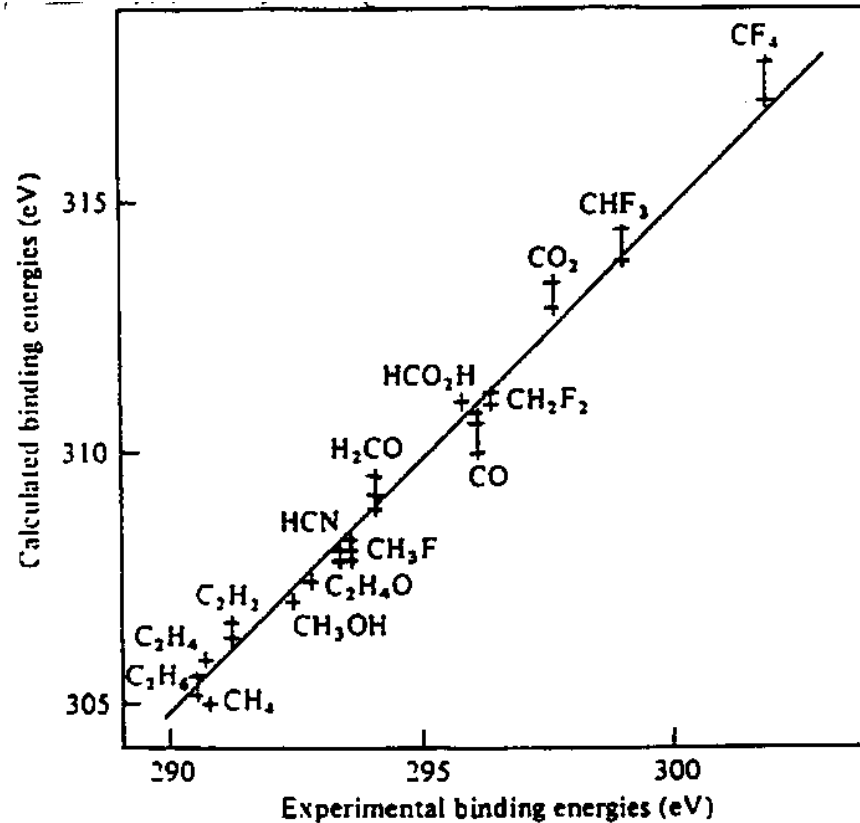


Table 3.2. Typical C_{1s} binding energies for organic samples*

Functional group		Binding energy (eV)
hydrocarbon	$C-H, \underline{C}-C$	285.0
amine	$C-N$	286.0
alcohol, ether	$\underline{C}-O-H, \underline{C}-O-C$	286.5
Cl bound to carbon	$\underline{C}-Cl$	286.5
F bound to carbon	$\underline{C}-F$	287.8
carbonyl	$\underline{C}=O$	288.0
amide	$N-\underline{C}=O$	288.2
acid, ester	$O-\underline{C}=O$	289.0
urea	$N-\overset{O}{\parallel}{\underline{C}}-N$	289.0
carbamate	$O-\overset{O}{\parallel}{\underline{C}}-N$	289.6
carbonate	$O-\overset{O}{\parallel}{\underline{C}}-O$	290.3
2F bound to carbon	$-CH_2CF_2-$	290.6
carbon in PTFE	$-CF_2CF_2-$	292.0
3F bound to carbon	$-CF_3$	293-294

*The observed binding energies will depend on the specific environment where the functional groups are located. Most ranges are ± 0.2 eV, but some (e.g., fluorocarbon samples) can be larger

Table 3.3. Typical O_{1s} binding energies for organic samples*

Functional group		Binding energy (eV)
carbonyl	$C=\underline{O}, O-C=\underline{O}$	532.2
alcohol, ether	$C-\underline{O}-H, C-\underline{O}-C$	532.8
ester	$C-\underline{O}-C=O$	533.7

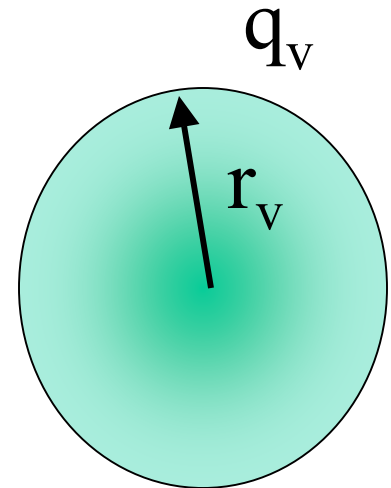
*The observed binding energies will depend on the specific environment where the functional groups are located. Most ranges are ± 0.2 eV.

The Chemical Shift: Charged Sphere Model

For a single atom j:

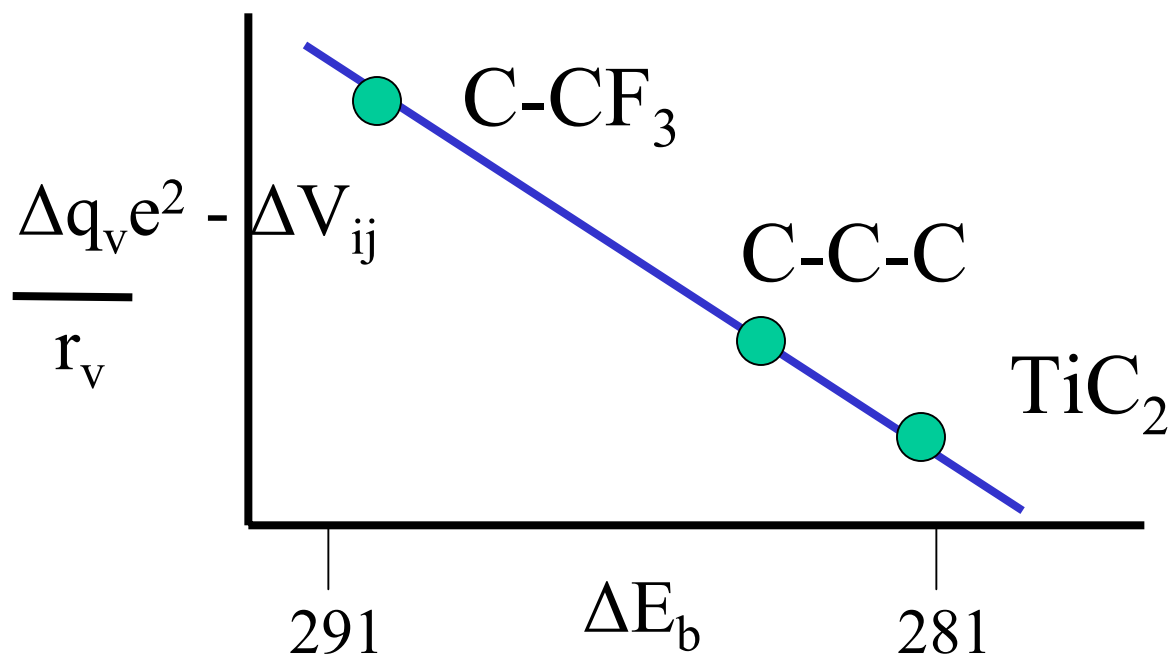
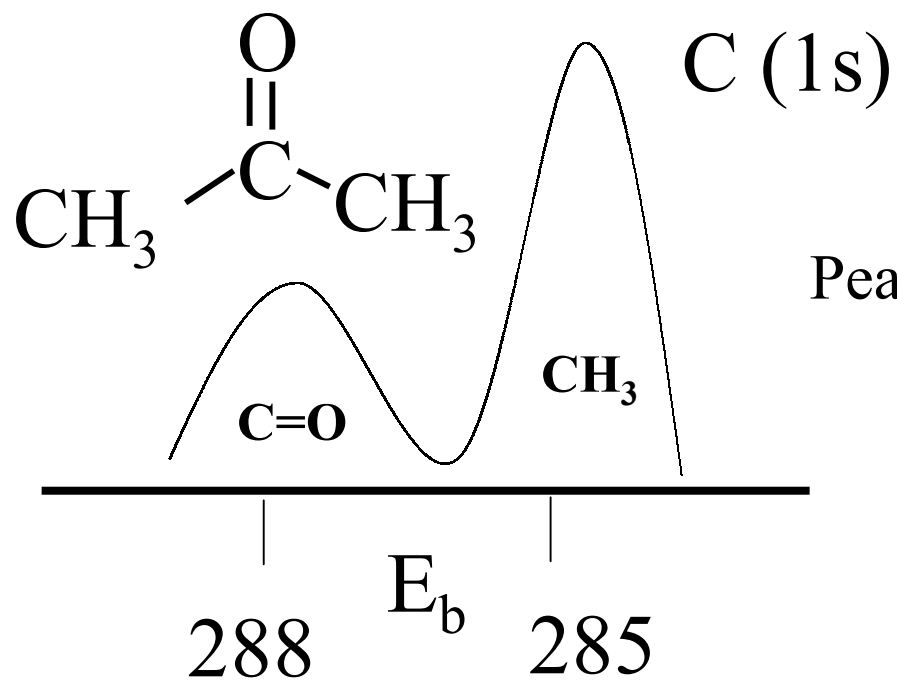
$$E = \frac{q_v e^2}{r_v} \quad \begin{array}{l} q_v = \text{no. of valence electrons} \\ r_v = \text{average radius of valence} \\ \text{electrons} \end{array}$$

$$\Delta E_b = \frac{\Delta q_v e^2}{r_v}$$

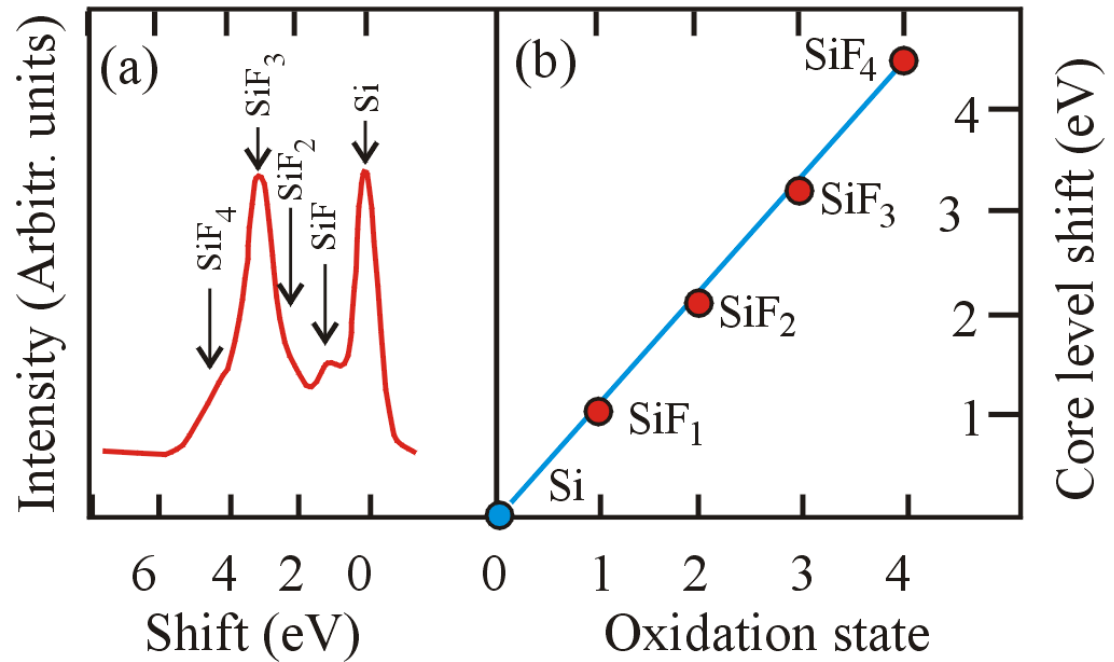
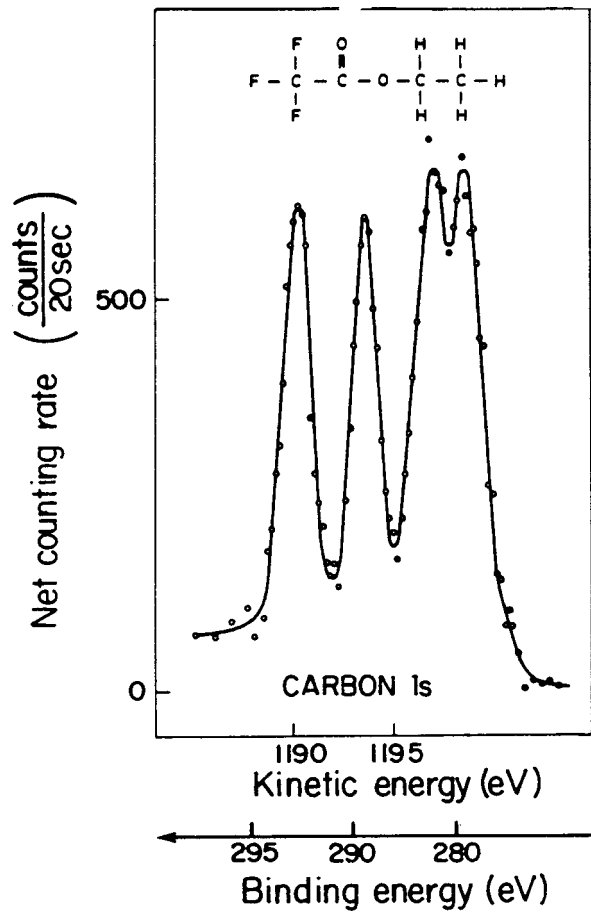


Add change in interatomic potential

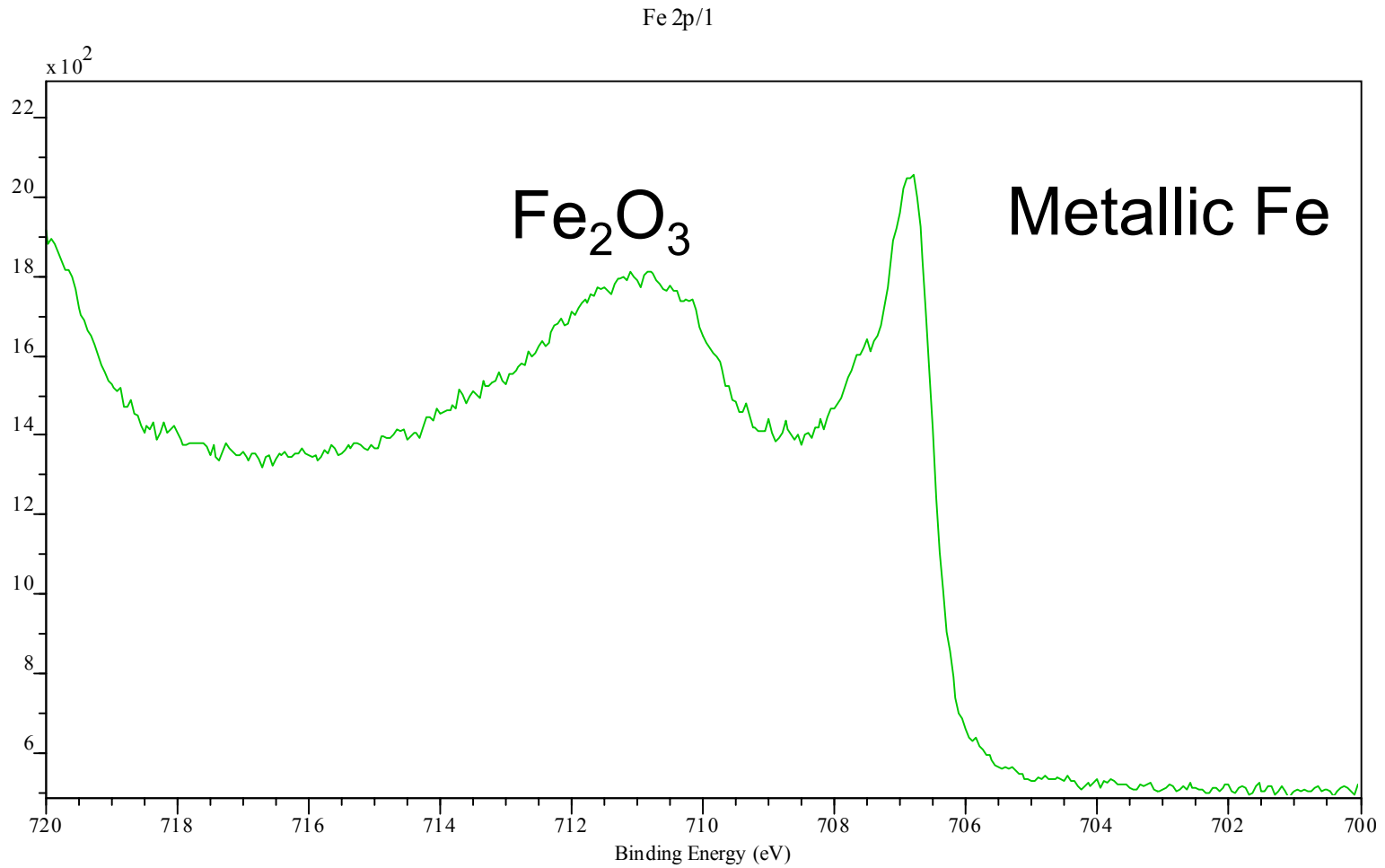
$$E_b = \frac{\Delta q_v e^2}{r_v} - \Delta V_{ij} \quad \text{where } V_{ij} = \text{potential of atom } i \text{ on } j$$



Examples of Chemical Shifts

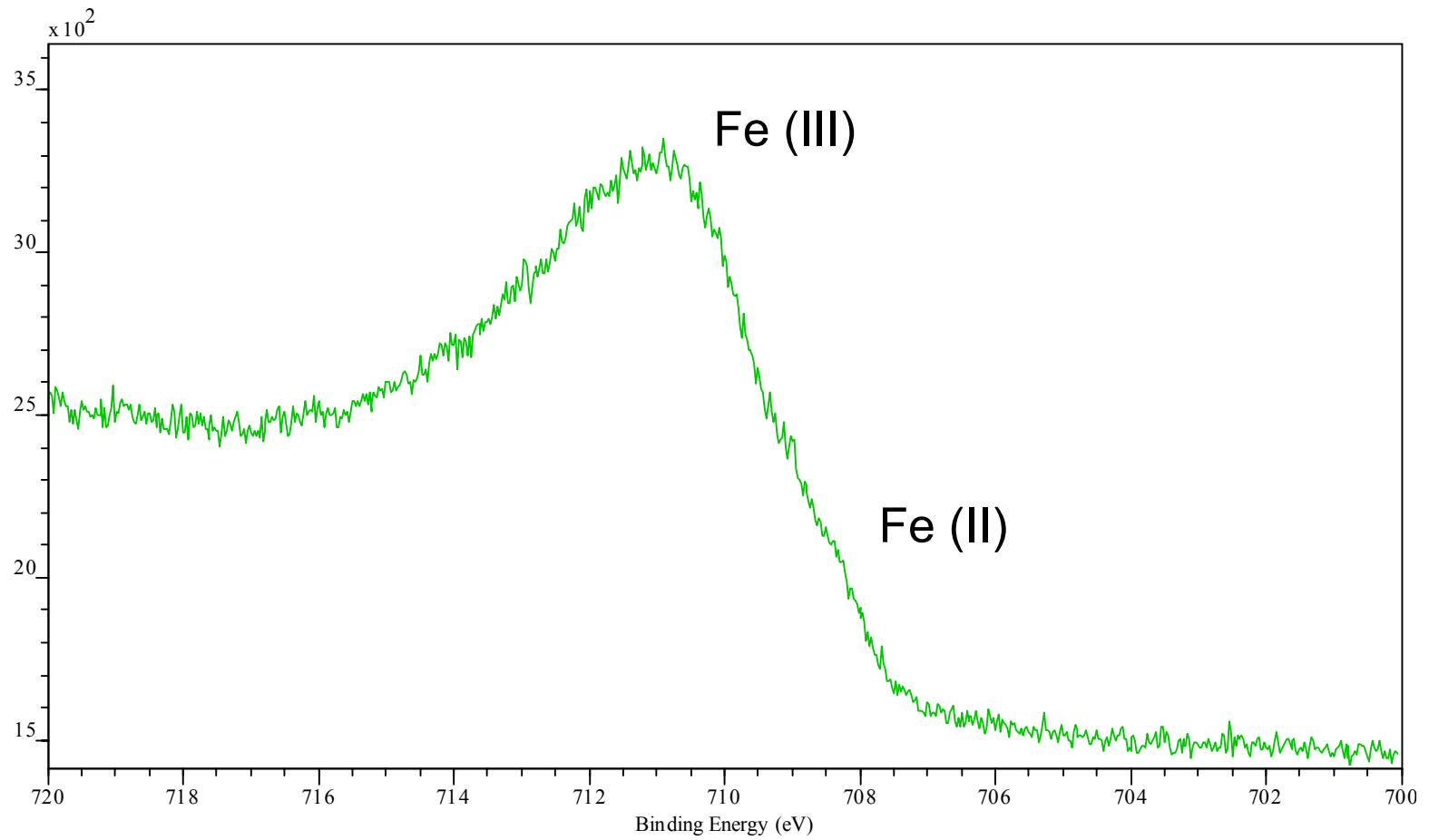


Detailed Iron 2p Spectrum of High Purity Iron

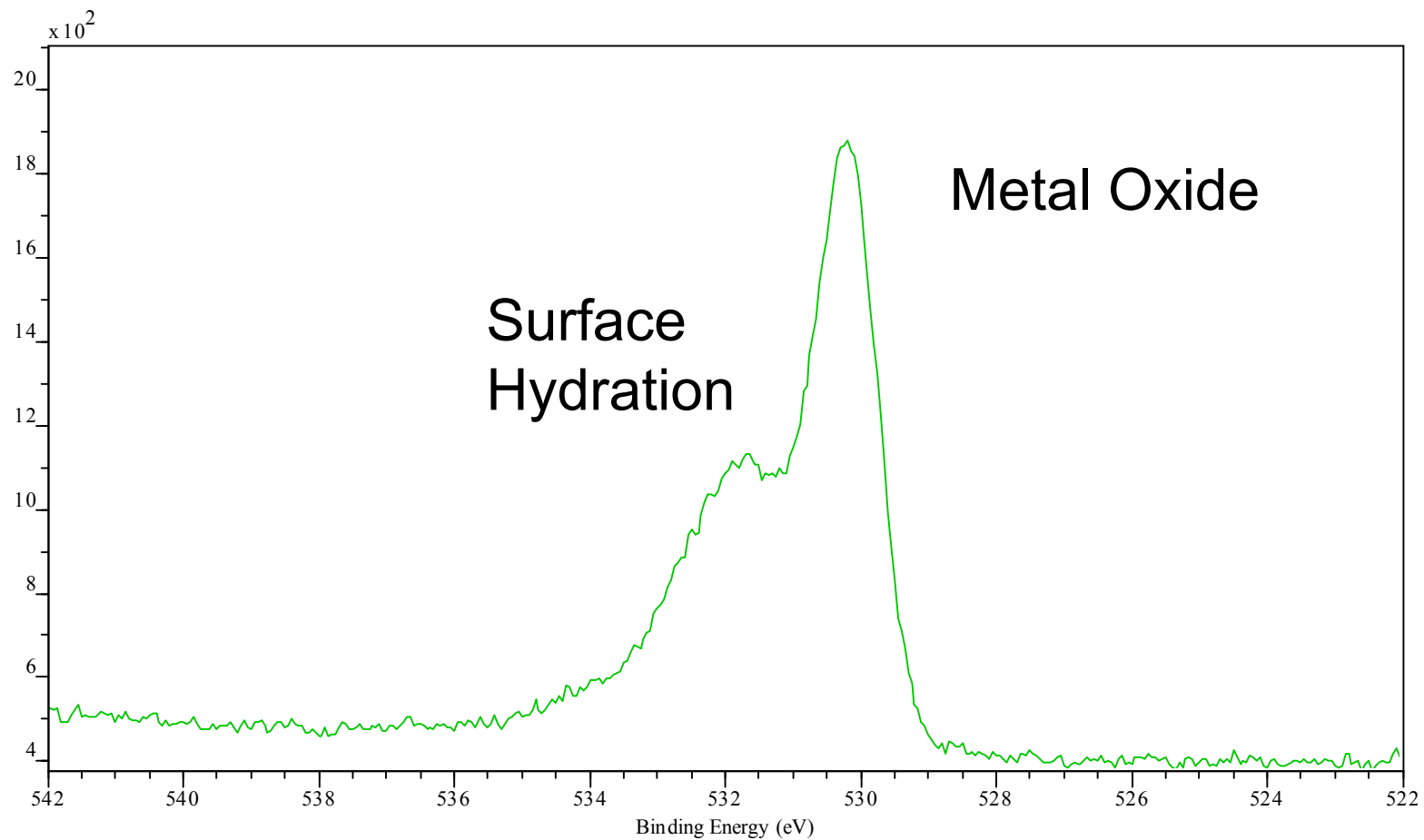


Detailed Spectrum of Fe 2p line for Magnetite (partly oxidized)

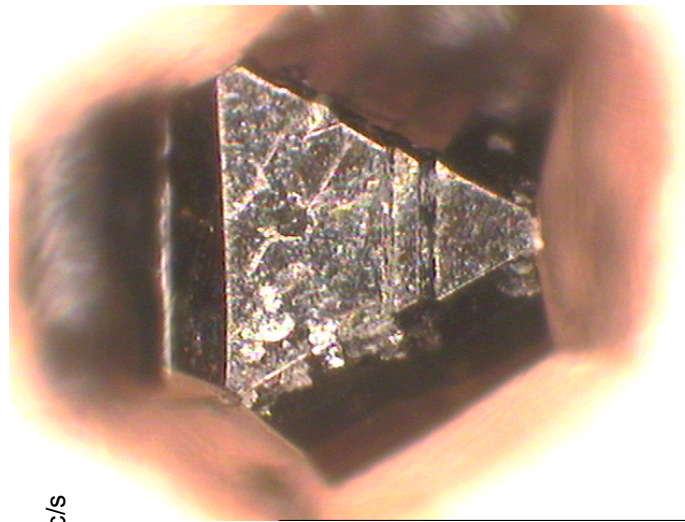
Fe 2p_HSS2_3/33



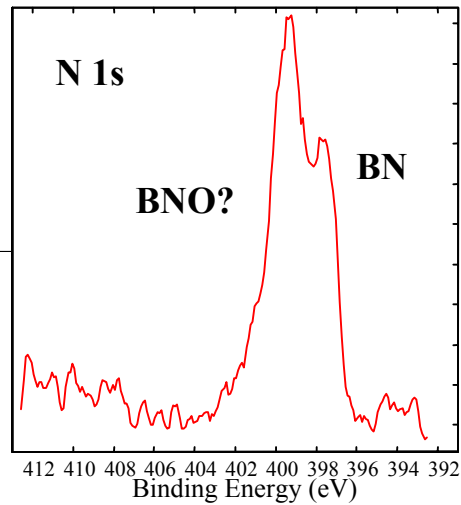
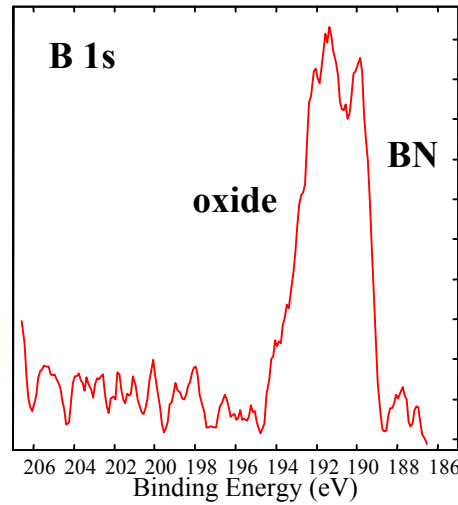
Detailed Oxygen 1s Spectrum



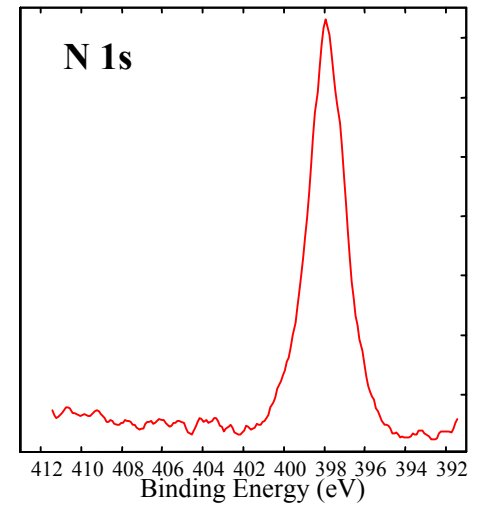
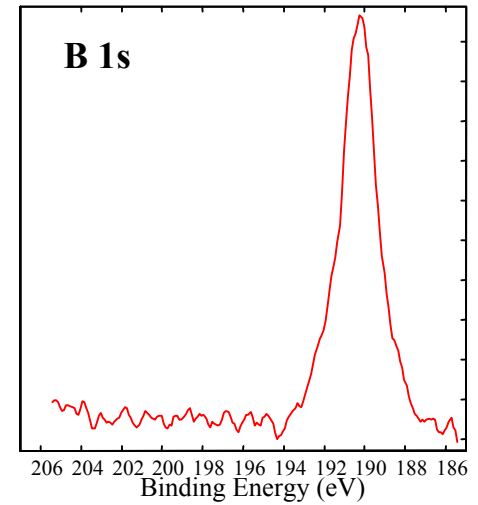
Cubic-BN Crystal



**Before
sputtering**

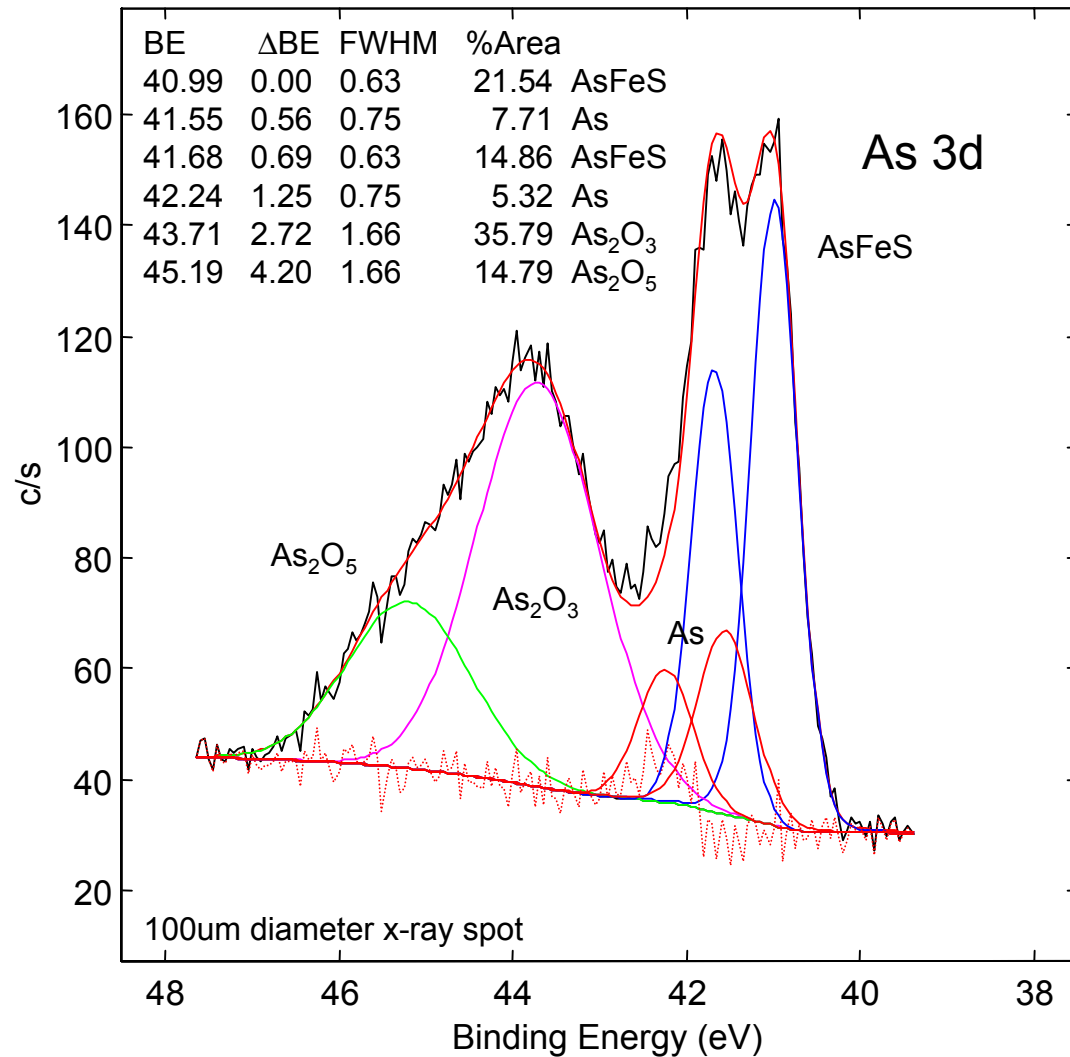


**After 200eV
Ar⁺ sputtering**

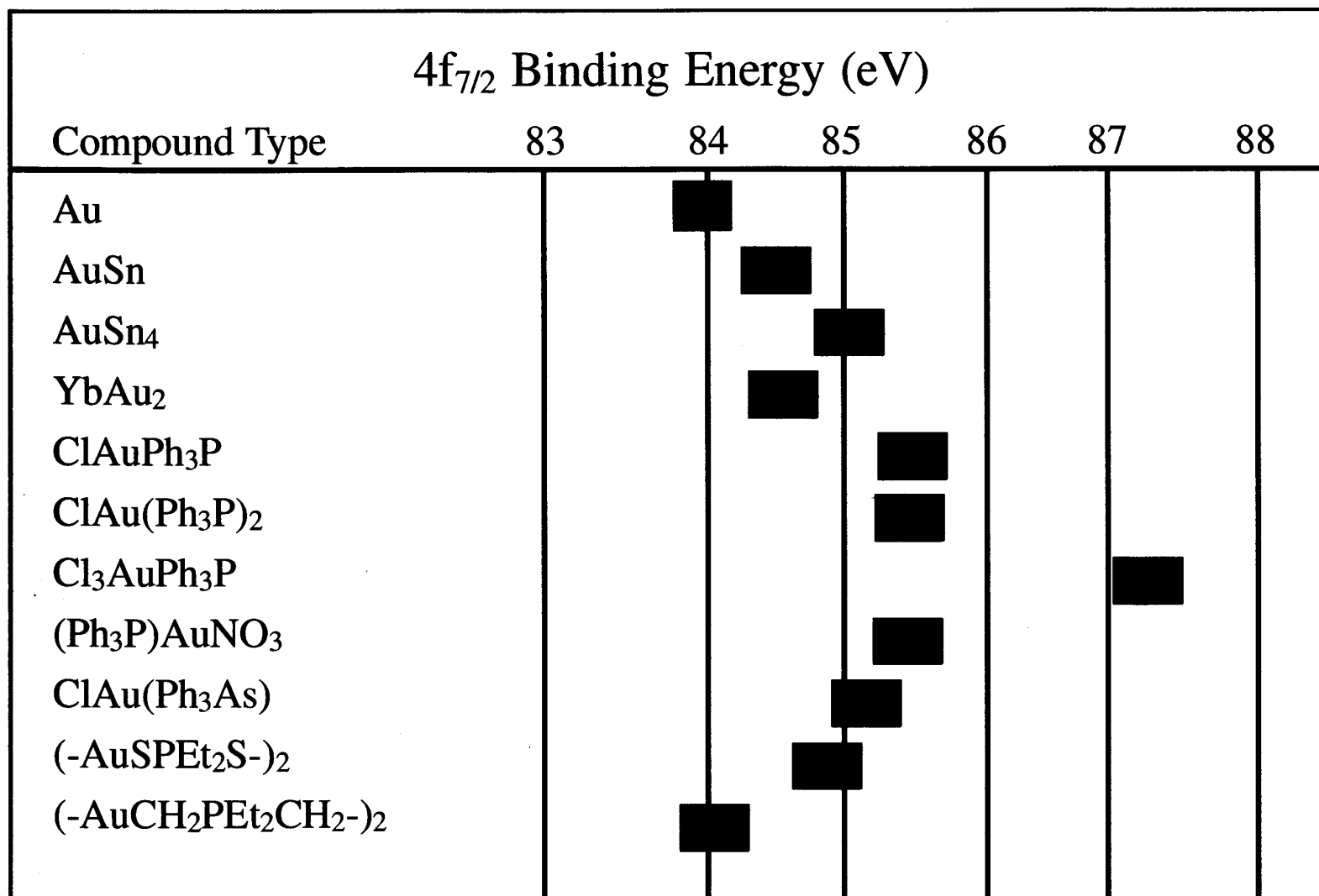


High Resolution Spectra

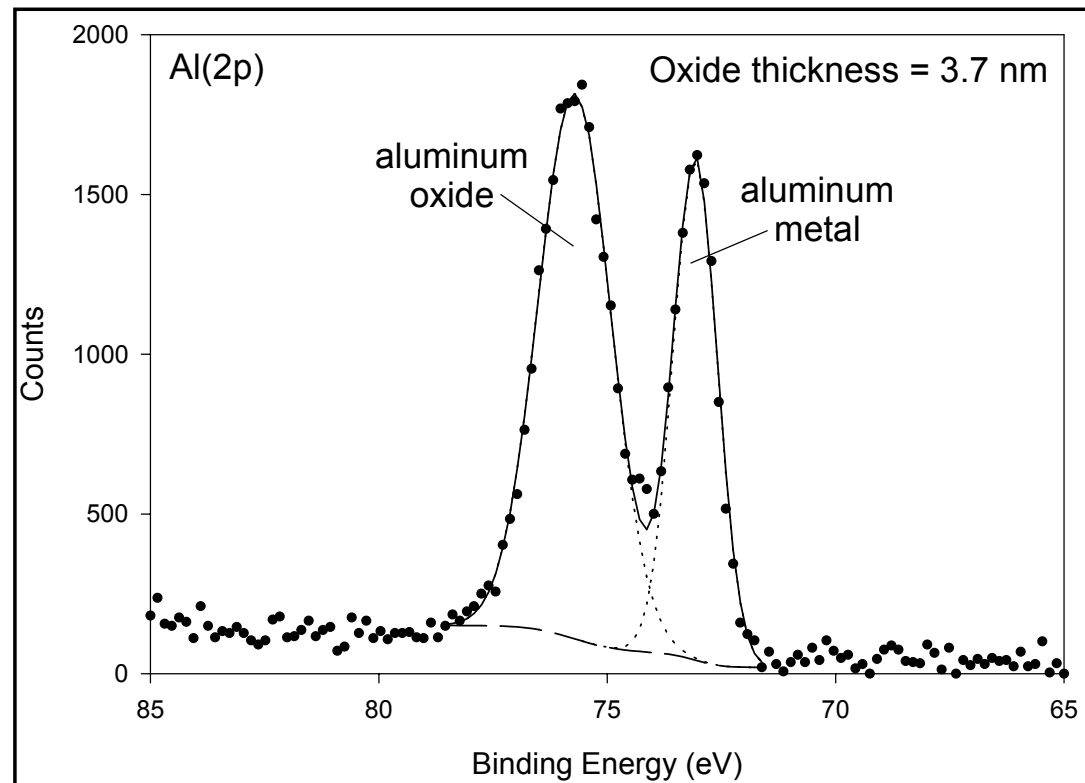
Arsenopyrite



Chemical Shift



Aluminum Oxide Thickness



High resolution Al (2p) spectrum of an aluminum surface. The aluminum metal and oxide peaks shown can be used to determine oxide thickness, in this case 3.7 nanometres.

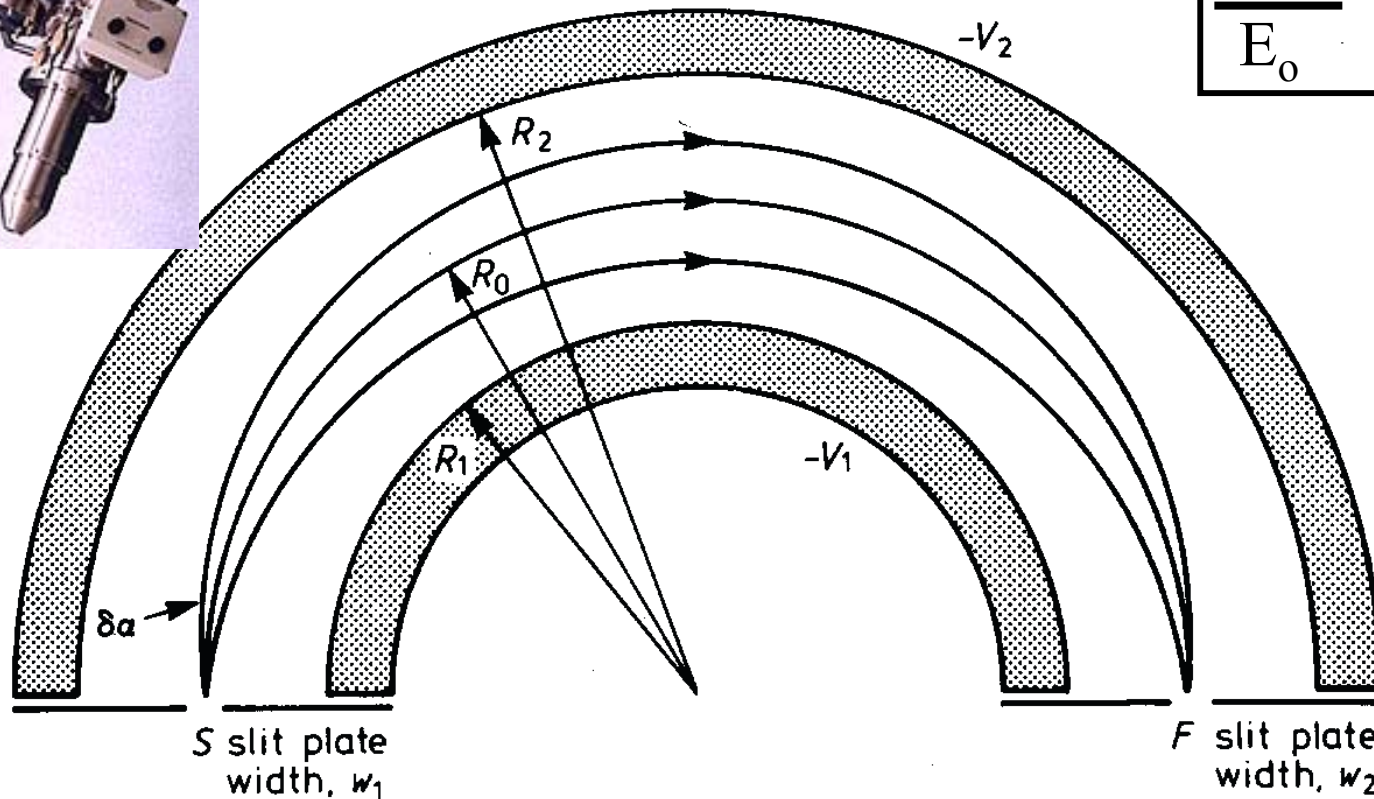
Estimation of Oxide Thickness

- Usually, the binding energies of the oxide and the metallic species are separated by a few electron volts.
- Thus, when the oxide is thin (< 9 nm), it is possible to distinguish the contribution from both oxide and metal photoelectrons.
- For aluminum, oxide thickness (d) is given as:
 - d (nm) = $2.8 \ln ((1.4(I_o/I_m))+1)$
 - where I_o and I_m are the intensities (peak areas) of the oxide and metal photoelectron peaks respectively.

Instrumentation

Electron Energy Analyzer

Concentric hemispherical analyzer (CHA)



For an electron of energy E_0 at S

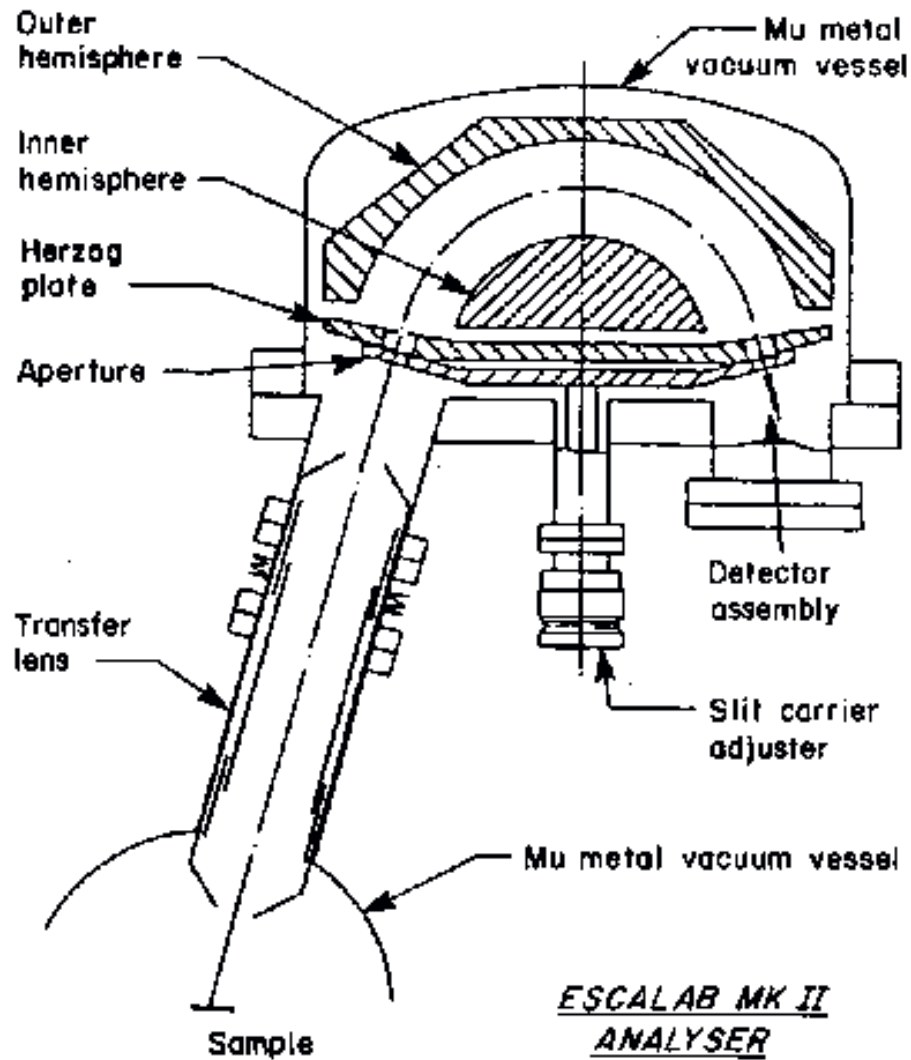
$$\frac{\Delta E}{E_0} = 0.63 \frac{\overline{w_1}}{R_0}$$

Pass Energies and Transfer Lens

(1) To resolve a 1000 eV electron to ± 0.5 eV would require an analyser with $w=1$ mm and $R=1.2$ metres!

Therefore, it is convenient to retard the energy of the incoming electrons so that they have a lower (and constant) energy as they pass through the analyser.

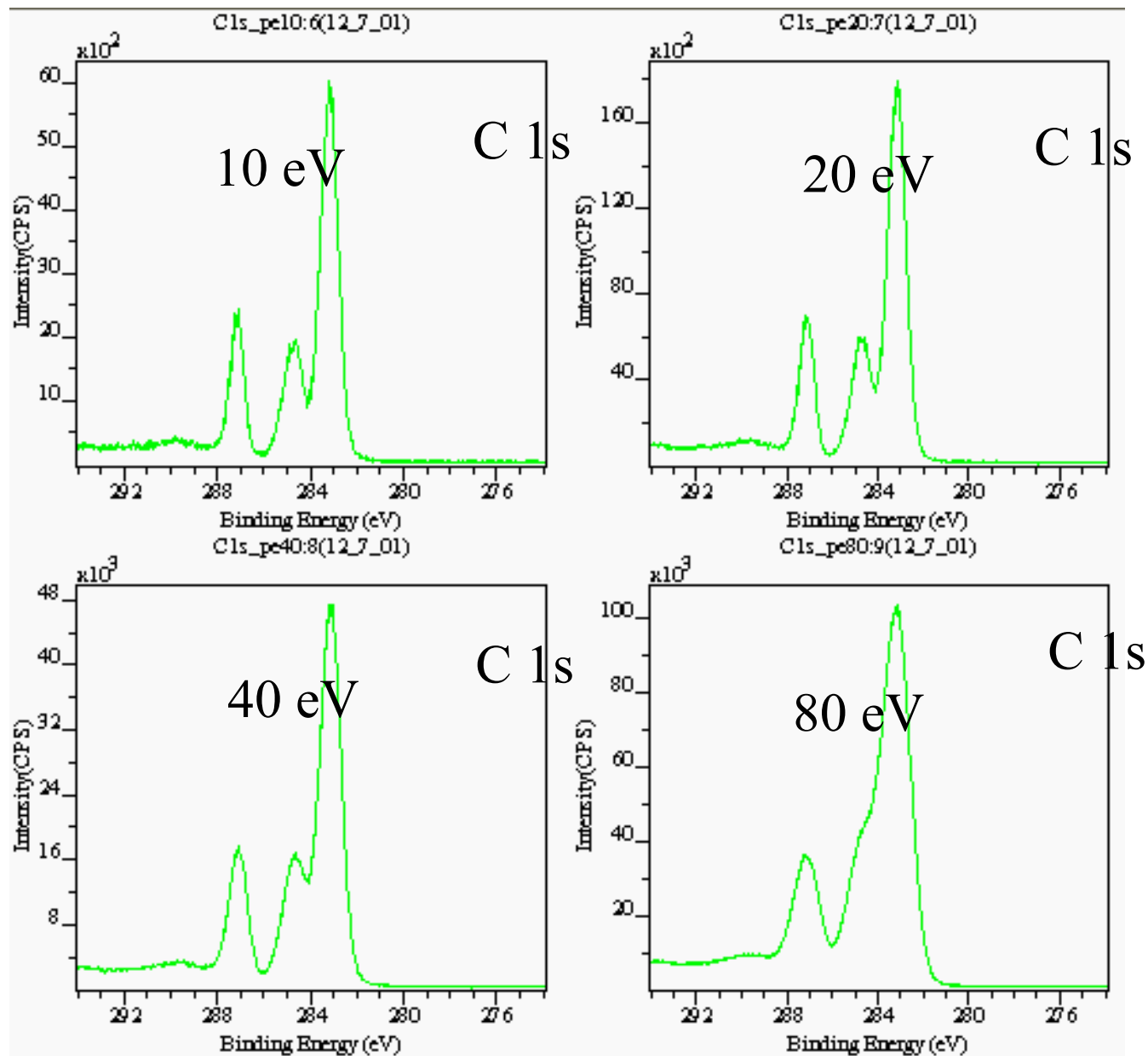
The lens system which retards the electron energy also **focuses** the electrons energy from the sample to increase the throughput.



Factors

- Pass energy
- Analyzer radius
- Slit width
- Elements in the transfer lens
- Energy of the photoelectrons

PET : Polyethylene terephthalate



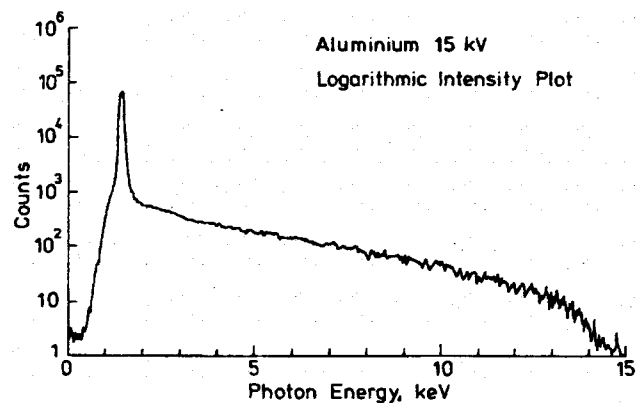
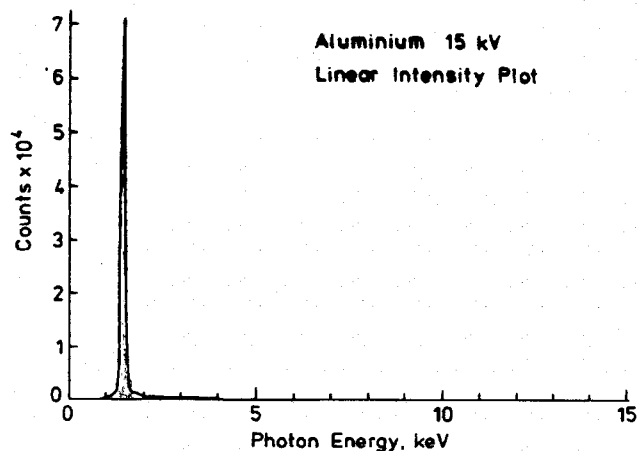
Different
Pass Energies
10-80 eV

CHA Analysers – Operating Modes

- “CAT” Retardation Mode: Constant Analyser Transmission
- Characteristics:
 - Constant Pass Energy across spectrum, therefore fixed resolution across spectrum
 - Easier quantitation since transmission is fixed
 - However, fixed transmission works against high KE photoelectrons since most electrons here are scattered
 - narrow acceptance angle
 - Pass Energy \propto “Entendue”

CRR Mode – Constant Retarding Ratio, not used for XPS

Satellite peaks

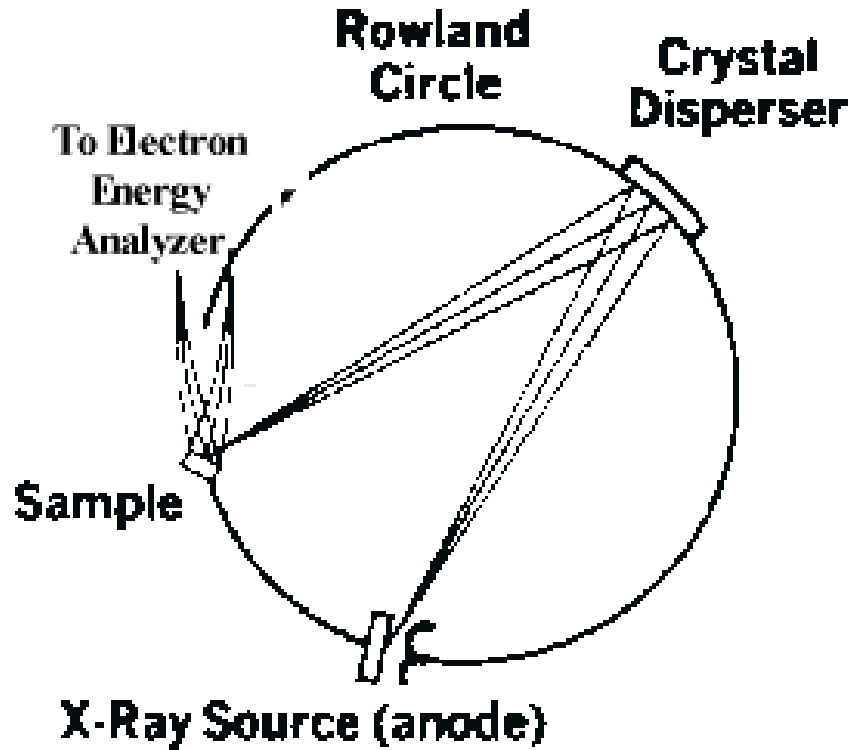


High energy satellite lines from magnesium and aluminium targets

Separation from $K\alpha_{1,2}$ (eV) and relative intensity ($K\alpha_{1,2} = 100$)

X-ray line	Mg	Al
$K\alpha'$	4.5(1.0)	5.6(1.0)
$K\alpha_3$	8.4(9.2)	9.6(7.8)
$K\alpha_4$	10.0(5.1)	11.5(3.3)
$K\alpha_5$	17.3(0.8)	19.8(0.4)
$K\alpha_6$	20.5(0.5)	23.4(0.3)
$K\beta$	48.0(2.0)	70.0(2.0)

X-ray monochromator



$$n\lambda = 2d\sin\theta$$

For Al K_{α}

$$\lambda = 8.3\text{\AA}$$

use $(10\bar{1}0)$ planes
of quartz crystal

$$d = 4.25\text{\AA}$$

$$\theta = 78.5^{\circ}$$

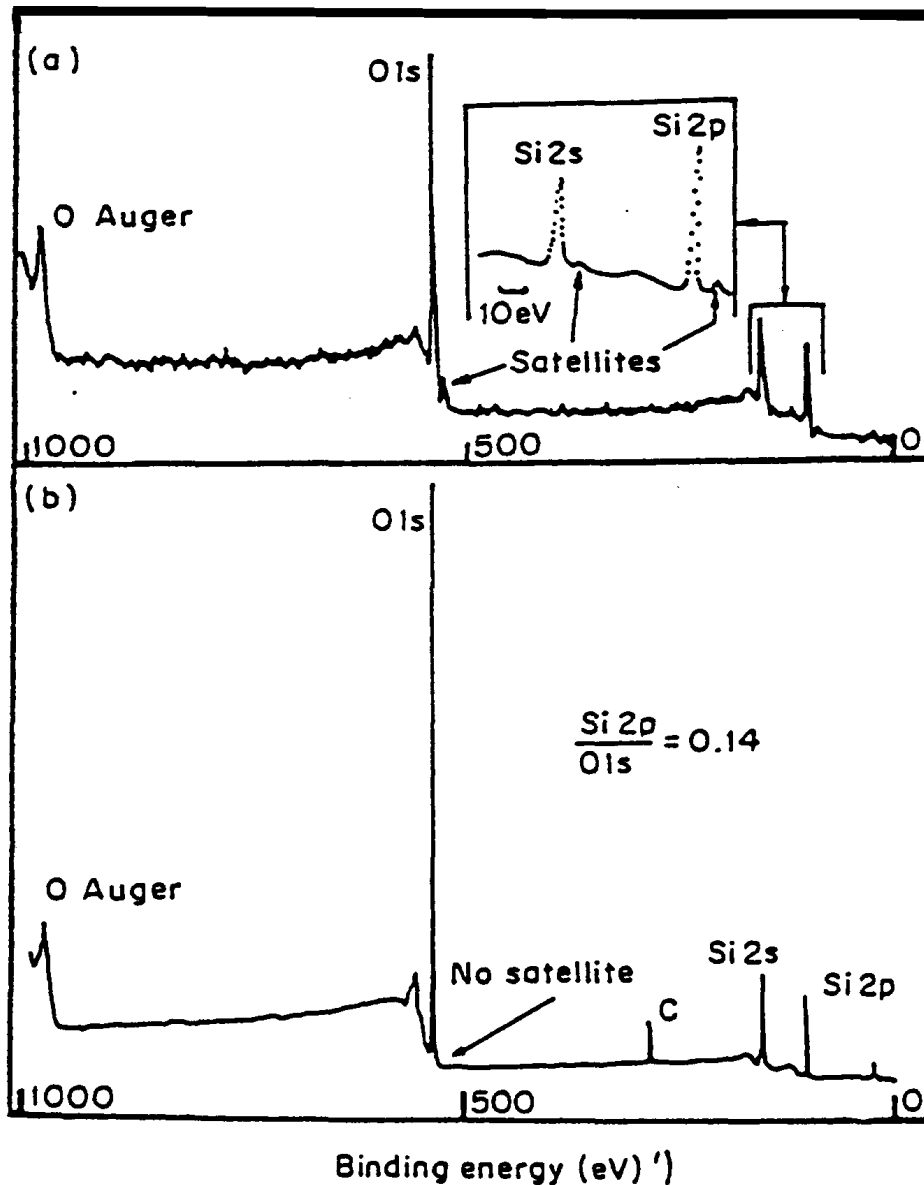
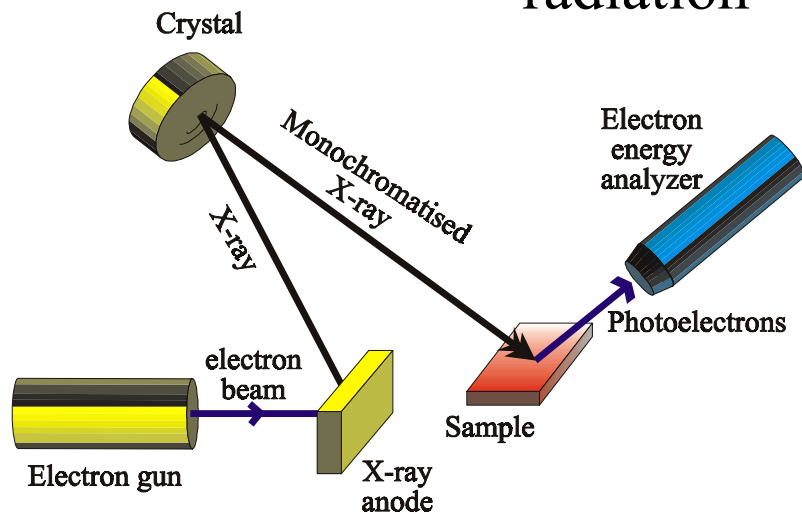
Advantages of using X-ray monochromator

- Narrow peak width
- Reduced background
- No satellite & Ghost peaks

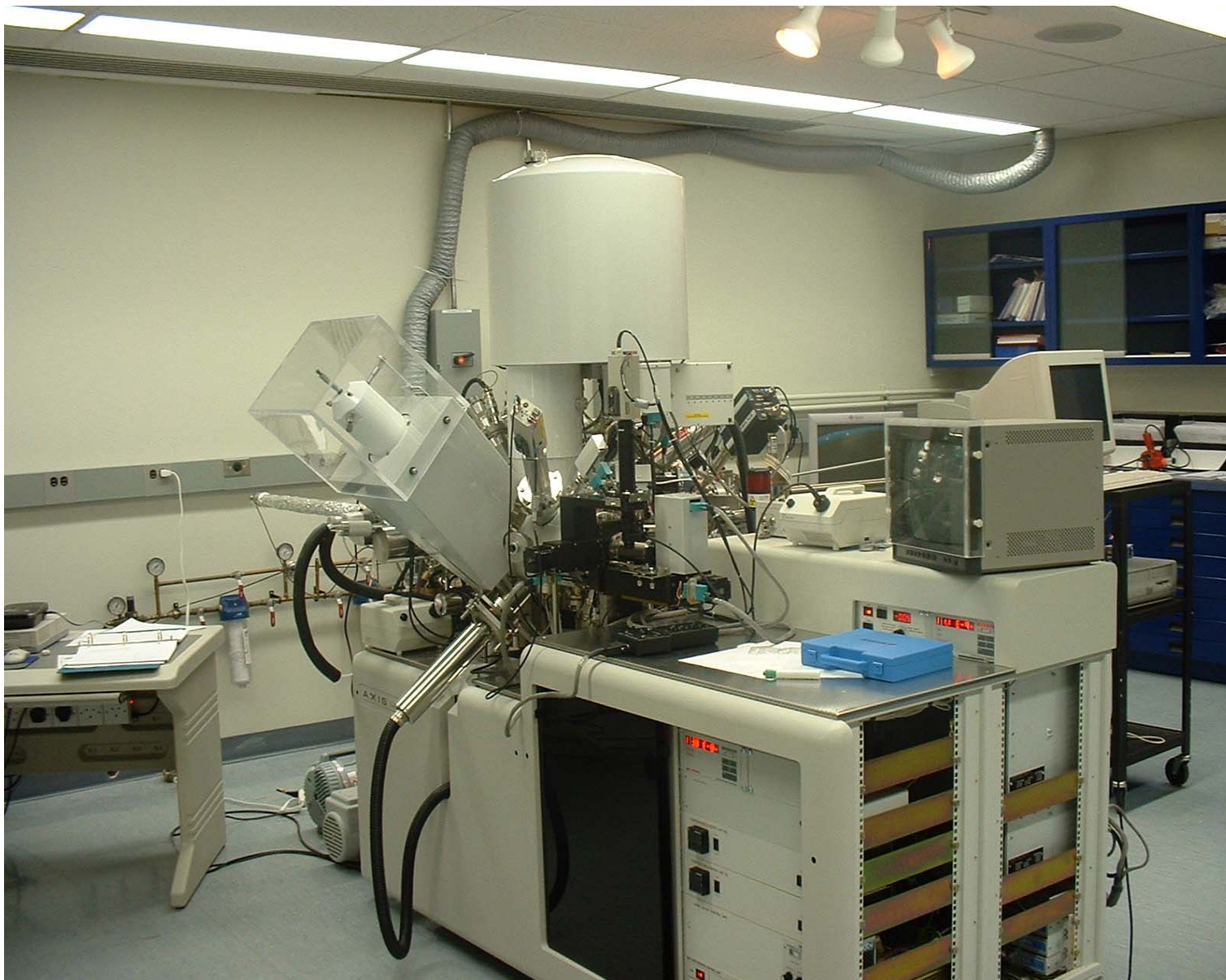
Photoelectron spectra of SiO₂ excited with Al K_α radiation

Unfiltered radiation

Monochromatized radiation



Kratos Axis Ultra at SSW



Photoelectron Line Widths

Contributions to width

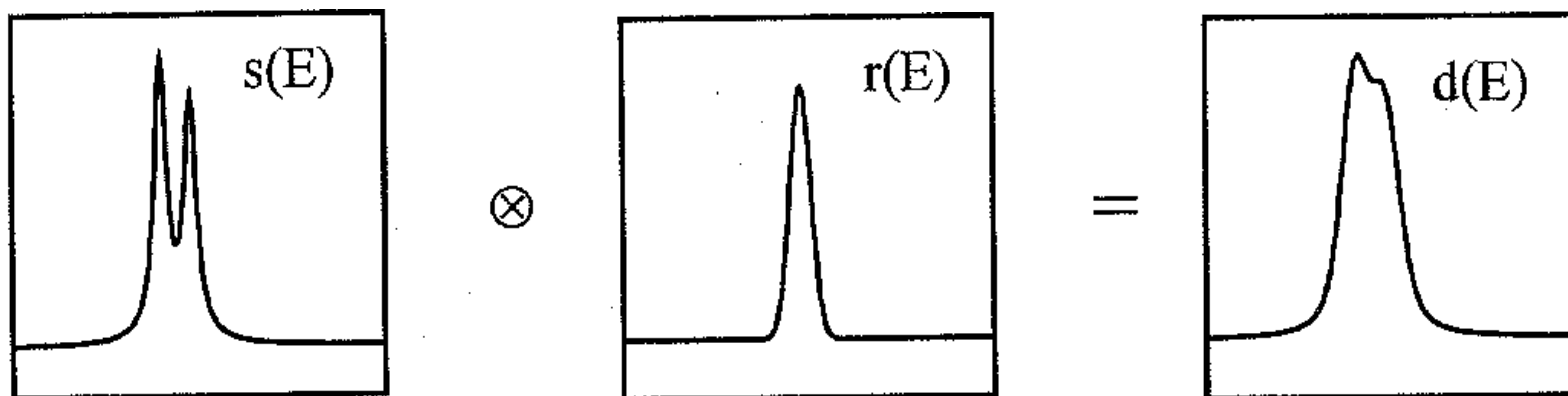
1. Inherent linewidth of the photoelectron production event
 - lifetime-dependent
 - temperature-dependent
 - Lorentzian-shape
2. Width of Exciting line
 - $\text{MgK}\alpha < \text{AlK}\alpha$
 - Monochromatised $\text{AlK}\alpha$ is better. Two component shape is modelled as a Gaussian
3. Analyser Resolution – determined by pass energy and slit width, modelled as a “box” function.

X-ray lines

Commonly used

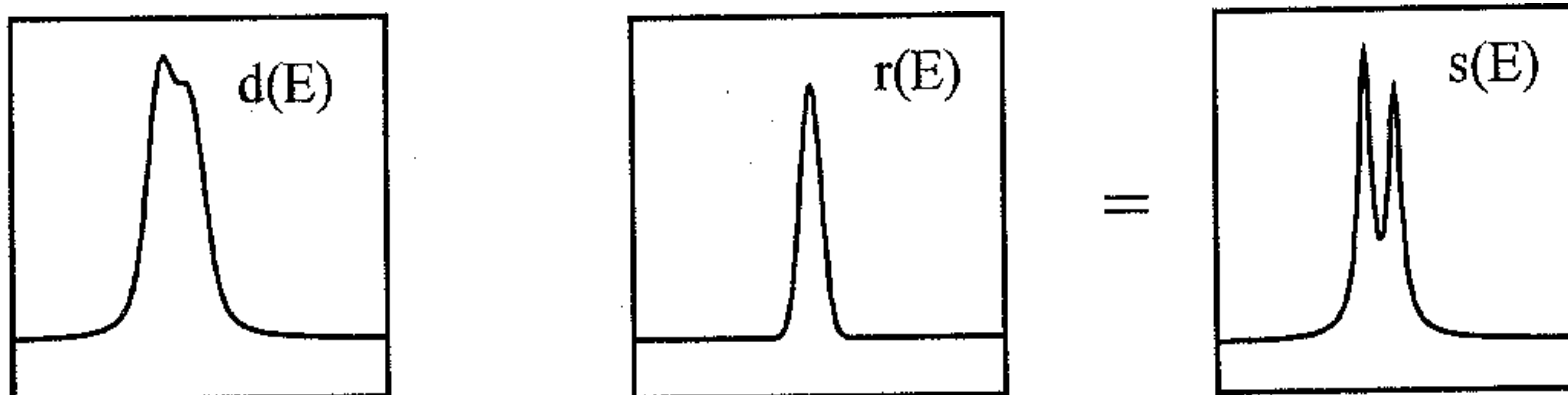
Line	Energy, eV	Width, eV
Y $M\zeta$	132.3	0.47
Zr $M\zeta$	151.4	0.77
Nb $M\zeta$	171.4	1.21
Mo $M\zeta$	192.3	1.53
Ti $L\alpha$	395.3	3.0
Cr $L\alpha$	572.8	3.0
Ni $L\alpha$	851.5	2.5
Cu $L\alpha$	929.7	3.8
Mg $K\alpha$	1253.6	0.7
Al $K\alpha$	1486.6	0.85
Si $K\alpha$	1739.5	1.0
Y $L\alpha$	1922.6	1.5
Zr $L\alpha$	2042.4	1.7
Ti $K\alpha$	4510.0	2.0
Cr $K\alpha$	5417.0	2.1
Cu $K\alpha$	8048.0	2.6

Analytical Methods



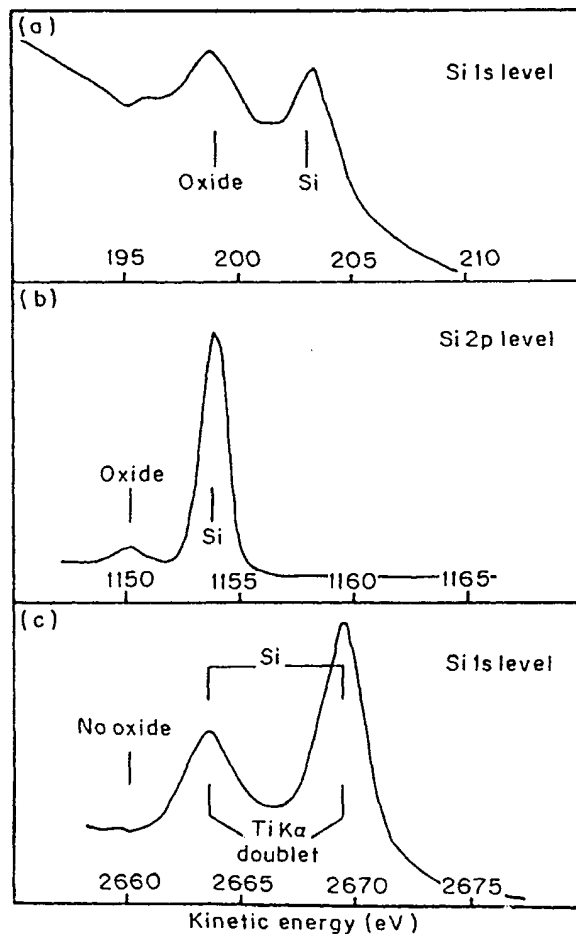
Convolution

How to obtain high-resolution XPS spectra?



Deconvolution

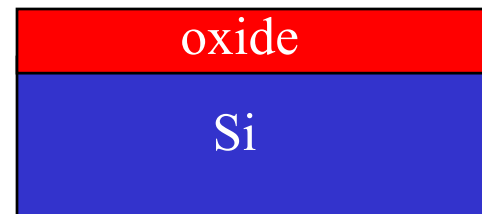
The Use of Different Photon Energy



(a) ZrL α 2040 eV

(b) Mg K α 1253.6 eV

(c) Ti K α 4510 eV



SESSION 3

Energy losses: extrinsic and intrinsic

Electron attenuation: inelastic scattering

Interpretive models: QASES

Plasmon losses, shake-up and shake-off satellites

Multiplet interactions

Depth profiling

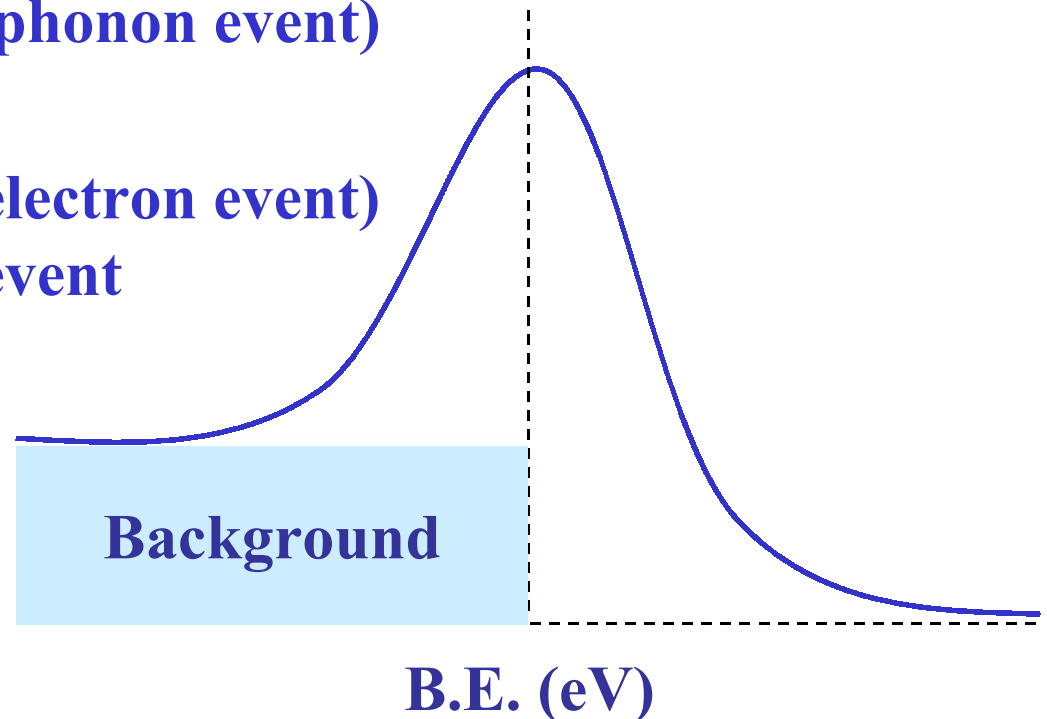
Intrinsic and Extrinsic Losses

--- Variation of Al2p energy loss structure

Origins of the XPS background

- Extrinsic losses (electron-phonon event)
inelastic scattering
- Intrinsic losses (electron-electron event)
A part of photoemission event
Alternative final states

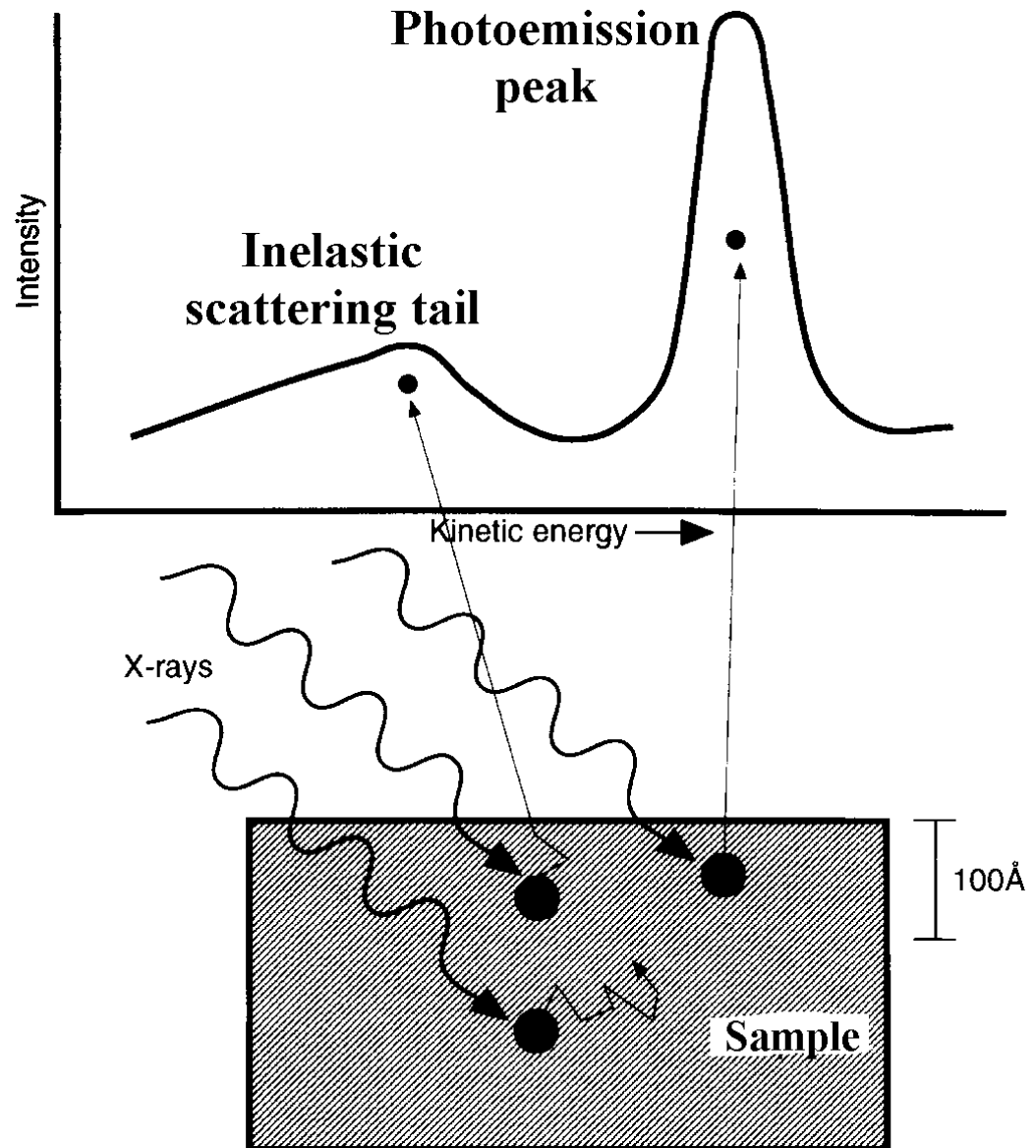
Why study intrinsic backgrounds?



- Information about the depth and lateral distributions of elements using the QUASES method developed by Sven Tougaard

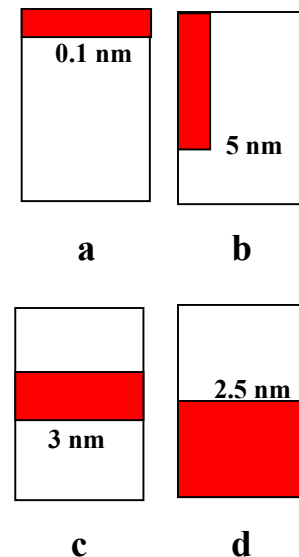
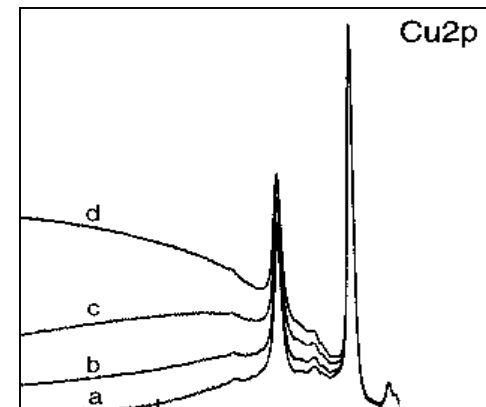
Inelastic Scattering Background

Tougaard developed a fitting procedure for the inelastic scattering tail, which may give some information about the structure of the surface layer, such as, complete coverage by a metal layer or formation of metal clusters.



Analysis of XPS Spectra Using QUASES

- Traditional XPS quantification assumes
 - Outer surface of sample is homogeneous
 - Outer surface concentration is directly proportional to the peak intensity
- More accurate quantification should include peak intensity, peak shape and background energy
- In photoelectron spectroscopy electrons detected result from two processes
 - the *intrinsic electrons* – from photoelectron process
 - the *extrinsic electrons* – from scattering of photoelectrons passing through surrounding atoms
- Depending on the depth of the emitting atom within the surface, as well as its lateral distribution, the extrinsic portion will change dramatically
- The figure shows a theoretical calculation of the extrinsic portion of a copper 2p spectrum as a function of the position and distribution of the emitting copper atoms within a matrix of another element

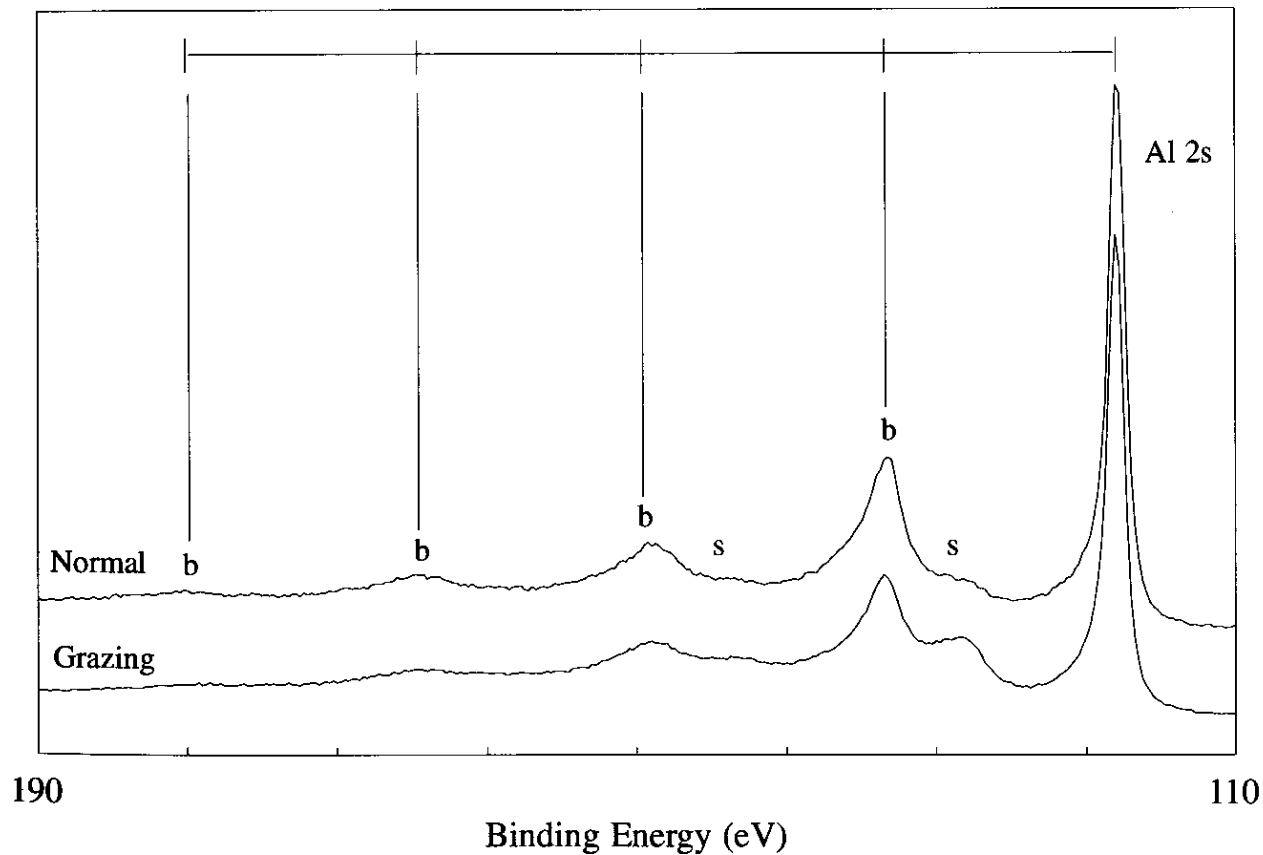


The above example courtesy of www.quases.com

Plasmon Loss Peaks

For some materials, there is an enhanced probability for loss of a specific amount of energy due to interaction between the photoelectron and other electrons.

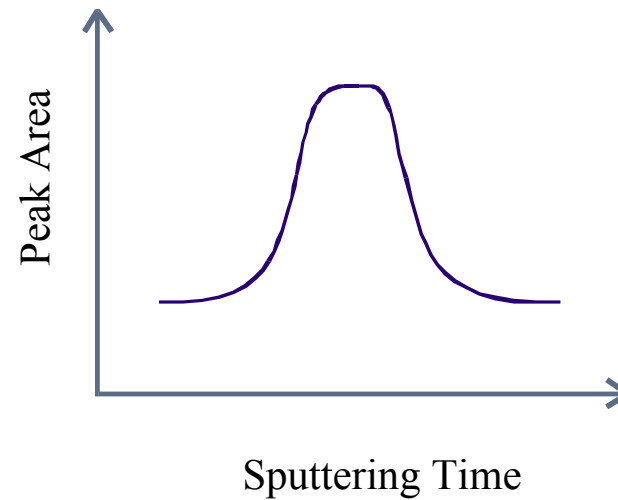
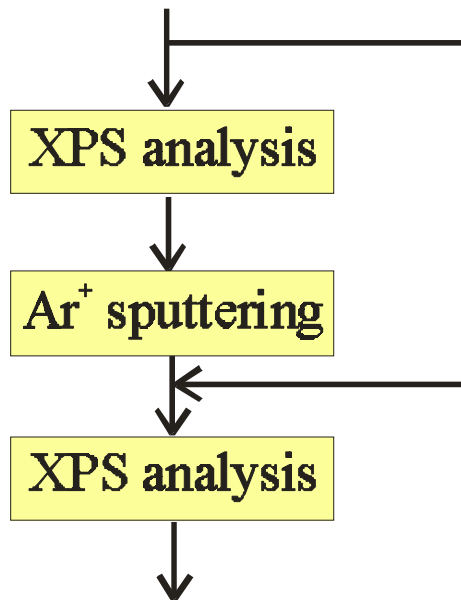
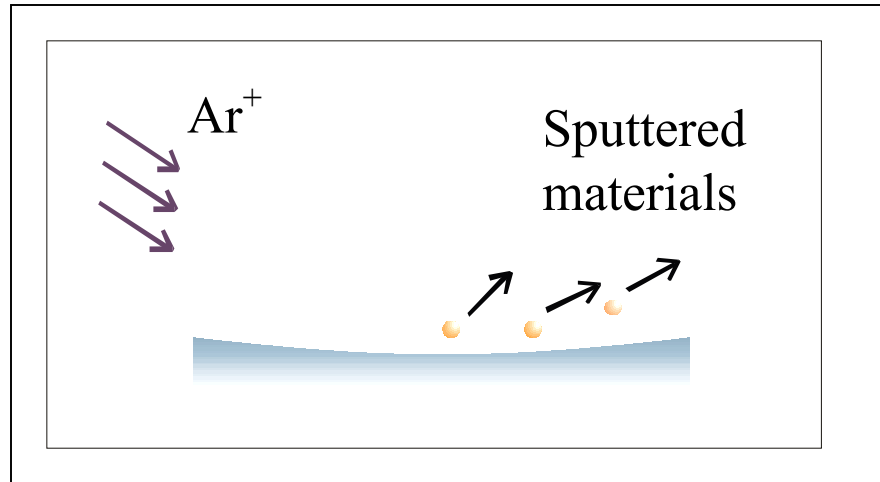
Al 2s spectrum of sapphire (Al_2O_3)

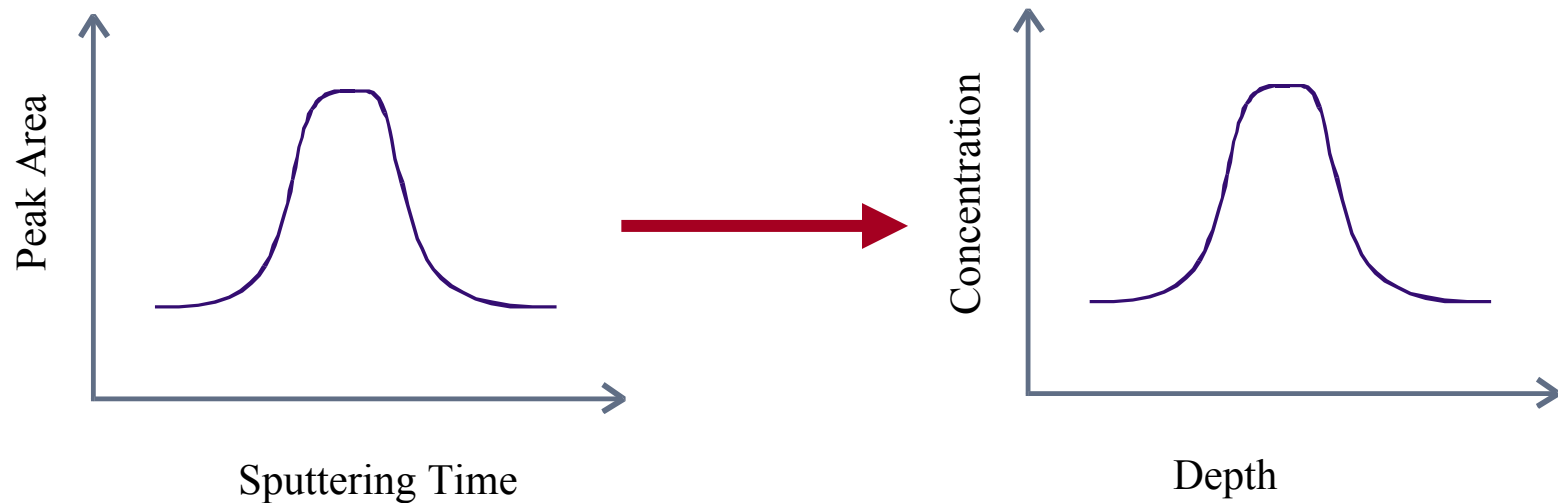


S: surface plasmon
B: bulk plasmon

Some photoelectrons lose more than once

Depth Profiling

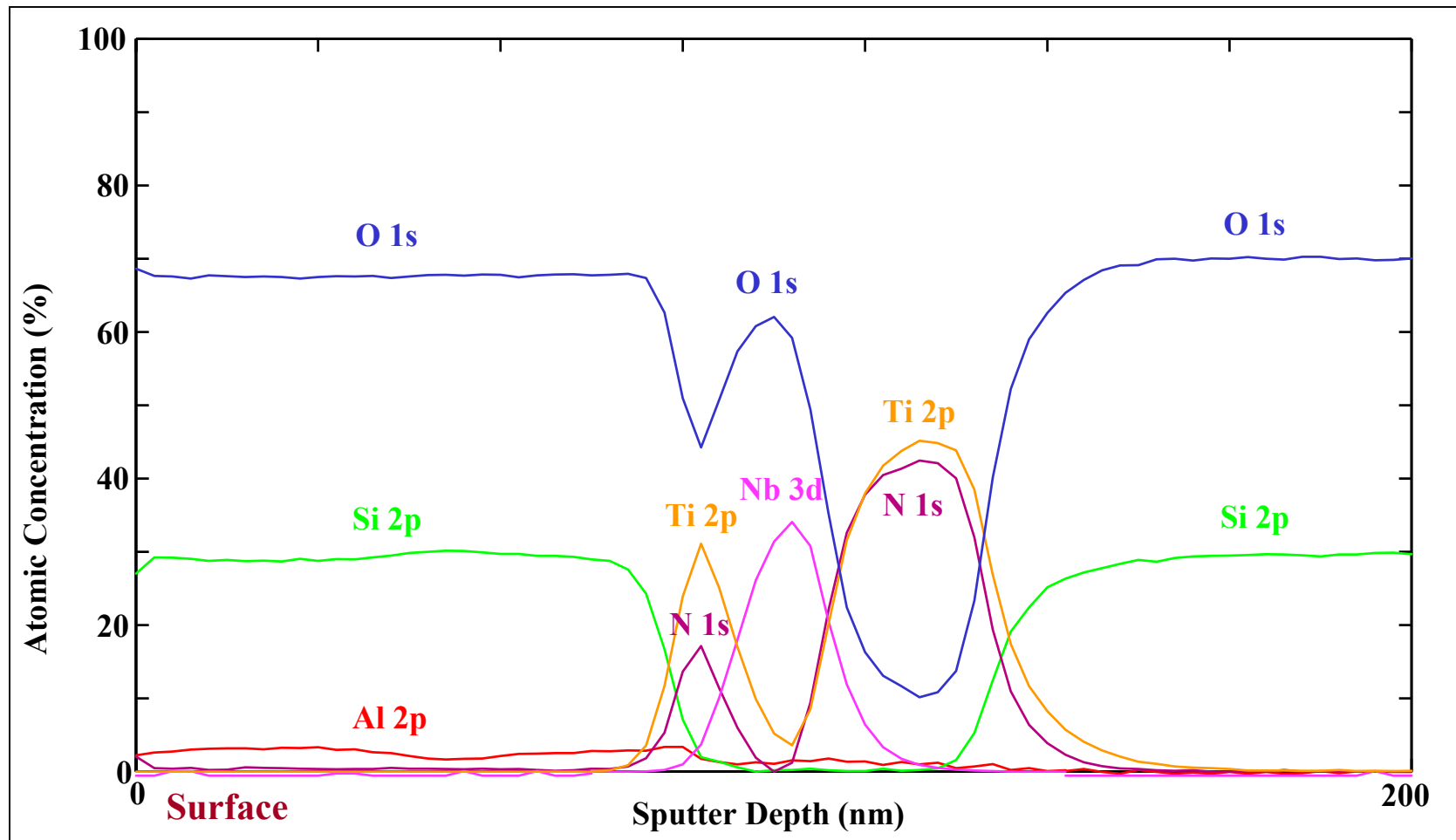




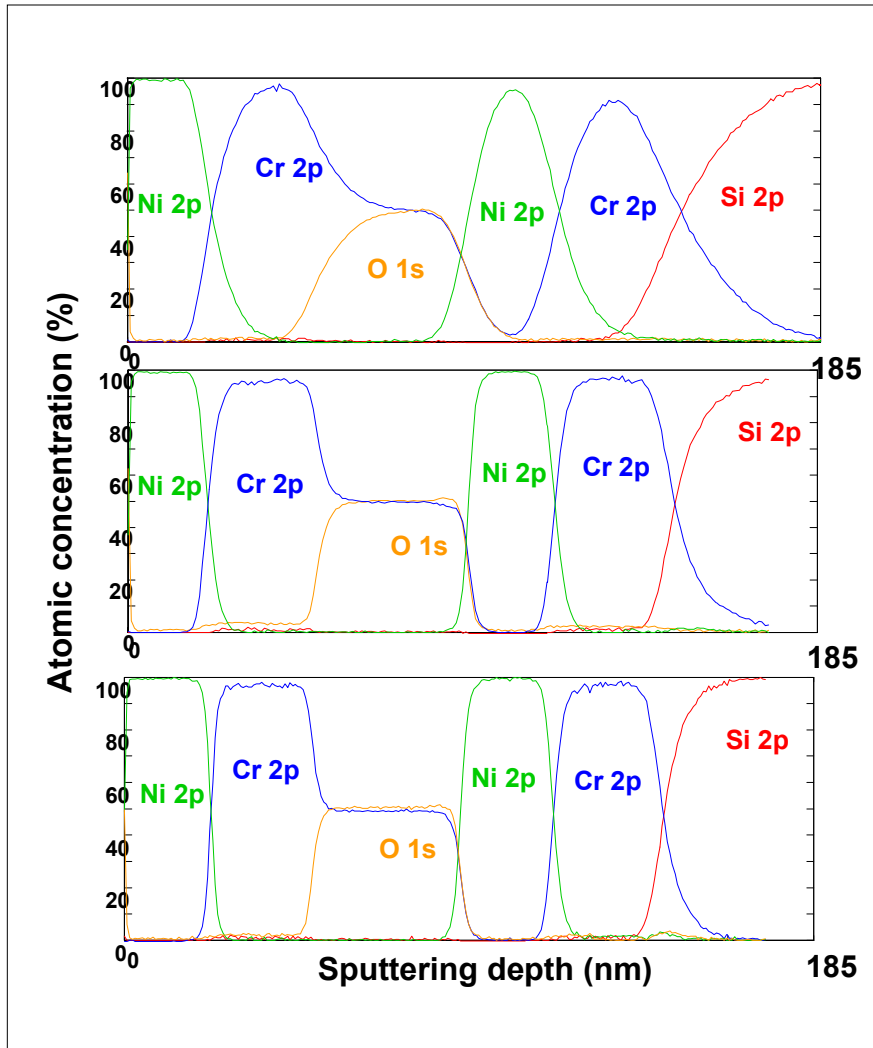
Calibration of depth scale

1. Sputtering rate determined from the time required to sputter through a layer of the same material of known thickness.
2. After the sputtering analysis, the crater depth is measured using depth profilometer. A constant sputtering rate is assumed.

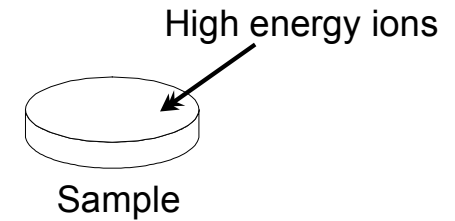
Depth profile of Architectural Glass Coating



Depth Profile with Sample Rotation

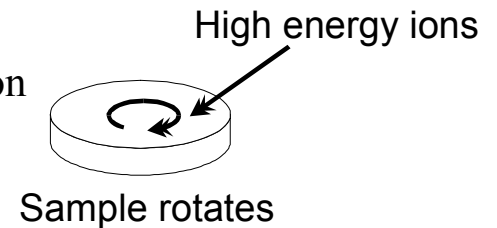


Ions: 4 keV
Sample still



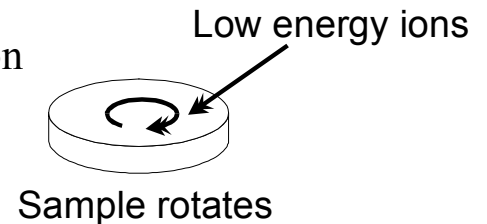
Cr/Si interface width (80/20%) = 23.5nm

Ions: 4 keV
With Zalar rotation



Cr/Si interface width (80/20%) = 11.5nm

Ions: 500 eV
With Zalar rotation



Cr/Si interface width (80/20%) = 8.5nm

Factor Affecting Depth Profiling

● Instrumental factors

- Adsorption from residual gas atmosphere
- Redeposition of sputtered species
- Impurities in ion beam
- Non-uniform ion beam intensity
- Time-dependent ion beam intensity

● Sample characteristics

- Depth information (IMFP)
- Original surface roughness
- Crystalline structure and defects (Channelling)
- Alloys, compounds, second phases (Preferential sputtering and induced roughness)

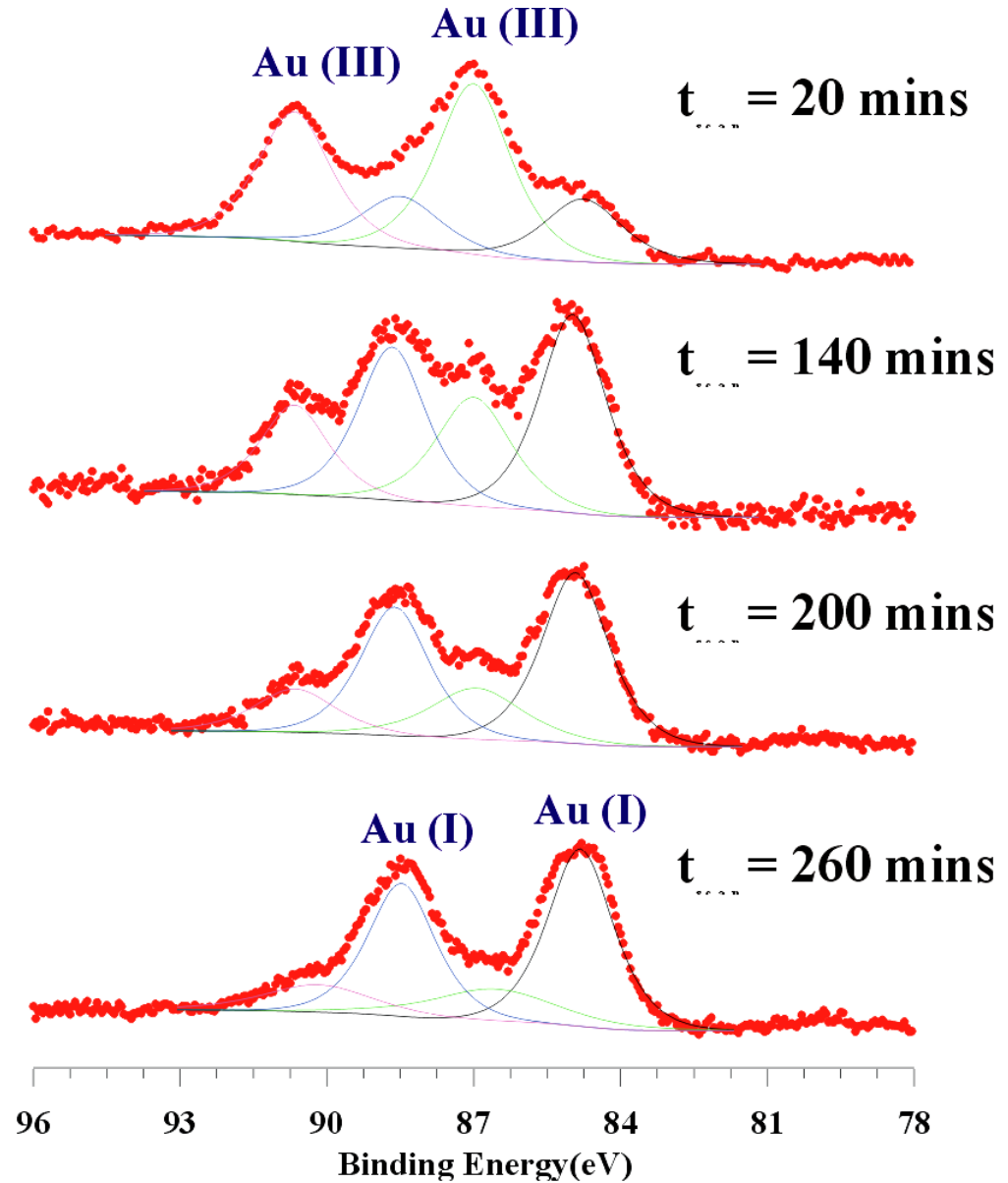
● Radiation-induced effects

- Primary ion implantation
- **Atomic mixing**
- Sputtering-induced roughness
- **Preferential sputtering and decomposition of compounds**
- Enhanced diffusion and segregation
- Electron-induced desorption
- Charging of insulators (analysis distortion; electromigration)

X-ray damage

Some samples can be damaged by the x-ray

For sensitive samples, repeat the measurement twice to check for x-ray damage.

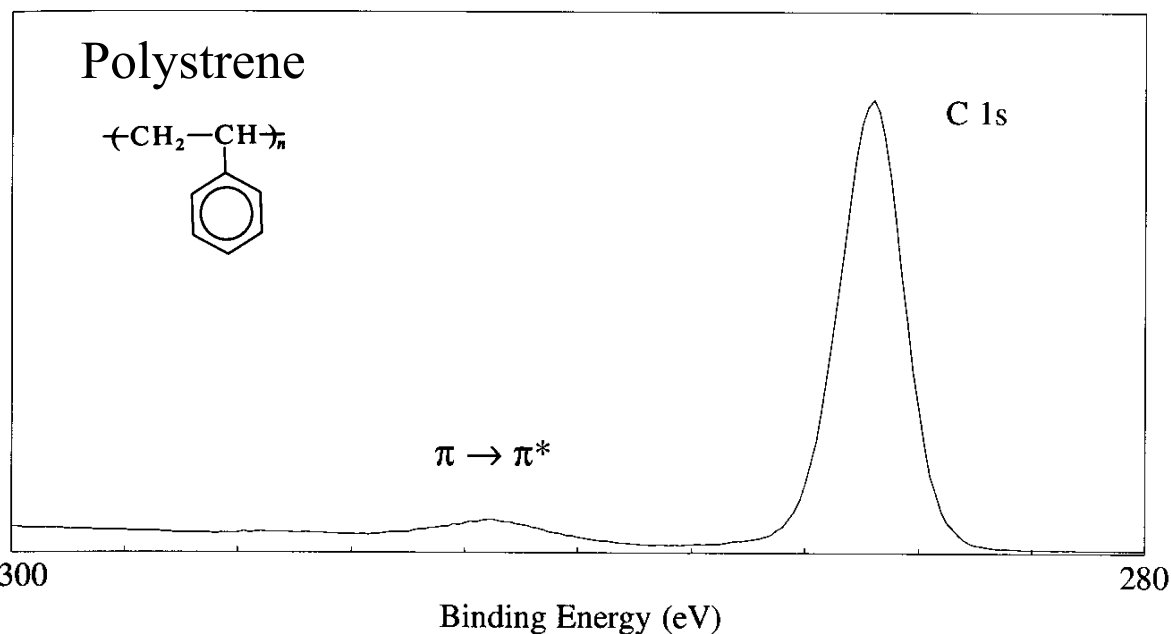
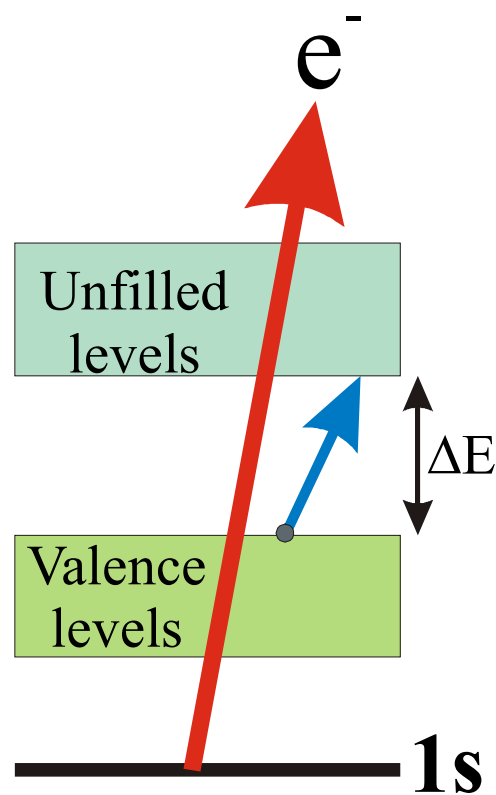


Shake-up Peaks

$$\text{K.E.'} = \text{K.E.} - \Delta E$$

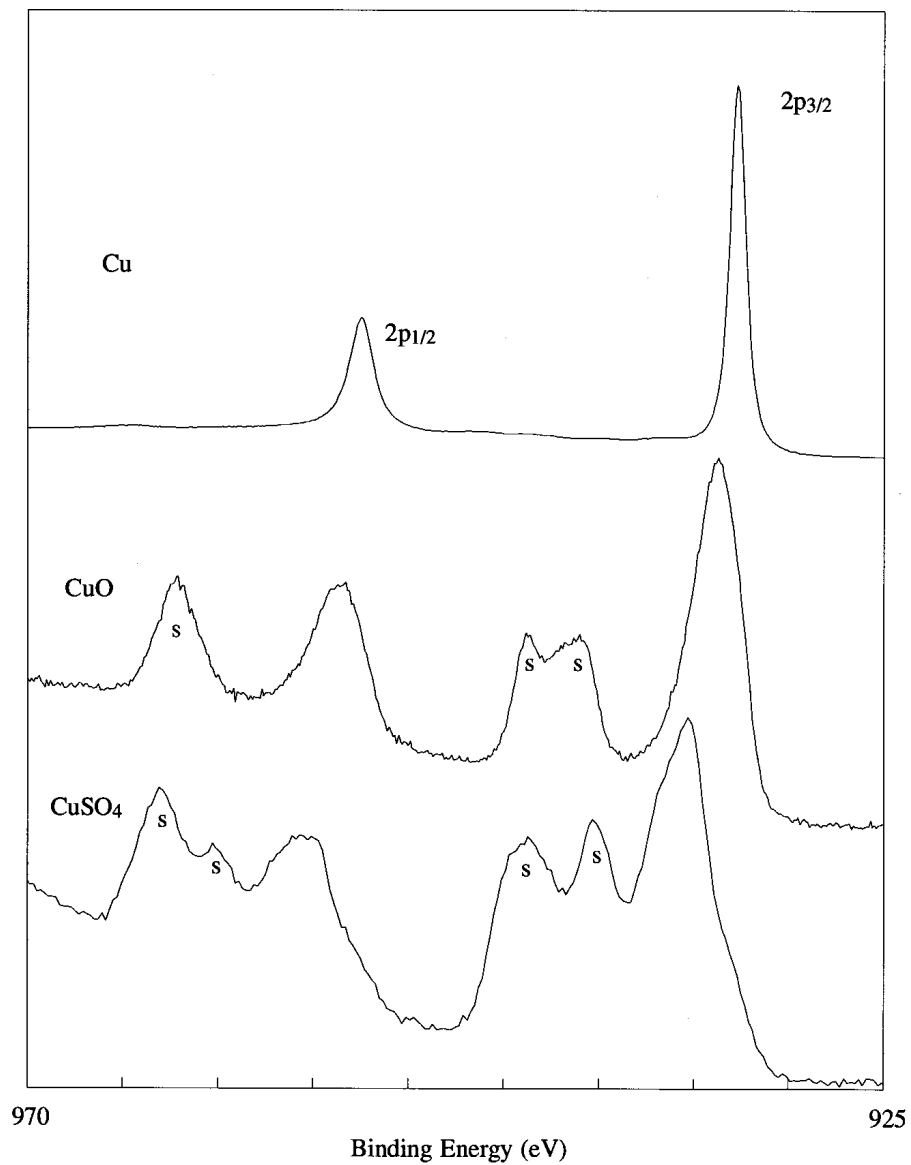
$$\text{B.E.'} = \text{B.E.} + \Delta E$$

For some materials, there is a finite probability that the photoelectronic process leads to the formation of an ion in its excited state with a few eV above the ground state.



Cu (II) Shake-up Peaks

A feature for the identification of Cu (II)



Other Chemical Effects in XPS

Multiplet Interaction

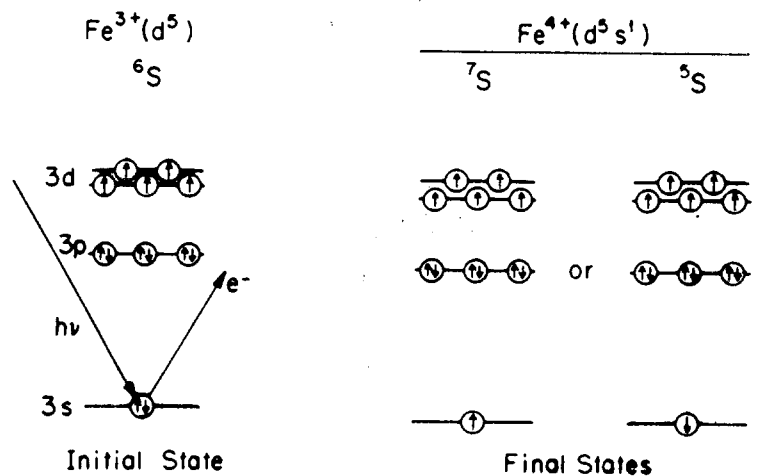


FIGURE 5.24. Schematic of multiplet splitting following photoionization in Fe^{3+} .

S level interaction

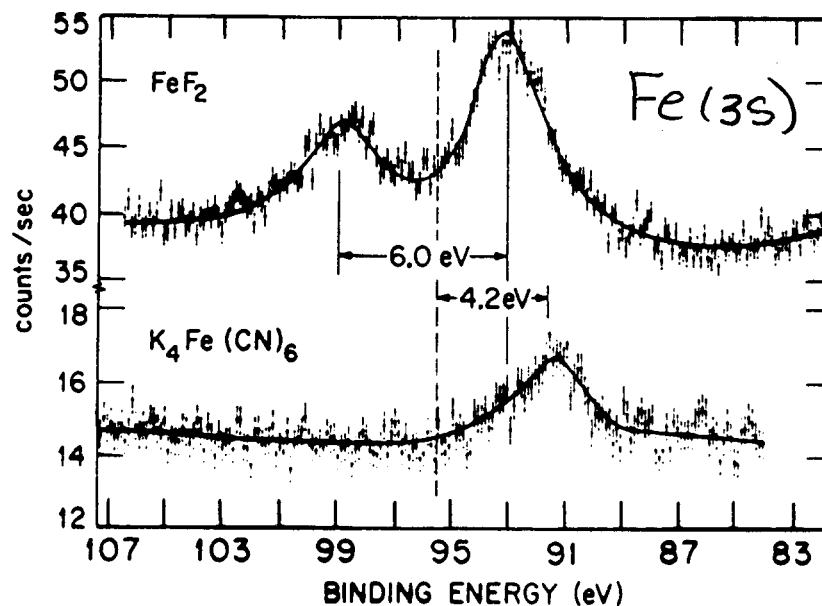


FIGURE 5.25. Photoelectron spectra of 3s shell in some transition metal compounds showing effect of multiplet splitting. [Reproduced from Carver *et al.*,⁽¹¹⁷⁾ Figure 2.]

(b) 2p level interaction

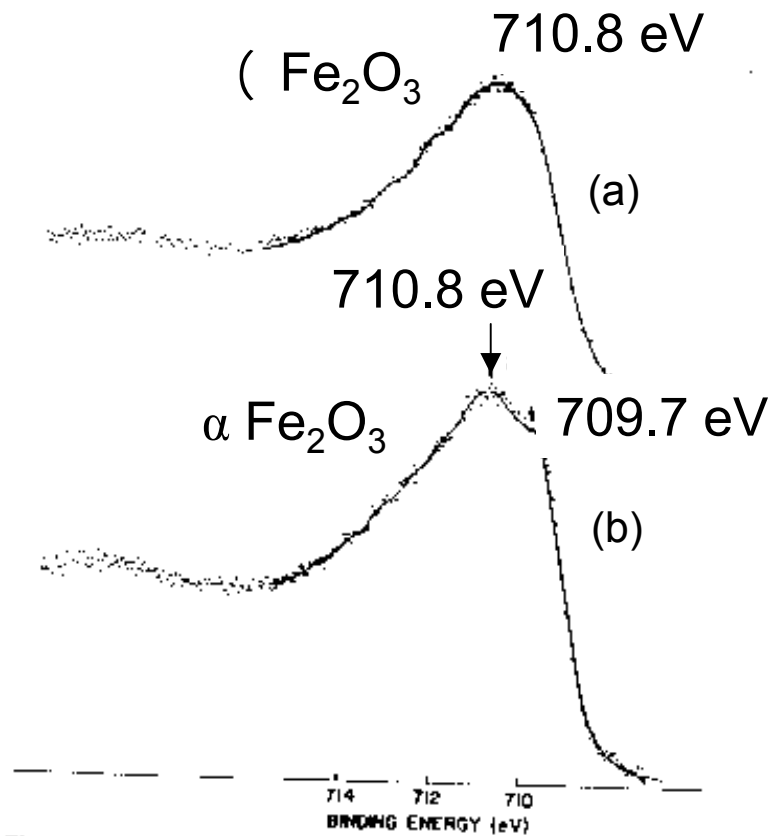
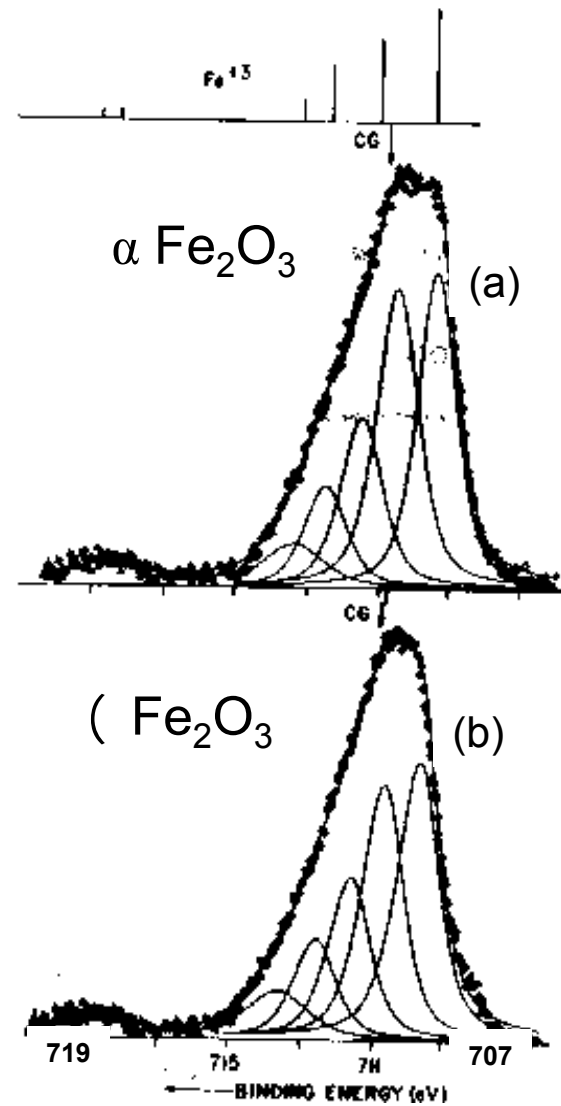


Figure 2. Detailed Fe(2p^{3/2}) spectra of (a) γ-Fe₂O₃, (b) α-Fe₂O₃



Detailed Fe(2p^{3/2}) spectra of (a) (Fe₂O₃, (b) α-Fe₂O₃

SESSION 4

Sample charging: compensation

Small area analysis and imaging

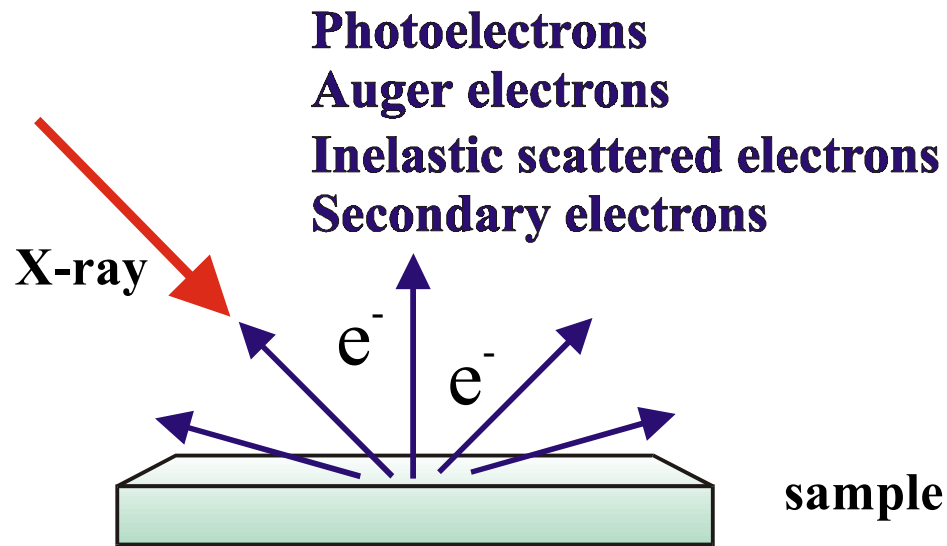
Angle dependent profiling

Modified Auger parameter

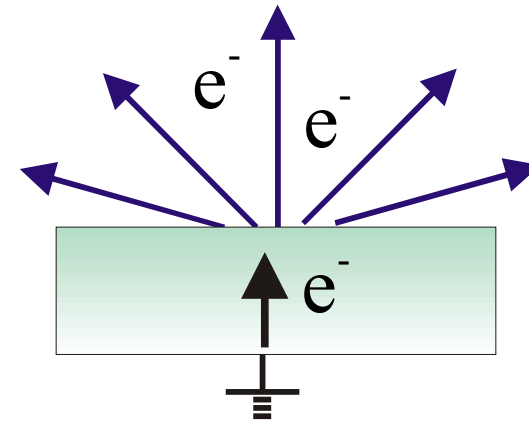
Case studies

Charging Compensation

Electron loss and compensation



For metal or other conducting samples that grounded to the spectrometer

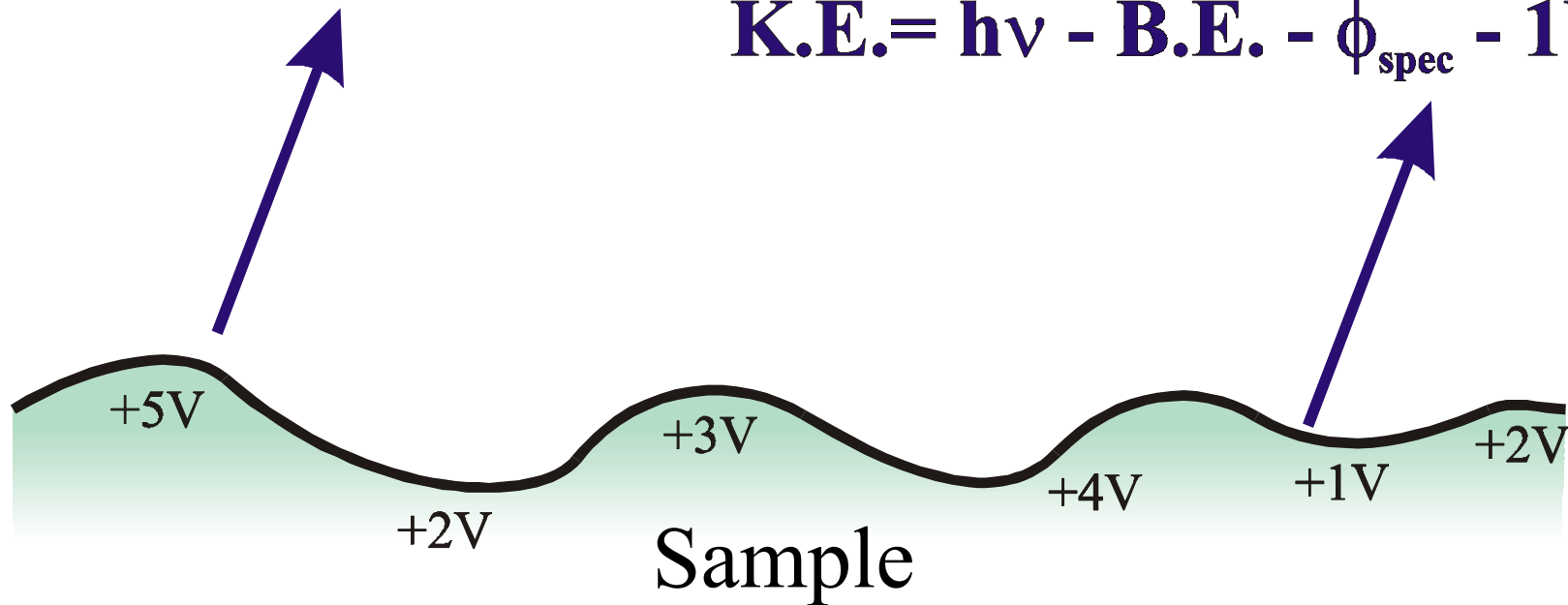


Electrons move to the surface continuously to compensate the electron loss at the surface region.

Differential (non-uniform) surface charging

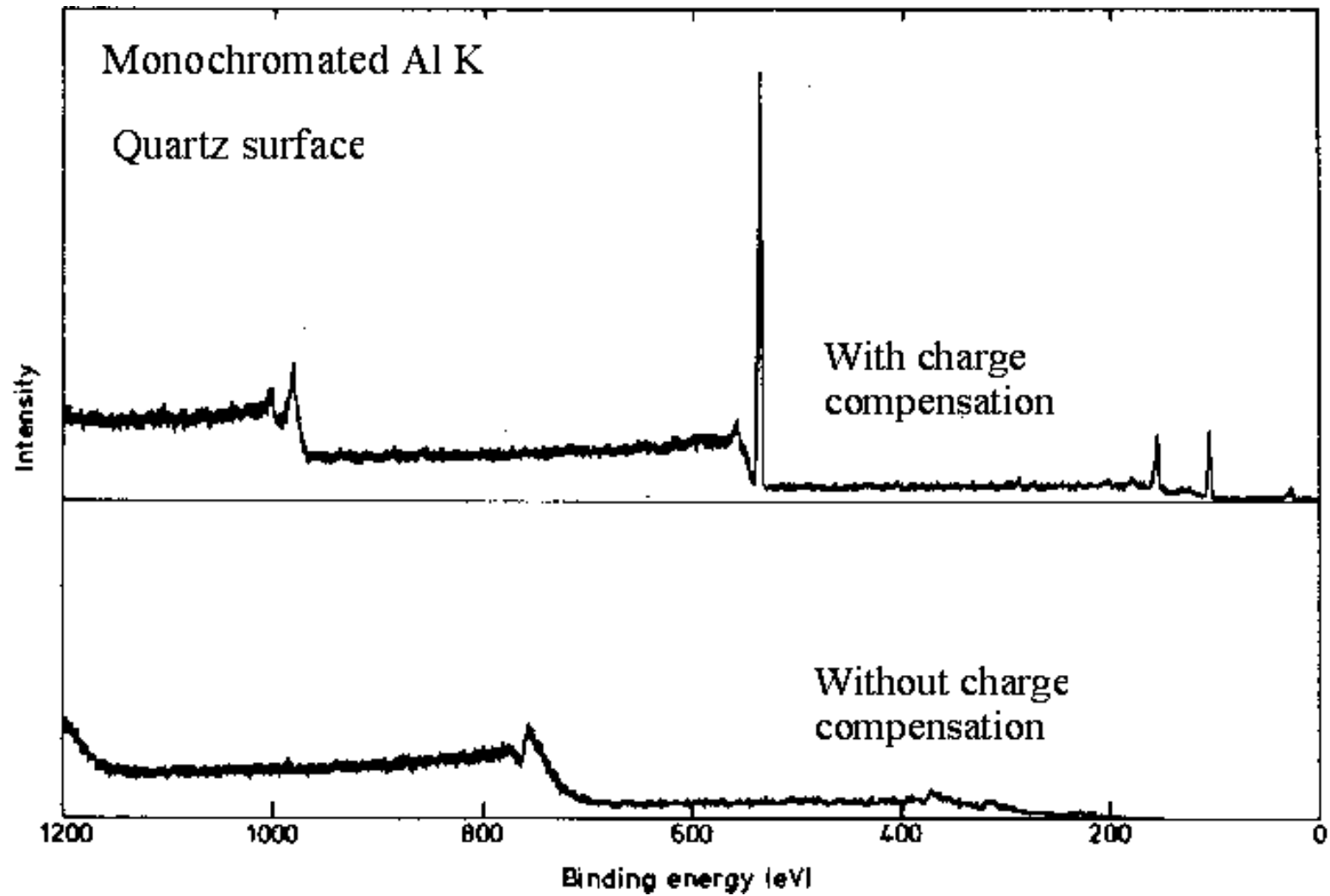
$$\text{K.E.} = h\nu - \text{B.E.} - \phi_{\text{spec}} - 5\text{V}$$

$$\text{K.E.} = h\nu - \text{B.E.} - \phi_{\text{spec}} - 1\text{V}$$



Broadening of peak

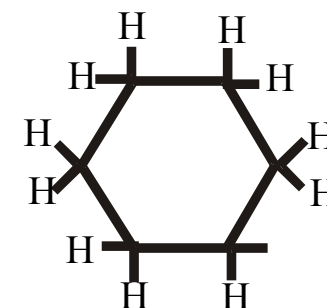
An example of differential surface charging



Binding Energy Referencing technique on insulating samples

Use of adventitious carbon-based contaminants

- (i) air exposure
- (ii) contamination due to pumping oil
- (iii) add cyclohexane

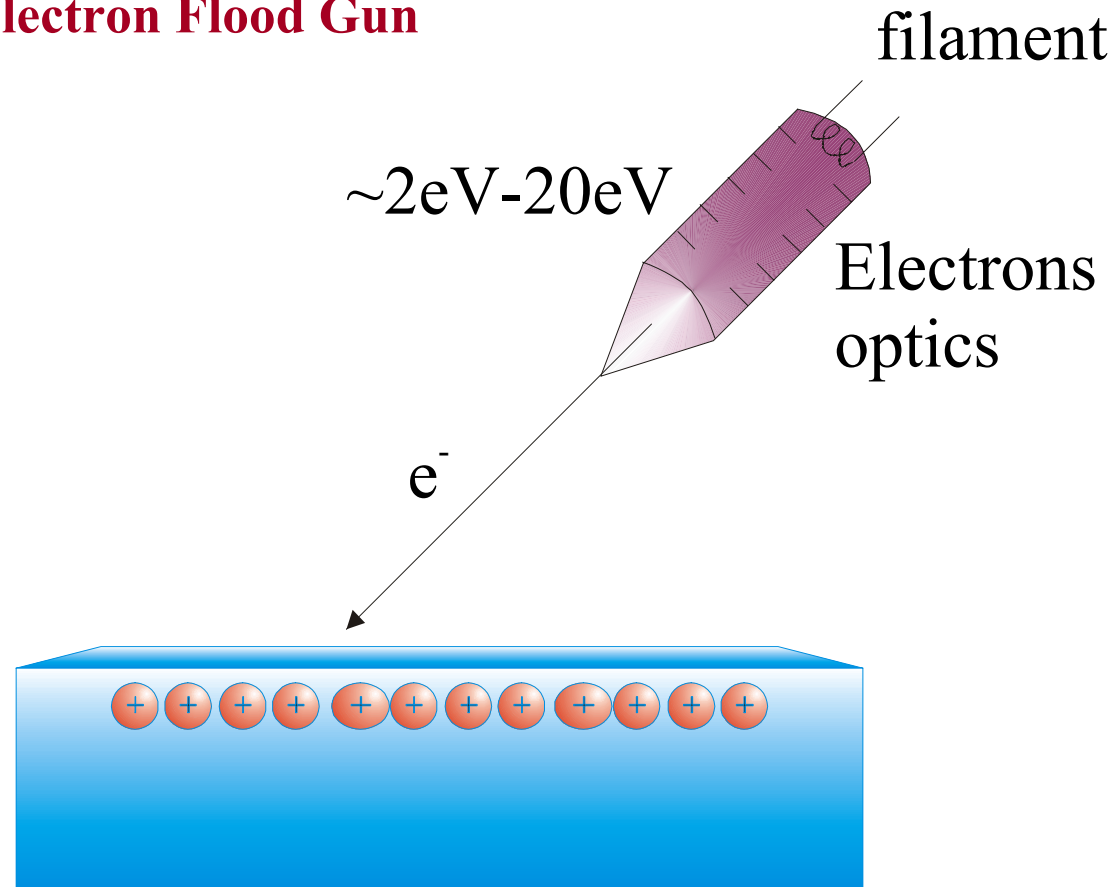


Often used BE = $285.0 \pm 0.2 \text{ eV}$ (aliphatic carbon)
with referenced to Au $4f_{7/2} = 84.0 \text{ eV}$

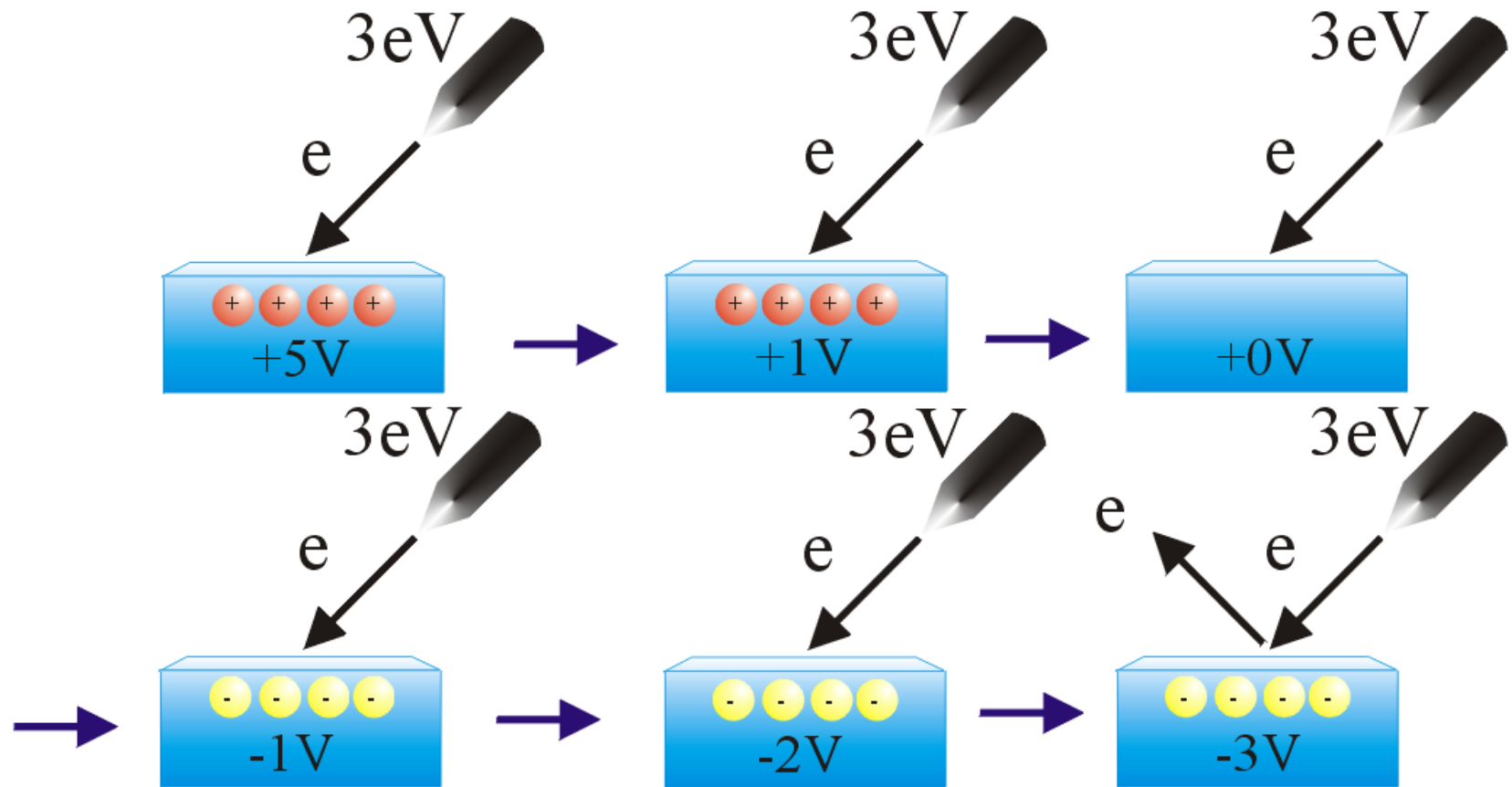
Or other peaks with known peak position in the sample

Charge Compensation Techniques

Low Energy Electron Flood Gun



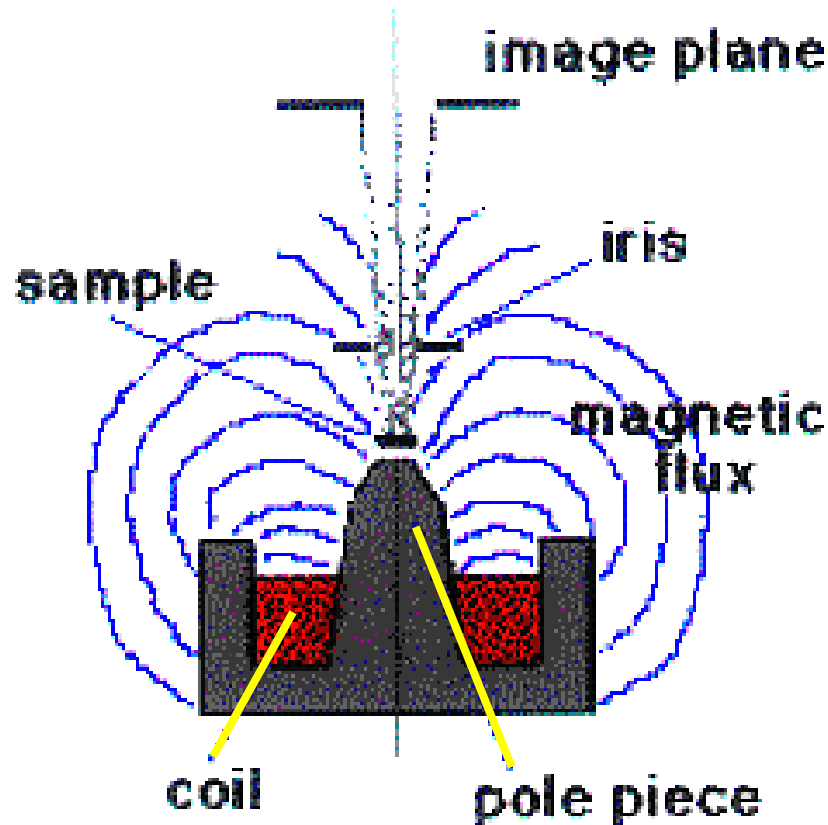
If the electron intensity is high enough



At equilibrium, Surface potential = electron beam energy

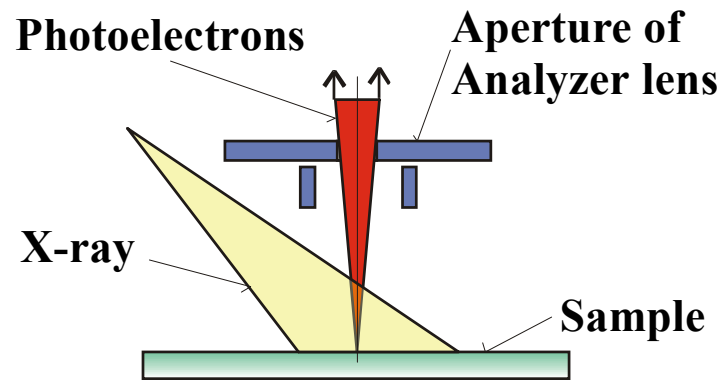
Usually, at equilibrium, surface potential < electron beam energy

Microscopic Analysis and Imaging Using Photoelectron Spectroscopy



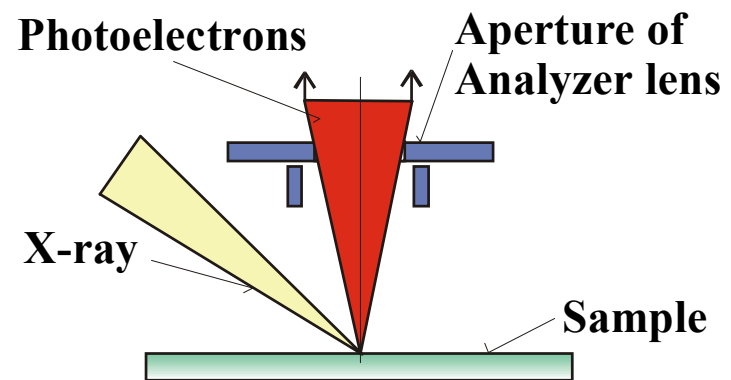
- Strong magnetic immersion fields are used to extract photoelectrons from localized phases.
- High collection efficiency allows images to be acquired within a few minutes.
- Images “corrected” for surface geometry
- Present resolution $\sim 1\ \mu\text{m}$
- Spectra can be extracted from regions as small as $15\ \mu\text{m}$

Small area analysis and XPS Imaging



Spot size determined by the analyser

Both monochromated and dual anode x-ray sources can be used



Spot size determined by the x-ray beam

XPS Imaging (1) Moving sample stage Techniques

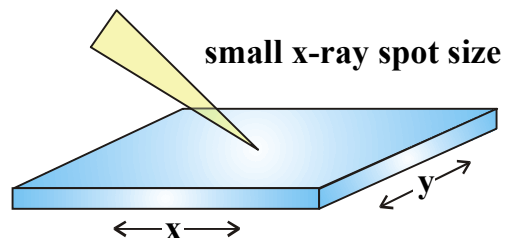


Image: x,y position versus photoelectron intensity

Resolution: $\sim 50\mu\text{m}$

(2) Use of scanning plates

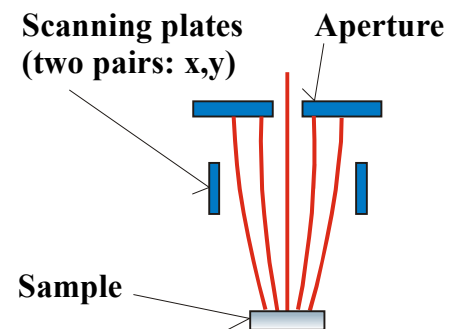
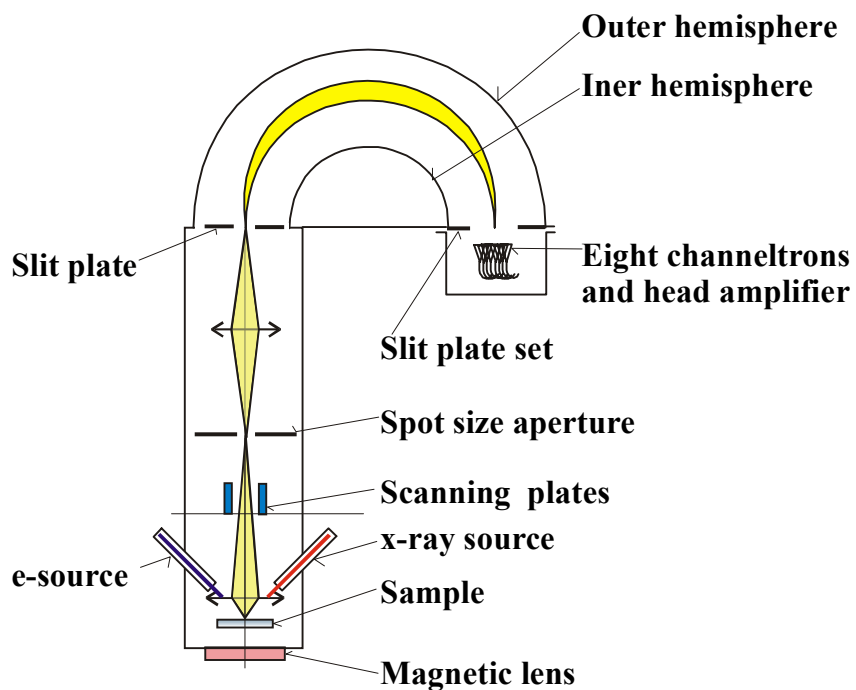
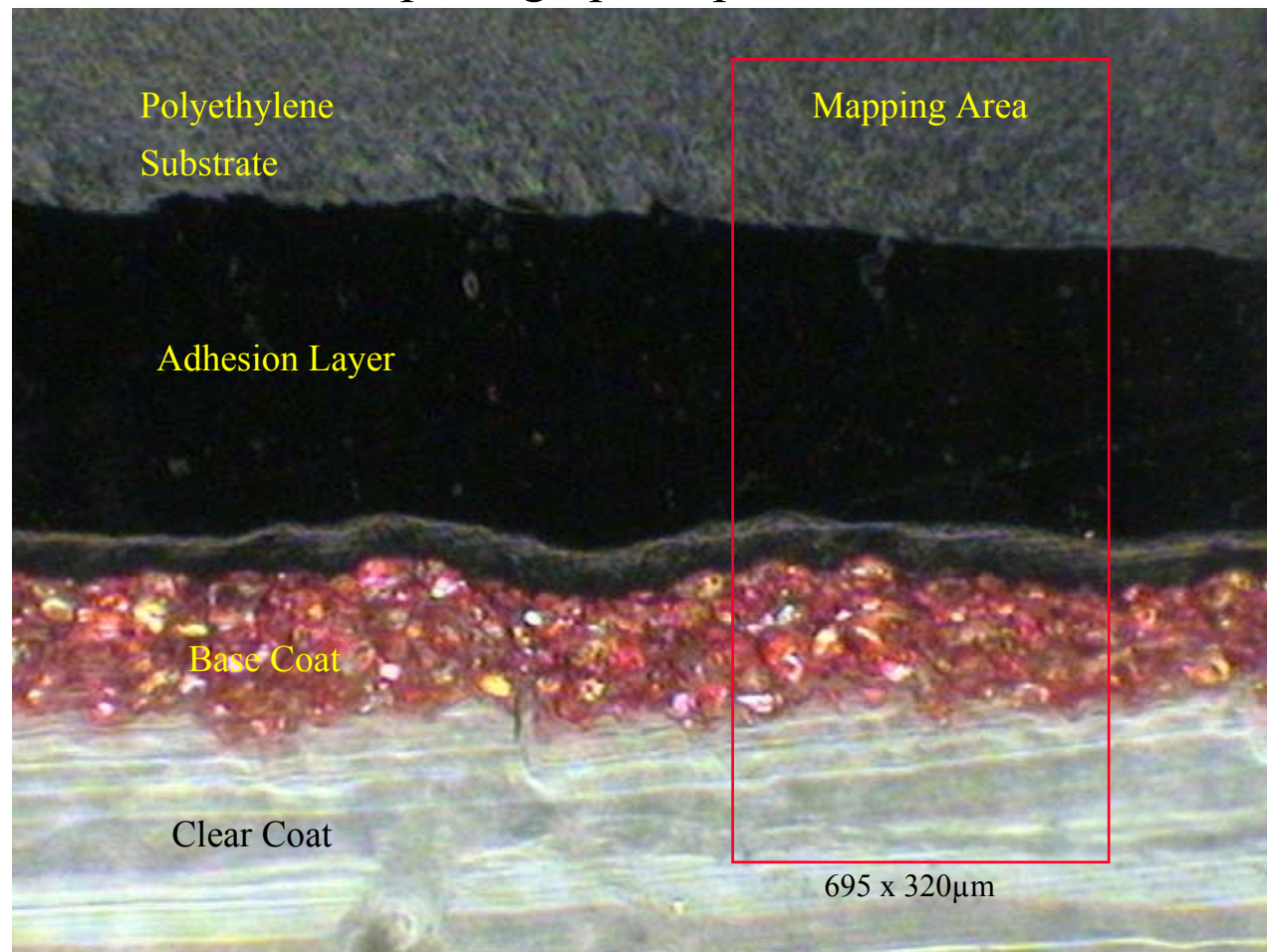


Image: Voltages V_x & V_y scanned:
Photointensity collected from different points in time sequence

Resolution: $\sim 10\mu\text{m}$

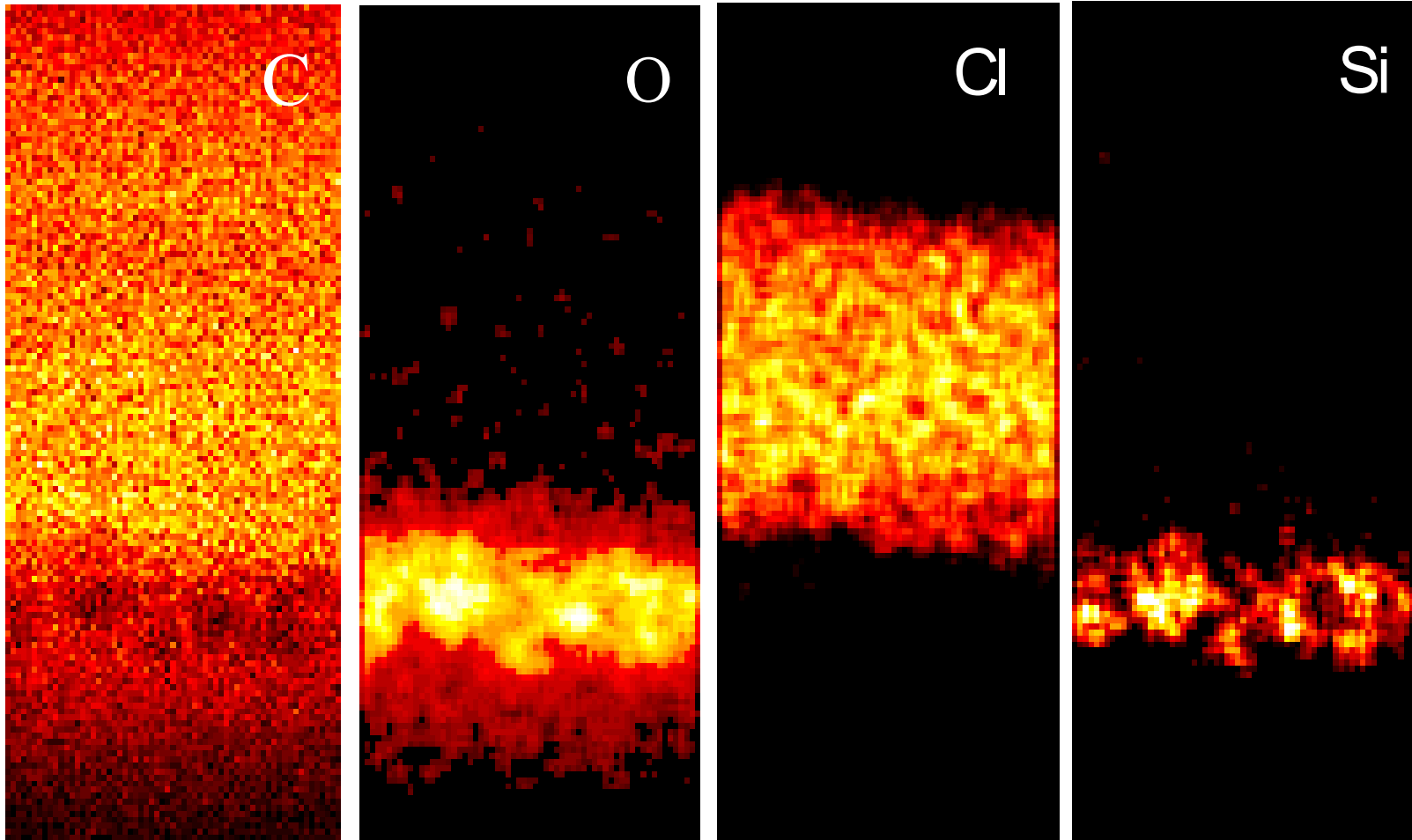
XPS study of paint

SPS photograph of paint cross section



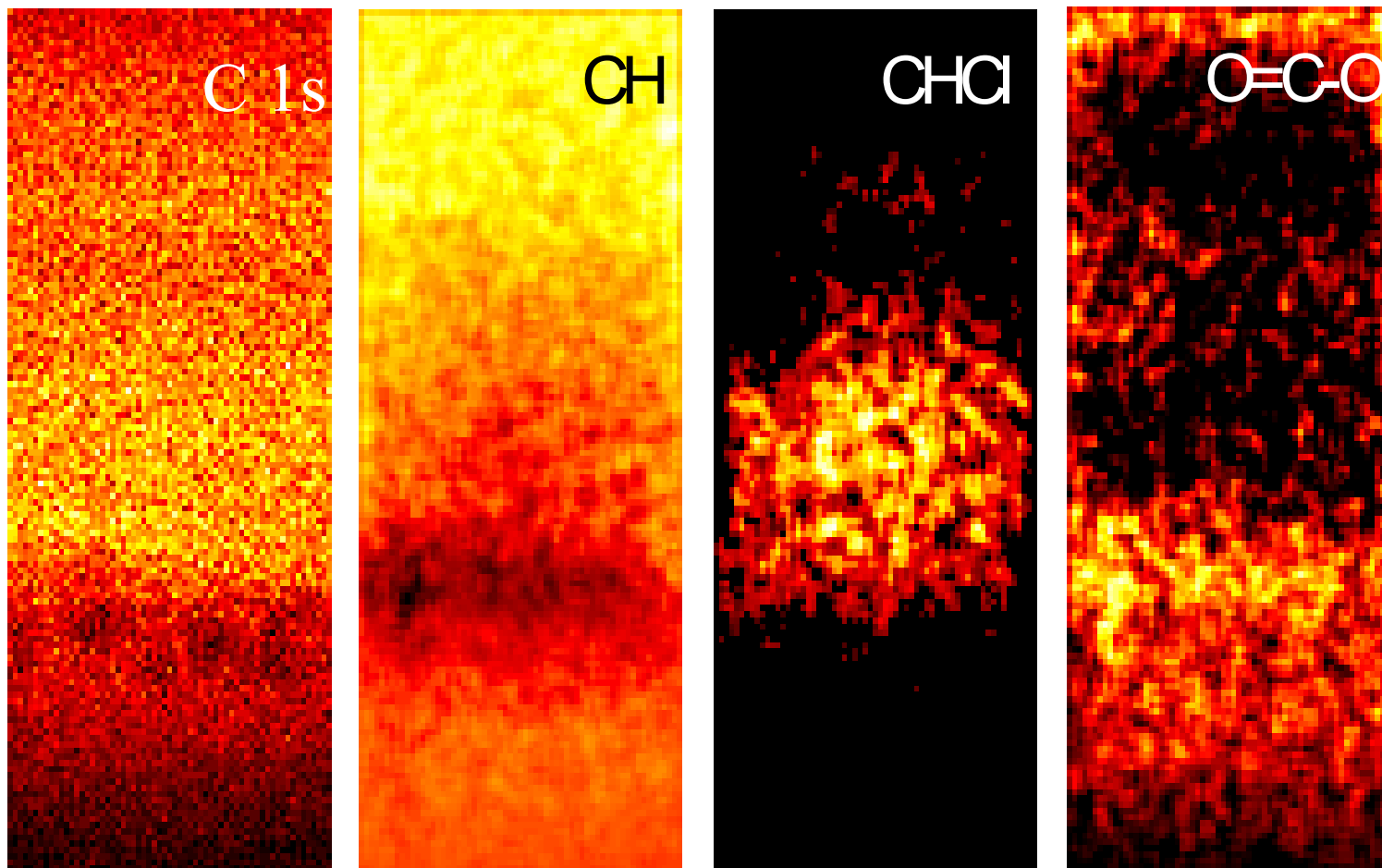
1072 x 812mm

Elemental ESCA Maps using C 1s, O 1s, Cl 2p and Si 2p signals



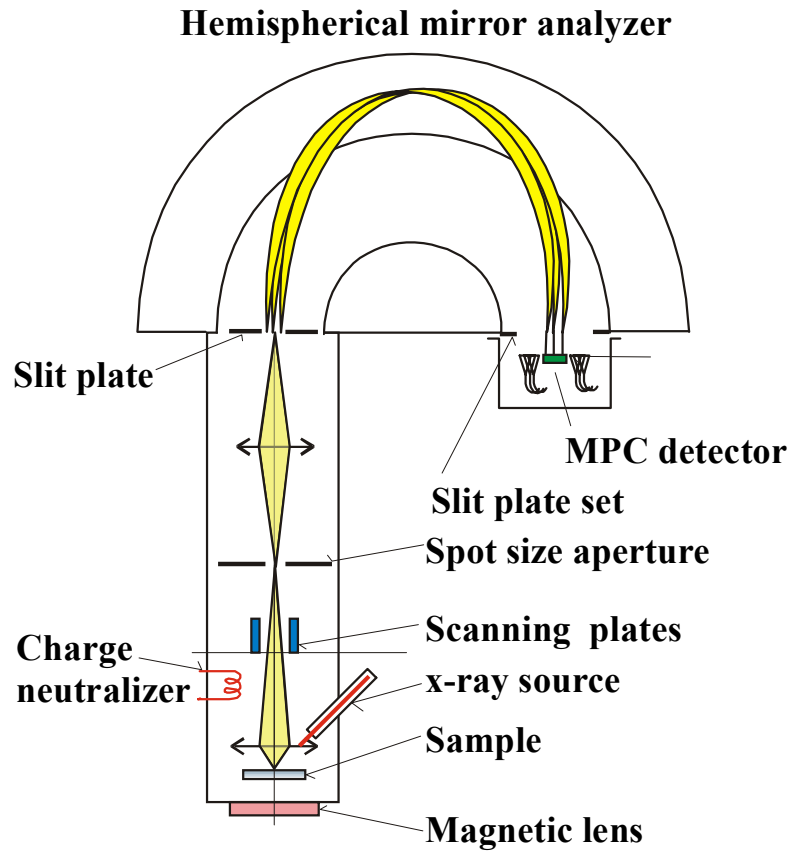
695 x 320mm

C 1s Chemical State Maps



695 x 320mm

(3) Use of multichannel plate



MCP An array of e-detectors

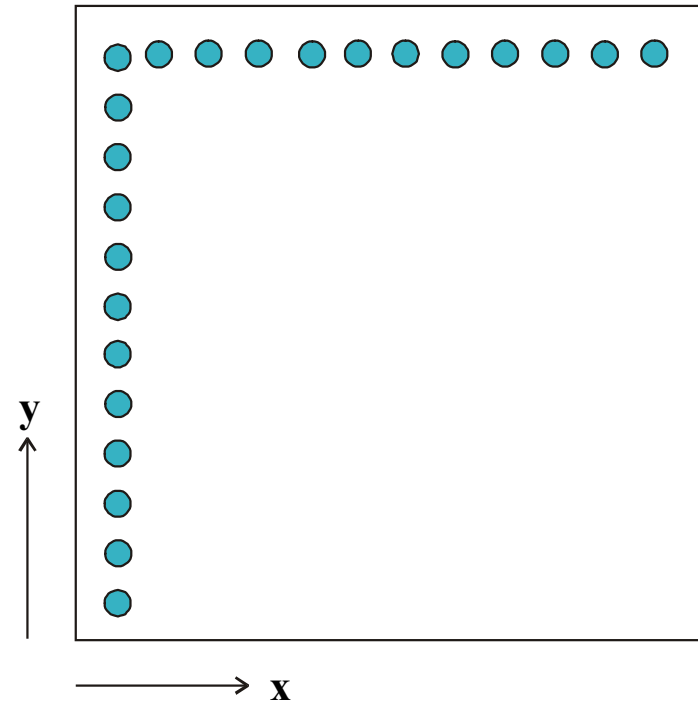


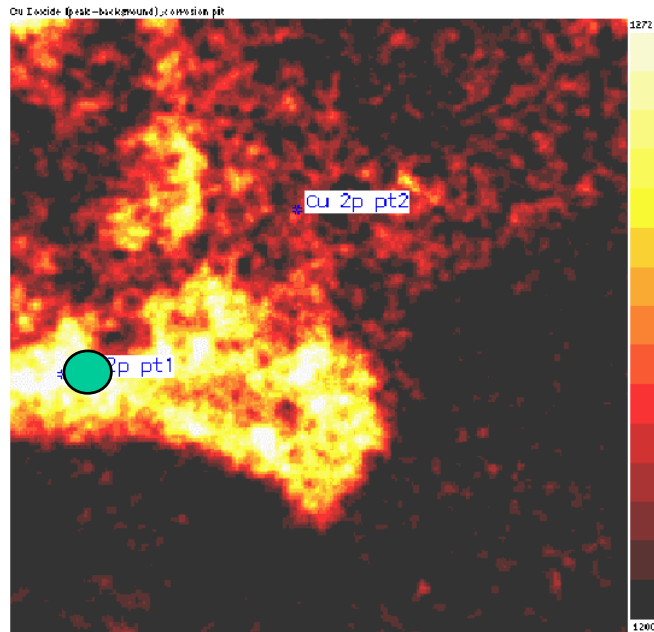
**Image: x, y position of e- detector
versus photoelectron intensity**

Best resolution: $\sim 3 \mu\text{m}$

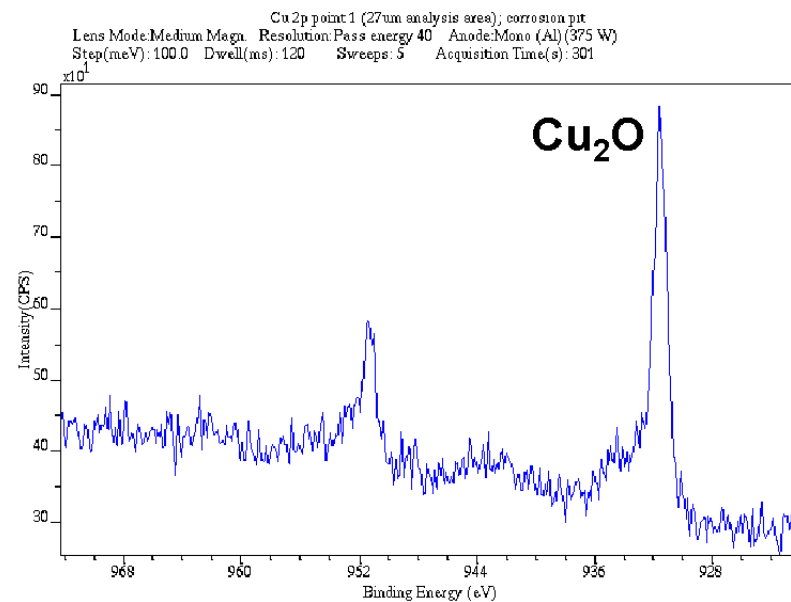
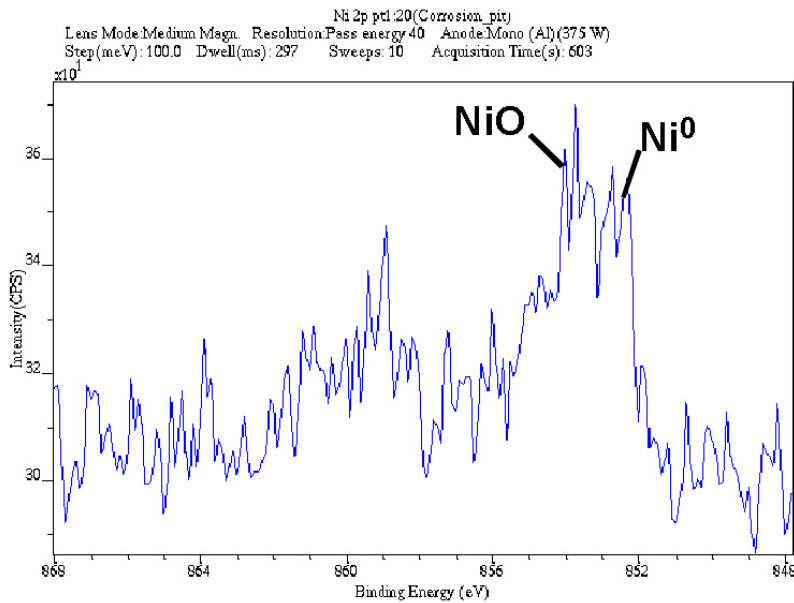
'Spot' High Resolution Analysis: Cathodic Region?

Cu₂O Map

**100
microns**



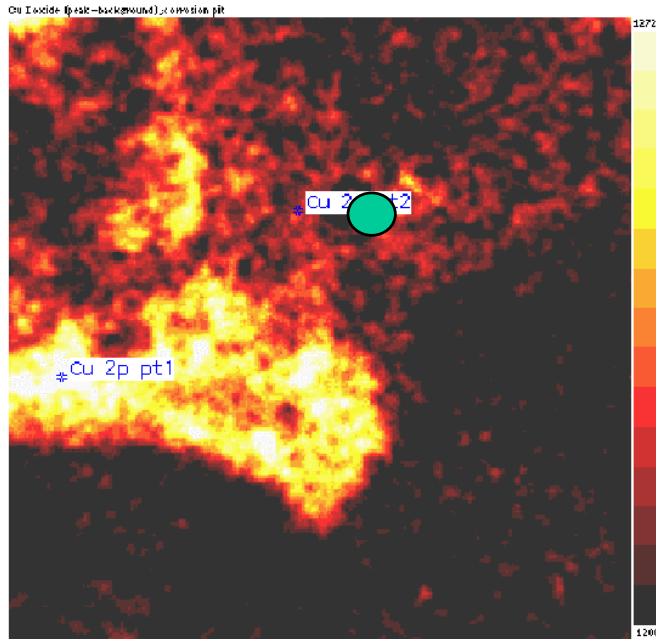
'Spot' chemical state analysis within this map enables identification of a local cathodic site.



'Spot' High Resolution Analysis: Anodic Region?

Cu₂O Map

**100
microns**



'Spot' chemical state analysis within this map enables identification of a local anodic site.

